ANALYSIS AND IDENTIFICATION
OF ROBUST LINEAR MODELS
FOR MULTIVARIABLE CONTROL

By

CHING-WEI KOUNG, M.Sc.

A Thesis
Submitted to the School of Graduate Studies
in Partial Fulfillment of the Requirements
for the Degree
Doctor of Philosophy

McMaster University

ANALYSIS AND IDENTIFICATION OF ROBUST LINEAR MODELS FOR MULTIVARIABLE CONTROL

In memoriam

My Grandmother	and	My Father-in-law
(1906 - 1989)		(1915 - 1989)

DOCTOR OF PHILOSOPHY (1991) McMASTER UNIVERSITY

(Chemical Engineering) Hamilton, Ontario, Canada

TITLE : Analysis and Identification of Robust Linear Models for Multivariable Control

AUTHOR : Ching-Wei Koung, B.Sc. (National Taiwan University)

M.Sc. (Queen's University)

SUPERVISOR : Professor John F. MacGregor

NUMBER OF PAGES : xiii, 132

Abstract

This study considers control problems associated with robust stability and performance of linear, time-invariant multivariable controllers. The robust stability and performance problems considered here are determined exclusively by the steady-state properties of closed-loop systems, and therefore they are independent of controller design and tuning methods. New approaches, one based on geometric interpretations and the other on singular value decomposition, are proposed to analyze the effects of steady-state model mismatches. The new analysis approaches are able to distinguish the critical differences between a process and its model that cause the control problems, and to identify the crucial process characteristics that must be preserved in the model if the closed-loop system is to be robust. This study shows that these properties are related to specific geometric differences and to particular elements in the singular value decomposition matrices, and that it is the structure rather than the magnitude of multivariate model mismatch that dominates the robustness properties. These results explain the fact that many nonlinear processes can be controlled by linear controllers with robustness over a wide range of operating conditions, in spite of the large mismatch magnitudes arising from process nonlinearities. Physical examples of these processes are given in this thesis. The analysis results are also used to specify new criteria for experimental designs to identify linear models that lead to robust multivariable controllers. The new experimental designs are based on minimizing model uncertainties in the multivariate model structure rather than simply the mismatch magnitude. The significance of the new experimental design approach is that it can identify robust models that yields high-performance control even for ill-conditioned processes. These robust identification designs usually require input perturbations that are drastically different from traditional designs.

Acknowledgement

I would like to express my greatest gratitude to my supervisor, Professor John F. MacGregor, for his extraordinarily intelligent guidance and kindly encouragements.

I would also like to thank:

Department of Chemical Engineering, McMaster University, for the financial support.

Professor Thomas E. Marlin for his many helpful comments.

My father for his generosity in supporting me and my wife financially.

I am in debt to my wife, Shou-Fen, for taking excellent care of our first baby girl, Fan-Pei.

Table of Contents

Table of Figures

Table of Tables

1 Introduction

Multivariable control always needs a process model explicitly or implicitly in designing the controller. The most commonly used controllers today are still formulated as a linear, time-invariant control law, and therefore linear dynamic models such as transfer functions are sufficient for designs of these controllers. Transfer function models are mostly obtained from process identification in practice. The major problems in linear, time-invariant control arise from the fact that: 1) the relationship between the manipulated inputs and the controlled outputs in real chemical processes are virtually never linear and time-invariant, and 2) experimental identification always has errors. The existence of the mismatch between a true process (nonlinear and time-variant) and its identified transfer function model makes the controller have a different performance from that specified in the design, and may even endanger the closed-loop stability. Therefore, the effect of model mismatch on the stability and performance of the closed-loop systems is of utmost importance.

It is important to clarify the difference between model mismatch and model uncertainty prior to discussing robustness issues. Model mismatch is defined here as the difference between the true process at a specific condition (approximated by a *fixed* transfer function model) and the linear model that the controller design is based upon. Since the true process is subjected to many changing conditions (ie. changing operating points, disturbances, etc.), one specific model mismatch cannot characterize any real process over its operating range. A collection of all possible model mismatches that might be encountered in the true process defines the model uncertainty region. Rigorously speaking, it is specific model mismatches, rather than the model uncertainties, that cause control problems. In a deterministic situation, it is not very difficult to find out some ("good") model mismatches that have no effect on the control stability or minimal impact on the control system performance, and to pinpoint some ("bad") mismatches that have severe impacts. The major difficulty is that we never know the true model uncertainties in a stochastic situation. In the past, robustness studies always assume certain descriptions of model uncertainty regions to approximate the true model uncertainties, and for many valid reasons, never distinguish between the "good" and "bad" model mismatches within the assumed model uncertainty region.

The thrust of recent robust controller design research has been to incorporate a description of the model uncertainties explicitly into the design methodology in order to enhance the robustness of the control system. The difficulty in obtaining a realistic uncertainty description usually leads to conservative designs. However, the ultimate limitation in controller performance and stability is not the uncertainty characterization, but the actual model mismatches themselves. In other words, even if we could characterize precisely the model uncertainty region in one model which contained many "bad" model mismatches, and use a very sophisticated robust controller design to minimize their impact, the control performance would never be better than the one from the same design with a better model, that is, one with better model mismatches.

This thesis focuses on the new problem of *robust linear models*. A robust linear model is defined here as a linear model that will lead to more robust linear, time-invariant controllers by any design method. The major contribution of this thesis is the presentation of some preliminary research results on the analysis and identification of robust linear models for Multiple-Input-Multiple-Output (MIMO) processes.

The objective in the analysis of robust linear model, in the simplest words, is to recognize what constitutes "good" and "bad" model mismatches for an arbitrarily given linear MIMO model. If we have the answer to this question, we will know exactly what types of identification errors, process nonlinearities and time-variant properties make the given model robust or sensitive. Note that in this study the model mismatches arising from nonlinear, time-variant processes are examined only as locally linearized, time-invariant processes.

The objective in the identification or "synthesis" of robust linear models is to provide a methodology on how to identify a linear model whose model uncertainty region contains only the "good" mismatches arising from identification errors and/or process nonlinearities. However, for the latter situation, it is important to recognize that there are nonlinear processes in which controller designs based on linear models never yield robust control systems. This study will identify some special classes of nonlinear processes in which linear, time-invariant controllers can be robust.

The most powerful analysis and synthesis tools for *robust controller* designs up to date are based on the so-called unstructured and structured uncertainty descriptions (Doyle and Stein (1981), Doyle (1982)). Given an unknown process and a model that the controller design is based upon (ie. the true model uncertainties are fixed), the whole methodology is first to obtain an uncertainty description as close to the true uncertainties as possible (note that only the so-called norm-bounded uncertainties can be handled in these methods), and then either to analyze a given controller or to synthesize a robust controller. However, it provides no insights into what constitutes a robust model or how to obtain one. Consequently, the norm-bounded unstructured/structured uncertainties analysis/synthesis methods are not directly applicable to the *robust model synthesis* problem on how to obtain better model uncertainties via a better model. A major contribution of this study is that a new methodology on robust model synthesis is proposed to "manipulate" the model uncertainties through the designs of identification experiments.

This thesis contains six chapters. Chapter 2 first defines the control problems which can be resolved by using a more robust model in the controller design, through a simulation example, and then necessary conditions for robust performance and stability for these control problems are introduced.

Chapter 3 first summarizes the approaches from past research work for analyzing the impact of a given description of the model uncertainties on the defined control problems.

Then two new approaches proposed in this study are introduced in the rest of this chapter. The first one is a geometric approach in which the impact of model mismatches in 2×2 systems can be analyzed in terms of the geometric differences between the true process and its model. Most importantly, this approach is able to distinguish between "good" and "bad" model mismatches for the defined control problems, and therefore is well-suited for the robust model synthesis problem. The second approach is based on a new framework of describing the model uncertainties and is applicable to high-dimensional systems. Within this framework, some descriptions of model uncertainties that contain only the "good" mismatches for the defined control problems can be directly applied to the synthesis or identification of robust models. However, since the analysis can be conducted only for limited cases, this approach is less appropriate as a general tool for robust model analysis.

Chapter 4 considers specific classes of structured uncertainties arising from process nonlinearities or time variations, and investigates the robustness of linear time-invariant controllers. Suppose that we could obtain a perfect model for the true process at one specific condition and design a controller for it. Then in this chapter some sufficient conditions are given on how much and in what fashion the nonlinearities or time-variant properties can introduce mismatch into that particular process, without causing the defined control problems. Physical examples of nonlinear processes are given in the rest of this chapter to show that the theoretically derived sufficient conditions do exist in real world, and therefore high-performance robust linear controllers are feasible for this group of nonlinear processes.

Chapter 5 applies the new analysis and synthesis tools developed in Chapter 3 to the practical problem of identifying transfer function models that lead to controller designs. This problem is referred as *robust identification* in this thesis. It is well-known that the uncertainties in parameter estimates are controlled by the design of experiments, and therefore Chapter 5 focuses on this aspect. The designs of experiments for identifying robust models are rigorously derived for 2×2 processes and generalized to high-dimensional systems. Numerical examples are also provided at the end of this chapter to confirm the effectiveness of the new designs.

2 Control Problems Arising from Steady-State Mismatches

2.1 An Illustrative Example

To illustrate how steady-state model mismatches affect the stability and performance of a linear multivariable control, consider the following example of a hypothetical nonlinear process:

$$\bar{\mathbf{P}}(z)=\frac{0.4}{1-0.6z^{-1}}\begin{bmatrix}0.505 & -0.495\\ 0.495 & -0.505\end{bmatrix} \qquad (2-1.a)$$

$$\mathbf{P}(z)=\frac{0.4}{1-0.6z^{-1}}\begin{bmatrix}0.177 & -0.159\\ 0.750 & -0.754\end{bmatrix} \qquad (2-1.b)$$

(2-1.a) and (2-1.b) are the locally linearized discrete transfer function models of this process at two operating conditions (the former is specified as the nominal process). For simplicity, the nominal process is assumed to have the same dynamics in each pair of input/output variables, and moreover the common dynamic parameter (ie. 0.6 in the denominator term of (2-1.a)) is not affected by changing the operating condition such as (2-1.b).

Consider the following three estimates of nominal processess which might arise from an identification study:

$$\hat{\mathbf{P}}_{(1)}(z)=\frac{0.4}{1-0.6z^{-1}}\begin{bmatrix}0.466 & -0.461\\ 0.529 & -0.535\end{bmatrix},\ \|\bar{\mathbf{G}}-\hat{\mathbf{G}}_{(1)}\|_2=0.069,\ \|\mathbf{G}-\hat{\mathbf{G}}_{(1)}\|_2=0.521 \qquad (2-2.a)$$

$$\hat{\mathbf{P}}_{(2)}(z)=\frac{0.4}{1-0.6z^{-1}}\begin{bmatrix}0.452 & -0.513\\ 0.432 & -0.532\end{bmatrix},\ \|\bar{\mathbf{G}}-\hat{\mathbf{G}}_{(2)}\|_2=0.088,\ \|\mathbf{G}-\hat{\mathbf{G}}_{(2)}\|_2=0.586 \qquad (2-2.b)$$

$$\hat{\mathbf{P}}_{(3)}(z)=\frac{0.4}{1-0.6z^{-1}}\begin{bmatrix}0.493 & -0.504\\ 0.524 & -0.507\end{bmatrix},\ \|\bar{\mathbf{G}}-\hat{\mathbf{G}}_{(3)}\|_2=0.031,\ \|\mathbf{G}-\hat{\mathbf{G}}_{(3)}\|_2=0.575 \qquad (2-2.c)$$

where $\mathbf{G}=\mathbf{P}(1)$, $\|\bar{\mathbf{G}}-\hat{\mathbf{G}}\|_2$ and $\|\mathbf{G}-\hat{\mathbf{G}}\|_2$ are the additive steady-state mismatch magnitudes of these models measured by the 2-norm (Stewart, 1973), with respect to the gain matrices at the nominal and the other operating conditions. It is clear that the three models have similar mismatch magnitudes. However, it will be shown later that the multivariable control performance based on them are very different.

The Internal Model Control (IMC) design with decoupled output responses (Garcia and Morari, 1985) will be used to test the robustness of these models. Figure-2.1 shows the simulated closed-loop output responses to the same sequence of set-point changes for the cases of the three models being used to design the controllers for the two locally linearized processes. The only controller design parameters are the diagonal filter constants, and they are chosen to be 0.7 for both outputs in all six cases.

We can observe two major control problems in Figure-2.1, one being related to the control stability and the other the control performance. Let's first examine the good control cases where the first identified model is used in the IMC design (Figure-2.1(a) and (b)). The first model yields a controller that has very robust performance not only to control the nominal process but also the other process in which gain nonlinearities introduce more than 5 times of mismatch magnitude compared with that between the nominal process and the model. On the contrary, the performance of the same design method using the second identified model to control the nominal process (Figure-2.1(c)) is much worse than that of using the first model. Remember that *decoupled* responses to the first set-point change are the ideal situation when the model is perfect. The mismatch in the second identified model makes the closed-loop response not only far from the ideal response but also worse than that in Figure-2.1(b), in spite of much larger mismatch magnitude in the latter. This result clearly indicates that the closeness between the identified and true processes cannot be judged exclusively by the mismatch magnitude, and the critical characteristics of MIMO model mismatch are yet to be recognized. When the second model is used to control the other process, the additional mismatch due to process nonlinearities leads to an unstable closed-loop system. We can see from Figure-2.1(d) that the outputs slowly drift away from the set-point values and finally settle down simply because the inputs are saturated. This controller behaves as though it has positive feedback. Finally, the third identified model with the smallest mismatch magnitude with respect to the nominal process cannot be used to control either the nominal process (Figure-2.1(e)) or the other process (Figure-2.1(f)).

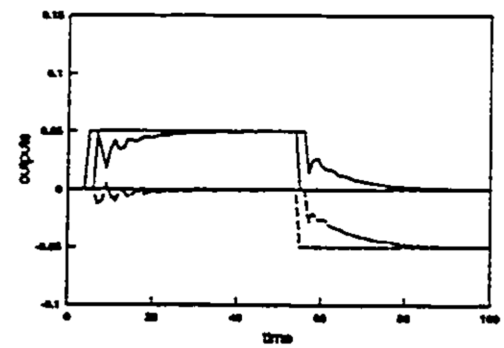

(a) Model 1 for the nominal process

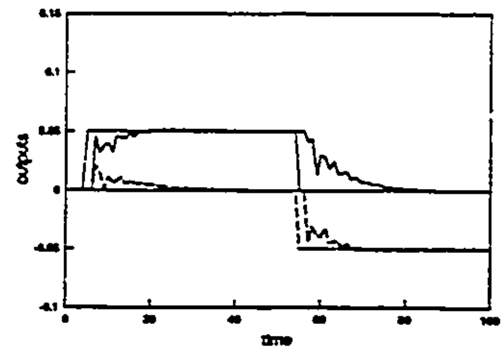

(b) Model 1 for the other process

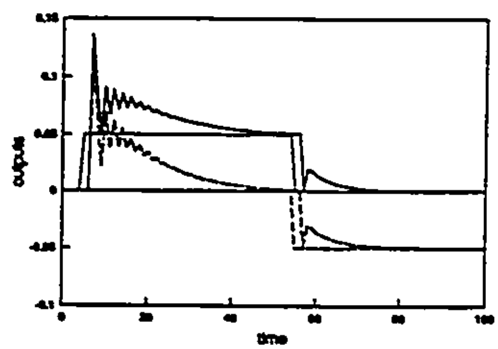

(c) Model 2 for the nominal process

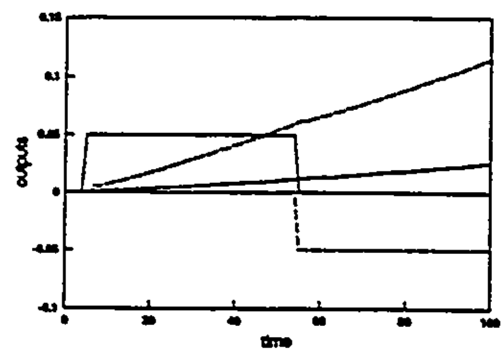

(d) Model 2 for the other process

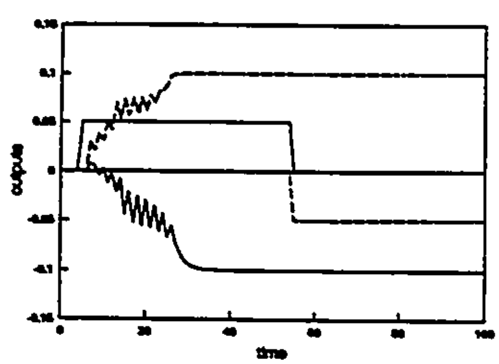

(e) Model 3 for the nominal process

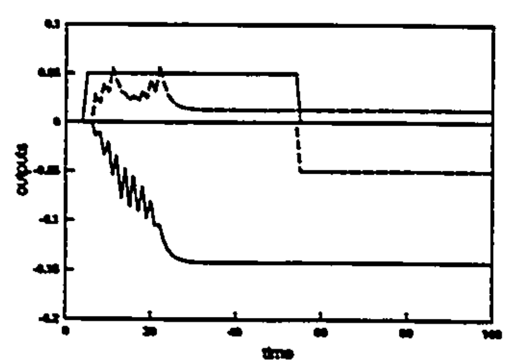

(f) Model 3 for the other process

Figure-2.1 Closed-loop responses using three identified models

This thesis is aimed at analyzing and explaining the behavior noted in these examples, and at developing methods for the design of experiments that will lead to robust models similar to Model 1 above.

2.2 Steady-State Mismatch Conditions

The IMC or Q-parameterization structure (Frank (1974), Zames (1981), Garcia and Morari (1982)) shown in Figure-2.2 is a useful one for robustness analysis.

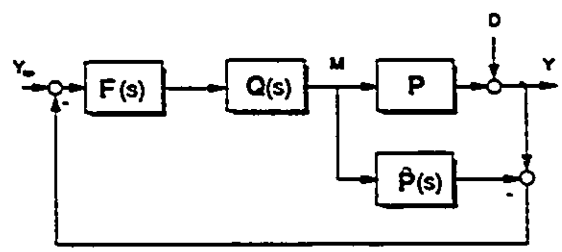

Figure-2.2 The IMC structure

The structure contains four major elements: a process block **P**, a model prediction block $\hat{\mathbf{P}}$ which in practice is obtained by an identification study, a controller block **Q** which is an approximate inverse of the identified model. Note that, for integral control action, the steady-state gain of **Q** must be the exact inverse of that of the identified model (ie. $\mathbf{Q}(0) = \hat{\mathbf{P}}^{-1}(0)$). Finally, a filter block **F** is added to ensure closed-loop stability in the presence of model mismatch.

The main objective of this study is to present methodology to analyze and identify linear models that lead to robust control. However, in general, robust control properties are determined not only by the identified model but also by the controller design. The only exception is where robustness properties involve only the steady-state conditions of a closed-loop system (Grosdidier, *et al* 1985), because the steady-state conditions are the same for all controller designs with integral action (ie. $\mathbf{Q}(0) = \hat{\mathbf{P}}^{-1}(0)$ and $\mathbf{F}(0) = \mathbf{I}$ in IMC structure). Since it is necessary that closed-loop robust stability and performance at zero frequency are ensured, we will focus on analyzing the effects of steady-state model mismatches. In the following, two steady-state mismatch conditions on this aspect are introduced.

2.2.1 Stabilizability Condition

Garcia and Morari (1985) have shown that a diagonal first-order exponential filter,

$$\mathbf{F}(s) = diag\left(\frac{1}{f_i s + 1}\right) \tag{2-3}$$

can always stabilize the approximate model inverse $\mathbf{Q}$ in the presence of model mismatch, if and only if

$$Re(\lambda_i(\mathbf{G}\hat{\mathbf{G}}^{-1})) > 0 \quad \forall i \tag{2-4}$$

where λ_i is the i-th eigenvalue of a matrix, $\mathbf{G} \equiv \mathbf{P}(0)$ and $\hat{\mathbf{G}} \equiv \hat{\mathbf{P}}(0)$ are the steady-state gain matrices of the true and identified processes respectively. This condition indicates that, as long as the steady-state gains of the true process and its model satisfy (2-4), a stable closed-loop system with no steady-state offset can be obtained in spite of the model mismatch simply by making f_i's sufficiently large. In this study, we will refer to a control system satisfying this condition as "stabilizable". If the stabilizability condition is violated, no multivariable control system would ever work regardless of how sophisticated the controller design and tuning. The uncontrollable examples as shown in Figure-2.1(d), (e) and (f) are exactly the consequences of violating the stabilizability condition.

Therefore, one of the necessary conditions for robust linear models in terms of closed-loop stability is that the stabilizability condition is satisfied. In Single Input Single Output (SISO) systems, the stabilizability condition simply corresponds to the well-known uncontrollable situation where a process and its model have opposite signs in their steady-state gains. On the other hand, for MIMO processes, this condition requires that all the eigenvalues of $\mathbf{G}\hat{\mathbf{G}}^{-1}$ lie in the *right* half of the complex plane. Then the answer is not clear at all for the question of how to identify a robust model for the stabilizability condition.

2.2.2 Performance Variation Condition

This study proposes a simple measure for assessing the effect of steady-state mismatches on changing the nominal closed-loop performance, which is particularly useful for the simple situation as given in the illustration example. Based on this measure, a necessary condition for robust linear models in terms of closed-loop performance will be derived in this section. Consider a servo control problem where a step change vector, ΔY_{sp}, is made in the set-points. Then the output step response of the true process and that based on the model prediction are as the following respectively

$$Y_{true}(s) = \mathrm{P}(s)\mathrm{Q}(s)[\mathrm{I} + (\mathrm{P}(s) - \hat{\mathrm{P}}(s))\mathrm{Q}(s)]^{-1}\frac{\Delta Y_{sp}}{s} \qquad (2-5.a)$$

$$Y_{model}(s) = \hat{\mathrm{P}}(s)\mathrm{Q}(s)\frac{\Delta Y_{sp}}{s} \qquad (2-5.b)$$

(2-5.a) is a straightforward result from the closed-loop transfer function between the set-points and the controlled outputs in terms of IMC structure, and (2-5.b) is obtained simply by taking $\mathrm{P}(s) = \hat{\mathrm{P}}(s)$ in (2-5.a). We may use the integral of the differences between the two step responses, Ψ, to quantify how much the closed-loop performance are changed due to the model mismatch

$$\Psi \overset{\Delta}{=} \int_0^{\infty} Y_{true}(t) - Y_{model}(t)dt \qquad (2-6.a)$$

$$= \lim_{s \to 0}\{\mathrm{P}(s)\mathrm{Q}(s)[\mathrm{I} + (\mathrm{P}(s) - \hat{\mathrm{P}}(s))\mathrm{Q}(s)]^{-1} - \hat{\mathrm{P}}(s)\mathrm{Q}(s)\}\frac{\Delta Y_{sp}}{s} \quad (2-6.b)$$

Similar usage of above time integral has been reported by Marlin *et al* (1986). A measure of performance variation is then defined as the ratio of the 2-norms of the Ψ vector to the ΔY_{sp} vector. In MIMO systems, such a measure will be a function of the direction of ΔY_{sp} vector. Suppose that the set-point changes are made in all directions. Then it is more meaningful to use the maximum ratio of all directions to asses the problem of performance variations, and it is equal to the maximum singular value (ie. the 2-norm of a matrix) of the following matrix

$$\underset{\substack{\text{directions}\\ \text{of } \Delta Y_{sp}}}{\text{Max}} \frac{\|\Psi\|_2}{\|\Delta Y_{sp}\|_2} = \left\| \lim_{s \to 0} \frac{1}{s} \{\mathbf{P}(s)\mathbf{Q}(s)[\mathbf{I} + (\mathbf{P}(s) - \hat{\mathbf{P}}(s))\mathbf{Q}(s)]^{-1} - \hat{\mathbf{P}}(s)\mathbf{Q}(s)\} \right\|_2 \quad (2-7.a)$$

$$= \left\| \frac{d}{ds} \{\mathbf{P}(s)\mathbf{Q}(s)[\mathbf{I} + (\mathbf{P}(s) - \hat{\mathbf{P}}(s))\mathbf{Q}(s)]^{-1} - \hat{\mathbf{P}}(s)\mathbf{Q}(s)\}_{s=0} \right\|_2 \quad (2-7.b)$$

The matrix of the RHS of (2-7.b) will be referred as the performance variation matrix. If the identified model were the true process the performance variation matrix and its 2-norm would be 0. When this matrix has a large 2-norm, we can definitely say that the control does not have robust performance. Therefore, it is a necessary condition for robust linear models to have the 2-norm of their performance variation matrices as small as possible.

Next we will assume the model mismatch is in the steady-state gains only and examine the relationship between such a mismatch and the 2-norm of the performance variation matrix. Under this assumption, the $\mathbf{P}$, $\hat{\mathbf{P}}$ and $\mathbf{Q}$ are related as the following

$$\mathbf{P}(s)\hat{\mathbf{P}}^{-1}(s) = \mathbf{G}\hat{\mathbf{G}}^{-1} \quad (2-8.a)$$

$$\mathbf{Q}(s) = \hat{\mathbf{P}}^{-1}(s)\mathbf{F}^{*}(s) \quad (2-8.b)$$

where $\mathbf{F}^{*}(s)$ is a lumped transfer function matrix to include all the controller design considerations such as removing unstable process zero, making the controller realizable and filter design (Garcia and Morari, 1985). Substituting (2-8) to (2-7.b) we obtain the following simple relationship

$$\text{Max} \frac{\|\Psi\|_2}{\|\Delta Y_{sp}\|_2} = \left\| (\mathbf{G}\hat{\mathbf{G}}^{-1}) \frac{d\mathbf{F}^{*}}{ds}\Big|_{s=0} (\hat{\mathbf{G}}\mathbf{G}^{-1}) - [2\mathbf{I} - (\hat{\mathbf{G}}\mathbf{G}^{-1})] \frac{d\mathbf{F}^{*}}{ds}\Big|_{s=0} \right\|_2 \quad (2-9)$$

From the above equation, we can clear see that the 2-norm of the performance variation matrix is affected by two factors: the controller design $d\mathbf{F}^{*}(s=0)/ds$ and the steady-state model mismatch ($\mathbf{G}\hat{\mathbf{G}}^{-1}$ and $\hat{\mathbf{G}}\mathbf{G}^{-1}$). For general controller designs where $d\mathbf{F}^{*}(s=0)/ds$ is a full matrix, it is still difficult to see explicitly how the steady-state model mismatch by itself affects the performance. Since the main concern of this study is on robust models rather than robust controller designs, we will fix the controller design matrix to be a scalar matrix (ie. $\mathbf{F}^*(s) = f^*(s)\mathbf{I}$) in order to simplify (2-9) further. Such a controller design approach is practical when the identified model has similar deadtimes in all transfer function elements and when a diagonal factorization of $\hat{\mathbf{P}}(s)$ to remove unstable zeros is acceptable (Garcia and Morari, 1985). If this is not the case, to force the $\mathbf{F}^*(s)$ to be a scalar can be a conservative design.

With the fixed controller design, $\mathbf{F}^*(s) = f^*(s)\mathbf{I}$, (2-9) is then reduced to its simplest form as the following

$$\mathrm{Max}\frac{\|\Psi\|_2}{\|\Gamma\|_2} = \left\| (\hat{\mathbf{G}}\mathbf{G}^{-1} - \mathbf{I})\frac{df^*}{ds}\Big|_{s=0} \right\|_2 \qquad (2-10)$$

Since the controller design $f^*(s)$ is a constant in terms of modelling, the necessary condition for robust linear models is obviously that the $\|\hat{\mathbf{G}}\mathbf{G}^{-1} - \mathbf{I}\|_2$ be minimized for not having large performance variations. If the steady-state mismatch $\|\hat{\mathbf{G}}\mathbf{G}^{-1}\|_2$ in one identified model is much larger than another one, the robust performances of control systems based on these two models will be very different, and this is exactly the cause for the very different performances as shown between Figure-2.1(a) and (c). However, remember that the LHS of (2-10) being small is only a necessary condition for robust performance, and thus $\|\hat{\mathbf{G}}\mathbf{G}^{-1} - \mathbf{I}\|_2$ is meaningful only when it is of a large value (ie. lack of robust performance). Under this situation $|\|\hat{\mathbf{G}}\mathbf{G}^{-1}\|_2 - 1|$ can be used to approximate the $\|\hat{\mathbf{G}}\mathbf{G}^{-1} - \mathbf{I}\|_2$. In conclusion, a criterion that is necessary for robust performance has been derived as follows

$$\|\hat{\mathbf{G}}\mathbf{G}^{-1}\|_2 \rightarrow 1 \qquad (2-11)$$

Eq.(2-11) can also be regarded as a loose condition for robust models and it will be referred to as the performance variation condition, and $\|\hat{\mathbf{G}}\mathbf{G}^{-1}\|_2$ is referred to as the performance variation measure.

For SISO systems, the necessary condition for robust linear models, which yield controllers with robust performance, simply requires the magnitudes of the true process gain and its model gain to be similar. Unfortunately, such a simple conclusion is not applicable to MIMO systems. More analysis is needed to determine what are the critical characteristics in multivariate mismatches that cause the performance variation condition to be violated.

3 Analysis and Synthesis of Robust Linear Models

Having established the steady-state model mismatch conditions for the two control problems as shown in the illustration example, this chapter investigates the robust model analysis problem of when a MIMO process can be controlled with a given model such that the mismatch conditions in (2-4) and (2-11) are satisfied, and the robust model synthesis problem of what constitutes a robust model and how to obtain one.

In order to provide a synthesis procedure, the results of the analysis method for robust models must be able to provide the answers for the question of what are the critical process characteristics that must be preserved in the modelling to ensure the robustness properties. For SISO systems, it was discussed in Chapter 2 that the answers to this question are straightforward. However, the solutions to SISO problems cannot be generalized to MIMO problems. For examples, the model in (2-2.b) has the correct signs in all gain elements and it does not yield a stabilizable controller design for controlling the process in (2-1.b). This model also has almost the correct magnitude in terms of the 2-norm of its gain matrix and it still has severe performance variations in controlling the process in (2-1.a).

Most of the past robustness studies focus on the analysis problem but few on synthesis problems. This chapter introduces two new approaches that cover both robust model analysis and synthesis for the two simple control problems as given in Chapter 2. The new approaches distinguish themselves from the traditional ones in that they analyze the effects of model mismatches rather than model uncertainties. The difference between a mismatch analysis and an uncertainty analysis is elaborated in the following.

3.1 Mismatch Condition vs. Uncertainty Condition

There are two strategies to solve the robust model analysis problem. The first one considers a specific pair of G (process) and $\hat{G}$ (model) to develop conditions on how this specific model mismatch affects the control stability and performance. Such conditions are referred in this thesis as "mismatch conditions". For example, (2-4) and (2-11) are *mismatch* conditions for the stabilizability and the performance variation problem discussed in Chapter 2. Mismatch conditions are very important in theoretical studies because from these conditions we can see how different mismatches affect the control robustness. Therefore mismatch conditions may provide useful insights into robust model synthesis problems.

Granted the fact that a true process is virtually never characterizable by one specific **G** over its range of operation, it is important to consider the group or set of all possible process **G**'s, and to develop conditions on how the collection of all mismatches (ie. defined as the uncertainties) affects the control stability and performance. Such conditions are referred in this thesis as "uncertainty conditions". It is extremely important to recognize that uncertainty conditions do not provide us any information on the effects of individual mismatches. In other words, one should not check the robustness properties of a specific mismatch using the uncertainty conditions.

Most of the past robustness studies analyze the effects of model uncertainties rather than model mismatches. The most powerful and general analysis tool up to date is based on characterizing the multivariate model uncertainties by a matrix norm (in particular, the 2-norm), and develops uncertainty conditions in terms of the upper bound of an uncertainty matrix norm such that the robustness properties can be ensured. This norm-bounded approach shall be further divided as unstructured and structured approaches (Doyle and Stein (1981), Doyle (1982)). The former describes the MIMO uncertainties using a single matrix (ie. single source of uncertainties) while the latter uses multiple matrices (ie. multiple sources of uncertainties) (Figure-3.1).

The critical assumption behind the uncertainty conditions derived from both norm-bounded approaches is that all the mismatches within either Δ in Figure-3.1(a) or Δ_j in Figure-3.1(b) *must* exist. One major drawback of the norm-bounded approaches is exactly this very assumption, because not many true model uncertainties in real processes can be

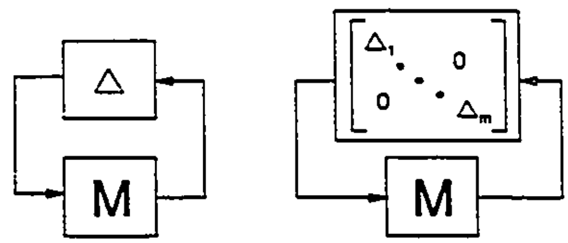

(a) unstructured (b) structured

Figure-3.1 Norm-bounded descriptions of model uncertainties

modelled as such. The other major deficiency in the uncertainty conditions is that no synthesis insight can be obtained, because the model uncertainties are modelled with a fixed structure. To better illustrate the latter argument, the particular applications of the norm-bounded approaches to the stabilizability condition (2-4) will be discussed in more details later in this chapter.

The main purpose of this chapter is to introduce two new analysis approaches that yield mismatch instead of uncertainty conditions for the stabilizability and performance variation problem. The geometric approach is applied to 2×2 systems only. Nevertheless, owing to this small dimension, this approach can provide mismatch conditions in terms of geometric differences between the true process and its model, which are applicable to arbitrary forms of mismatch. The second approach is based on mismatches in the singular values decomposition matrices of the model gain matrix and is applicable to high-dimensional systems. However, the latter approach imposes several restrictions on the model mismatches which make it more appropriate for the robust model synthesis than analysis.

3.2 Norm-Bounded Approaches

In this section, the stabilizability condition will be taken as an example to demonstrate how the well-developed, norm-bounded uncertainty approaches are used as an analysis tool. It will then be evident why we need alternative approaches for the robust model synthesis problem.

3.2.1 Unstructured Uncertainty Analysis

The unstructured, norm-bounded uncertainty approach describes the mismatch between $\mathbf{G}$ and $\hat{\mathbf{G}}$ in one of the following three ways

$$\mathbf{G} = \hat{\mathbf{G}} + \mathbf{L}_A \qquad (3-1.a)$$

$$\mathbf{G} = \hat{\mathbf{G}}(\mathbf{I} + \mathbf{L}_I) \qquad (3-1.b)$$

$$\mathbf{G} = (\mathbf{I} + \mathbf{L}_O)\hat{\mathbf{G}} \qquad (3-1.c)$$

The $\mathbf{L}_A$, $\mathbf{L}_I$, and $\mathbf{L}_O$ are referred as the additive, multiplicative input and multiplicative output mismatch matrices at steady state, respectively (Morari and Zafiriou, 1989). Then by specifying a magnitude of any of the above mismatch matrices (ie. a convenient matrix norm), this approach provides the most general description of multivariate model mismatches. A theorem which relates the 2-norm of an additive matrix perturbation with the eigenvalue variation is given as the following (Stewart, 1973)

<u>Theorem 1</u>

Let $\mathbf{A}$ be a $n \times n$ matrix and Γ be a non-singular matrix formed by the eigenvectors of $\mathbf{A}$. Let λ_i be the i-th eigenvalue of $\mathbf{A}$. Then, for any $n \times n$ matrix $\mathbf{E}$, the eigenvalues of $\mathbf{A} + \mathbf{E}$ lie in the union of the disks

$$\Omega_i = \{\lambda : |\lambda - \lambda_i| \le \|\Gamma\|_2 \|\Gamma^{-1}\|_2 \|\mathbf{E}\|_2\} \qquad (3-2)$$

To apply this theorem to the stabilizability problem, A should be replaced by $\hat{G}\hat{G}^{-1}$ (ie. the identity matrix) and A + E by $G\hat{G}^{-1}$. Then Γ is also an identity matrix and $\lambda_i = 1$ for all i, and therefore the eigenvalues of $G\hat{G}^{-1}$ must lie within the disk defined by

$$|\lambda - 1| \;\le\; 1 \cdot \| G\hat{G}^{-1} - I \|_2 = \| L_O \|_2 \qquad (3-3.a)$$

$$= \| (G - \hat{G})\hat{G}^{-1} \|_2$$

$$\le \| G - \hat{G} \|_2 \cdot \| \hat{G}^{-1} \|_2 = \| L_A \|_2 \cdot \frac{1}{\underline{\sigma}(\hat{G})} \qquad (3-3.b)$$

$$= \frac{\| L_A \|_2}{\| \hat{G} \|_2} \cdot \frac{\| \hat{G} \|_2}{\underline{\sigma}(\hat{G})} = \frac{\| L_A \|_2}{\| \hat{G} \|_2} \cdot \hat{\kappa} \qquad (3-3.c)$$

where $\hat{\kappa}$ is the condition number of the model gain matrix

Therefore if the norm of the multiplicative *output* mismatch in (3-3.a) is smaller than 1, or that of the additive mismatch in (3-3.b) is smaller than the minimum singular value of $\hat{G}$, the radius of the disk centered at (1,0) will be smaller than 1 and all the eigenvalues of $G\hat{G}^{-1}$ will satisfy the stabilizability condition. From (3-3.c) we also see that the relative magnitude of the additive mismatch to the nominal process should be smaller than the inverse of the condition number. This result explains the fact that an ill-conditioned process with a large condition number may be very sensitive to some model mismatches.

To obtain the upper limit of multiplicative *input* mismatch, we should substitute A + E by $\hat{G}^{-1}G$ and locate the boundaries of the eigenvalues of $\hat{G}^{-1}G$ as following

$$|\lambda - 1| \;\le\; 1 \cdot \| \hat{G}^{-1}G - I \|_2 = \| L_I \|_2 \qquad (3-4)$$

Since $\hat{G}^{-1}G$ can be obtained from $G\hat{G}^{-1}$ via a similarity transformation as following

$$\hat{G}^{-1}G = \hat{G}^{-1}(G\hat{G}^{-1})\hat{G} \qquad (3-5)$$

and since two matrices related with a similarity transformation have the same eigenvalues (Stewart, 1973), we can see that if the norm of the multiplicative input mismatch is smaller than 1 the eigenvalues of $G\hat{G}^{-1}$ will also satisfy the stabilizability condition.

So far the mismatch conditions have been established in terms of the norm bounds on different mismatch matrices,

$$\|\mathbf{L}_A\|_2 < \underline{\sigma}(\hat{\mathbf{G}}) \tag{3-6.a}$$

$$\|\mathbf{L}_I\|_2 < 1 \tag{3-6.b}$$

$$\|\mathbf{L}_O\|_2 < 1 \tag{3-6.c}$$

and these conditions are only *sufficient* for the stabilizability condition (2-4) to be true for any specific mismatch. To transform the above mismatch conditions into uncertainty conditions, Morari and Zafiriou (1989) used the unstructured, norm-bounded uncertainty assumption (Doyle and Stein, 1981).

$$\mathbf{L}_A \stackrel{\Delta}{=} l_A\Delta_A\,,\ \ \|\Delta_A\|_2 \le 1 \tag{3-7.a}$$

$$\mathbf{L}_I \stackrel{\Delta}{=} l_I\Delta_I\,,\ \ \|\Delta_I\|_2 \le 1 \tag{3-7.b}$$

$$\mathbf{L}_O \stackrel{\Delta}{=} l_O\Delta_O\,,\ \ \|\Delta_O\|_2 \le 1 \tag{3-7.c}$$

and derived exactly the same upper bounds for the three types of steady-state model uncertainties as follows:

$$l_A < \underline{\sigma}(\hat{\mathbf{G}}) \tag{3-8.a}$$

$$l_I < 1 \tag{3-8.b}$$

$$l_O < 1 \tag{3-8.c}$$

However, the above uncertainty conditions are both necessary and sufficient for the stabilizability (given the assumption that all mismatches in (3-7) are possible).

The unstructured, norm-bounded assumption of model uncertainties, which assumes that all possible members of **G** satisfying the norm bound must exist, is rarely justifiable in practice. In particular, for mechanistic model uncertainties such as those arising from process nonlinearities, the locally linearized processes almost always consist of only a very limited subset of **G**'s within the norm bound. Geometrically, given a norm bound, the unstructured norm-bounded uncertainty assumption yields a symmetrical disk of centered at (1,0) in the complex plane for the distribution of the eigenvalues of $G\hat{G}^{-1}$ (Figure-3.2(a)), while an asymmetrical distribution may be a result of a subset of G's and therefore may never across the imaginary axis regardless of the enormous magnitude of uncertainties (Figure-3.2(b)).

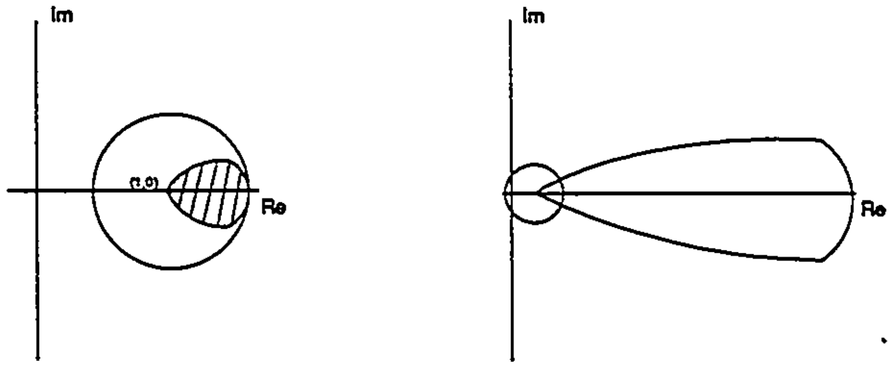

(a) (b)

(a) A subset (shaded area) vs. all (disk area) of G's given a bounded norm, (b) Unstructured (small) vs. structured (large) mismatch of very different magnitudes

Figure-3.2 Eigenvalue Distribution of $G\hat{G}^{-1}$

3.2.2 Structured Uncertainty Analysis

Characterizing the mismatch between G and $\hat{G}$ only by the norm of any of the mismatch matrices in (3-1) allows for the stabilizability condition be analyzed in a very general context, but it only yields sufficient condition for general model mismatches. For specific model mismatches we often have additional information other than its magnitude, and it is wasteful that we ignore this information and still analyze the problem using unstructured uncertainty approach. In the following, analysis results using the structured norm-bounded approach on the same stabilizability problem will be summarized for two situations, namely, structured uncertainties which arise from process nonlinearities and from identification errors.

3.2.2.1 Nonlinearity Effects

Model uncertainties due to process nonlinearities is definitely structured and it is impossible to have general descriptions for these structured uncertainties. In addition, even for a particular nonlinear process, to describe the true structured uncertainties can be so complicated that we have to rely on numerical or graphical descriptions such as the multivariable Nyquist plots used by McDonald *et al* (1988). However, there are still large classes of nonlinear processes whose structured uncertainties can be closely characterized using a structured, norm-bound description. For example, the structured uncertainties in high-purity binary distillation columns can be described by the following: (Skogestad and Morari, 1987)

$$\mathbf{G}-\bar{\mathbf{G}}=\begin{bmatrix} l_a\Delta & -l_a\Delta \\ -l_a\Delta & l_a\Delta \end{bmatrix} \qquad (3-9)$$

It can be derived from the structured, norm-bounded uncertainties theories that the structured uncertainties in (3-9), regardless of the magnitudes, will never make a controller based on the true nominal model unstabilizable (Morari and Zafiriou, 1989).

The structured norm-bounded approach does provide correct analysis on the fact that a linear controller designed for the true nominal process is able to control the nonlinear process over a wide region where the structured uncertainties defined in (3-9) hold. However, it does not provide us with any insight into the question whether there exist some process characteristics that are preserved despite the nonlinearity effects and which contribute to the controller robustness. As a result, we do not know which process characteristics are critical in robust model synthesis.

3.2.2.2 Identification Errors

Morari and Zafiriou (1989) also derived a sufficient condition for an identified model to have the stabilizability property (2-4). Under the structured uncertainty assumption that the uncertainties in the gain elements are independent, the stabilizability of an identified model in 2×2 systems is ensured if

$$\bar{r}_{max} < \frac{1}{\kappa^*(\hat{G})} \qquad (3-10)$$

where κ^* is the minimized conditioned number over all possible scaling of the input/output variables, and $\bar{r}_{max}$ is the maximum of the multiplicative mismatch bounds. It will be shown later in Chapter 5 that the magnitude bound with 95 percent confidence for the additive uncertainty of the kj-th gain element should be specified as

$$\bar{l}_{kj} = \frac{\sigma_{e_k}}{\sqrt{\sum_{i=1}^{n} m_{ji}^2}} \quad \forall k \qquad (3-11)$$

where $\bar{l}_{kj}$ is the upper bound of l_{kj}, ie. $l_{kj} = \bar{l}_{kj} \cdot \Delta$ and $|\Delta| < 1$, and m_{ji} is the value of the j-th manipulated variable for the i-th experiment. Then it is trivial to combine (3-10) and (3-11) to yield the magnitude bound for stabilizability

$$\bar{l}_e = \frac{\sigma_e}{\sqrt{n}} < \frac{g_{min}}{\kappa^*(\hat{G})} \qquad (3-12)$$

in which g_{min} is the minimum magnitude of the estimated gain element and it is assumed that the output variances are the same (ie. σ_e^2) and all input variables are coded between 1 and -1. Therefore we can see that the high-sensitivity of identified models of ill-conditioned processes arises from the fact that a large condition number requires a very small noise level and/or very large number of experiments to satisfy (3-12).

Similar to the situation discussed under nonlinearity effects, the structured norm-bounded approach is useful in analyzing the robustness of an identified model given a fixed structure for the uncertainties (ie. independent uncertainties among the gain elements). Fixing the uncertainty structure a priori certainly will not yield any insight into the possibility that there may exist another uncertainty structure which makes the identified model more robust. With respect to the robust model identification problem, the only usable information from the structured norm-bounded analysis result given in (3-12) is on the minimum number of experiments that is sufficient to reduce the uncertainty magnitude.

3.3 Geometric Approach for 2×2 Systems

A new geometric approach for the analysis and synthesis of robust models in 2×2 systems is introduced in this section. First, geometric characterizations of a gain matrix and the mismatch are introduced. Then the steady-state mismatch conditions are re-derived in terms of the geometric characteristics. The analysis on the resulting expressions will disclose a critical geometric characteristic of 2×2 processes that has the biggest impact on the robustness of multivariable control. Two applications of the geometric approach are given in this section. The first application is to analyze the robustness properties of multiloop SISO control and the second one is to develop a simple criterion for robust model synthesis.

3.3.1 Geometric Interpretations for Model Mismatches

A gain matrix can be interpreted geometrically in r-dimensional space as a set of the column vectors. These column vectors are often called the gain vectors of individual inputs. The components of a gain vector are the values of the process output changes due to an unit change of a specific input alone. For a model gain matrix of 2×2 systems, we can use polar coordinates to describe its two gain vectors by their lengths and angles with respect to the output coordinate axes (Figure-3.3(a)) and have the following expression:

$$\hat{\mathbf{G}}=\begin{bmatrix}\hat{l}_1\cos\hat{\alpha}_1 & \hat{l}_2\cos\hat{\alpha}_2\\ \hat{l}_1\sin\hat{\alpha}_1 & \hat{l}_2\sin\hat{\alpha}_2\end{bmatrix} \qquad (3-13)$$

where $\hat{l}_j$ and $\hat{\alpha}_j$ are the length and the angle of gain vector $\hat{G}_j$.

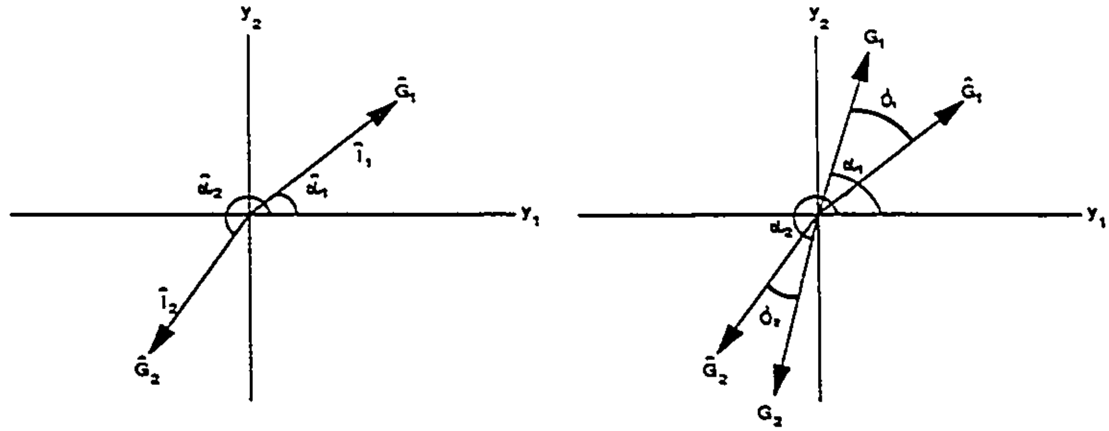

(a) (b)

Figure-3.3 Geometric interpretations of model mismatch

Based on the geometric expression in (3-13), model mismatches in a 2×2 gain matrix can be specified as mismatches in the vector lengths and/or angles. Therefore the true gain matrix can be expressed as:

$$\mathbf{G}=\begin{bmatrix} l_1\cos\alpha_1 & l_2\cos\alpha_2 \\ l_1\sin\alpha_1 & l_2\sin\alpha_2 \end{bmatrix}=\begin{bmatrix} n_1\hat{l}_1\cos(\hat{\alpha}_1+\delta_1) & n_2\hat{l}_2\cos(\hat{\alpha}_2+\delta_2) \\ n_1\hat{l}_1\sin(\hat{\alpha}_1+\delta_1) & n_2\hat{l}_2\sin(\hat{\alpha}_2+\delta_2) \end{bmatrix} \qquad (3-14)$$

and $n_j \geq 0$, $|\delta_j| \leq \pi$ for $j = 1,2$

where n_j is the multiplicative error in the length and δ_j is the additive error in the angle of the j-th process gain vector with respect to the model gain vector (Figure-3.3(b)).

3.3.2 Geometric Mismatch Conditions

In this section, the relationship between the geometric mismatches and the steady-state mismatch conditions in (2-4) and (2-11) will be derived. This objective is accomplished by: 1) substituting the geometric expressions of the true and model gain matrices as in (3-14) and (3-13) to reformulate $\mathbf{G}\hat{\mathbf{G}}^{-1}$ and $\hat{\mathbf{G}}\mathbf{G}^{-1}$ (see Appendix-1 for their final expressions), and 2) examining how the mismatches in the vector lengths and angles affect the eigenvalues of $\mathbf{G}\hat{\mathbf{G}}^{-1}$ as well as the 2-norm of $\hat{\mathbf{G}}\mathbf{G}^{-1}$.

Consider first the performance variation problem. Since the 2-norm and Euclidian norm of any 2×2 matrix have the following rank of magnitudes (Stewart(1973)):

$$\|\hat{G}G^{-1}\|_2 \le \|\hat{G}G^{-1}\|_E \le \frac{1}{\sqrt{2}}\|\hat{G}G^{-1}\|_2 \qquad (3-15)$$

the effects of model mismatches on changing either matrix norm are almost the same, and thus we can investigate the performance variation problem in 2×2 systems using the Euclidian norm instead. The Euclidian norm of $\hat{G}G^{-1}$ can be derived as the following:

$$\|\hat{G}G^{-1}\|_E = \frac{1}{|\sin\beta|}[\hat{n}_1^2 - 2\hat{n}_1\hat{n}_2\cos\beta\cos(\beta-\hat{\delta}_1+\hat{\delta}_2)+\hat{n}_2^2]^{\frac{1}{2}} \qquad (3-16)$$

where $\beta=\alpha_2-\alpha_1$, $\hat{n}_j=\frac{\hat{l}_j}{l_j}=\frac{1}{n_j}$ and $\hat{\delta}_j=\hat{\alpha}_j-\alpha_j=-\delta_j$

(3-16) clearly shows that the performance variation problem is determined by one true process characteristic β which is a measure of collinearity of the process gain vectors and, of course, the four mismatch terms ($\hat{n}_1$, $\hat{n}_2$, $\hat{\delta}_1$, and $\hat{\delta}_2$).

An important implication from (3-16) is that processes with $|\sin\beta|$ close to zero (ie. two gain vectors are nearly collinear) will have their multivariable controllers that are very sensitive to model uncertainties in terms of large performance variation, while processes with $|\sin\beta|$ equal to 1 (ie. two gain vectors are orthogonal) will be much less sensitive to the same ranges of model mismatches. Therefore, we shall conclude that the angle between the two gain vectors of the true process is one critical characteristic for robust performance of any multivariable control scheme. More details on the above two extreme situations will be covered in the discussions of multiloop SISO control.

As to the stabilizability condition, for 2×2 systems the two eigenvalues have positive real parts if and only if both the determinant and trace of $\mathbf{G}\hat{\mathbf{G}}^{-1}$ are positive. Therefore it is useful to derive some geometric conditions that determine their signs. The determinant and trace of $\mathbf{G}\hat{\mathbf{G}}^{-1}$ can be derived as below:

$$det(\mathbf{G}\hat{\mathbf{G}}^{-1}) = \lambda_1 \cdot \lambda_2 = n_1 n_2 \frac{\sin(\hat{\beta} + \delta_1 - \delta_2)}{\sin \hat{\beta}} \qquad (3-17.a)$$

$$tr(\mathbf{G}\hat{\mathbf{G}}^{-1}) = \lambda_1 + \lambda_2 = \frac{[n_1 \sin(\hat{\beta} + \delta_1) + n_2 \sin(\hat{\beta} - \delta_2)]}{\sin \hat{\beta}} \qquad (3-17.b)$$

Note that the eigenvalues of $\mathbf{G}\hat{\mathbf{G}}^{-1}$ are determined by the collinearity measure of the identified model rather than that of the true process (ie. $\hat{\beta}$ vs. β).

According to (3-14) the true process gain vectors (G_1, G_2) are interpreted as a result of the model gain vectors ($\hat{G}_1$, $\hat{G}_2$) being rotated and lengthened/shortened. Consider these rotations and length changes in two steps in which one gain vector is changed at a time. At each step, the fixed gain vector divides the space into two half planes. The following theorem is based on the half planes and its proof is given in Appendix-2:

<u>Theorem 2</u>

Define the *nominal half plane* as the half plane in which the model gain vector to be changed is located (Figure-3.4(a)). Suppose that the gain vectors of a 2×2 process are obtained by changing the nominal vectors in two steps where only one vector is changed at a time, then $det(\mathbf{G}\hat{\mathbf{G}}^{-1}) > 0$ if and only if the process and nominal gain vectors:

1) remain in their nominal half planes in both steps, or

2) are on the other side of their nominal half planes in both steps (Figure-3.4(b)).

As for the trace, since the RHS of (3-17.b) has additive terms, it is impossible to derive a general and simple geometric criterion which is both necessary and sufficient for the trace to be positive. However, some general sufficient conditions are obvious. The following geometric condition has been derived in Appendix-2:

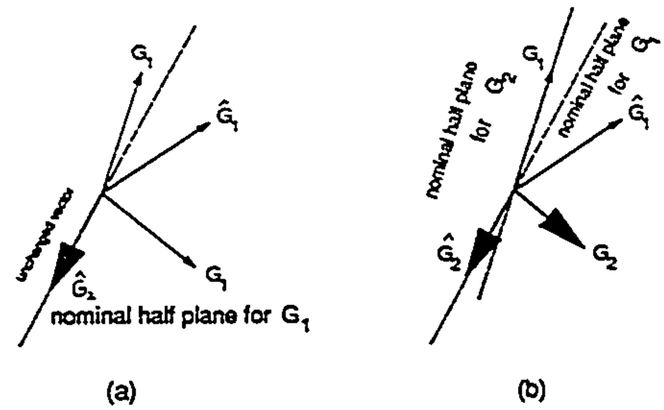

Figure-3.4 Nominal half plane mismatch conditions for $det(G\hat{G}^{-1})$

<u>Theorem 3</u>

Define an *original half plane* as the half plane, divided by one model gain vector, in which the other model gain vector is located (Figure-3.5). $tr(G\hat{G}^{-1})$ is

1) positive if both true gain vectors remain on their original half planes (Figure-3.5(a)),

2) negative if both true gain vectors are outside their original half planes (Figure-3.5(b)).

There is no general geometric condition to determine the sign of the trace, if one true gain vector is outside while the other is inside its original half plane.

All the geometric conditions given in Theorem 2 and 3 are based on setting boundaries to the angle mismatches of gain vector (ie. the half planes). It can be easily deducted from these two theorems that if there is no angle mismatch at all, both the trace and determinant of $G\hat{G}^{-1}$ must be positive and therefore the system is stabilizable. When there is no angle mismatch, the angle between the gain vectors of the true process (β) is preserved in the modelling, and this result once again stress the importance of β in affecting the robustness of multivariable control.

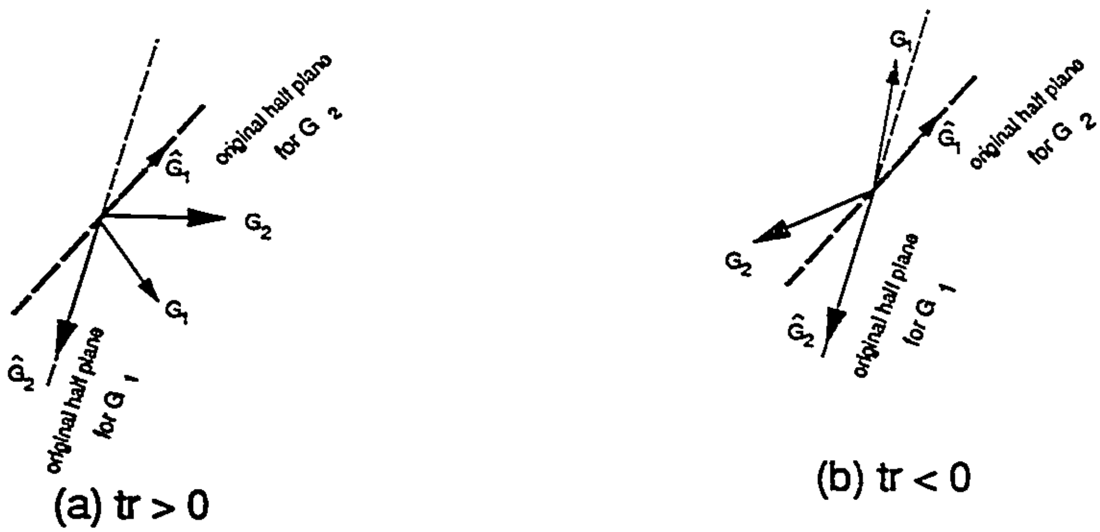

Figure-3.5 Original half plane conditions for $tr(G\hat{G}^{-1})$

A simple application of the above theorems is to analyze the sensitivity of the ill-conditioned models with nearly collinear gain vectors. Under this situation, the dividing lines of either the original half planes or the nominal half plane in the first step will almost overlap the two gain vectors. Therefore, small uncertainties in the angles can make the model violate the stabilizability condition.

3.3.3 Robustness of Multiloop SISO Control

MIMO processes are often controlled with multiloop SISO controllers. To use SISO controllers for MIMO control, one has to make the decision on pairing the input/output variables and then design each SISO controller based on a SISO model (implicitly or explicitly) for every input and output pair. The biggest problem in SISO control of MIMO processes is the interactions among the control loops, which usually deteriorate the originally well-tuned single loop performance of the individual input/output pair or even cause instability when all the loops are closed. In this section, the closed-loop performance and stability of multiloop SISO control will be treated from the viewpoint of MIMO model mismatch for the simplest situation of gain mismatch only. Multiloop SISO control is based on a diagonal model because all the interactions among the pairing (ie. off-diagonal elements) are not considered, and therefore has an inherent model mismatch for most of MIMO processes. More general analysis on the robustness of multiloop SISO control have been reported by Skogestad and Morari (1989) using the structured norm-bounded approach.

In 2×2 systems, a diagonal model gain matrix has two gain vectors aligned with the axes of two outputs and therefore they are perpendicular to each other (Figure-3.6). Depending on which input is assigned to the vector aligned with y_1 axis, the paring of SISO control can be determined geometrically. Two examples of pairing are given in Figure-3.6. In the following, the earlier geometric sensitivity analysis will be applied to derive some special robustness properties of multiloop SISO control.

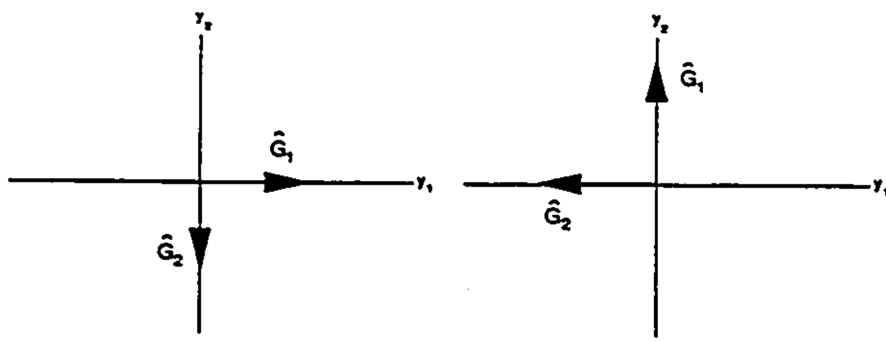

(a) y_1 - m_1 pairing (D1 model)

(b) y_1 - m_2 pairing (D2 model)

Figure-3.6 Geometric Representation of Pairing in SISO Control

3.3.3.1 The Performance Variation

For 2×2 systems, we may classify a process according to the angle between the two gain vectors (ie. $\beta=\alpha_2-\alpha_1$). Two extreme cases are the gain vectors being orthogonal ($\sin(\beta)=\pm1$) and nearly collinear ($\sin(\beta)\doteq0$) (Figure-3.7), which are referred as an orthogonal and a collinear process, respectively.

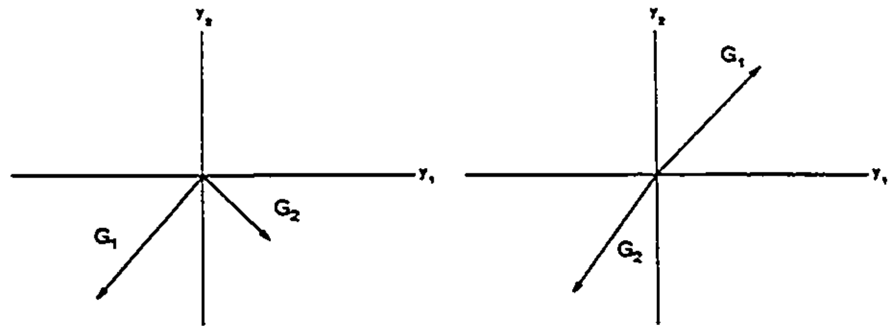

(a) Orthogonal process (b) Collinear process

Figure-3.7 Orthogonal and collinear processes

For orthogonal processes, by substituting $\beta=\pi/2$ into (3-16), the performance variation measure is reduced to:

$$\|\hat{G}G^{-1}\|_E=(\hat{n}_1^2+\hat{n}_2^2)^{\frac{1}{2}} \qquad (3-18)$$

which indicates that the performance variation measure in SISO control is affected by the mismatches in gain vector lengths only. Therefore, despite the large angle mismatches introduced by using a diagonal model for controller design, multiloop SISO control of orthogonal processes can meet the performance variation condition as given in (2-11) as long as the vector length mismatches are mild (ie. $\hat{n}_1$ and $\hat{n}_2$ are close to 1). Therefore we conclude the following property of performance variations using SISO control:

Property 1

For 2×2 orthogonal processes, closed-loop step responses of multiloop SISO control schemes usually have small performance variation measures defined in (2-11).

However, remember that a small $\|\hat{G}G^{-1}\|_E$ or $\|\hat{G}G^{-1}\|_2$ is only a necessary condition for robust performance. Closed-loop systems can have severe performance variations in a fashion that a set-point change response is very oscillatory but still yield a small integral as given in (2-6.a). It will be discussed later that multiloop SISO control of non-diagonal, orthogonal processes always have more oscillatory responses than the situation where only one loop is closed.

On the other hand, collinear processes have their $\sin\beta$ close to 0 and therefore the $\|\hat{G}G^{-1}\|_E$ in (3-16) in this situation can be asymptotically reduced to:

$$\|\hat{G}G^{-1}\|_E=\frac{1}{|\sin\beta|}(\hat{n}_1^2-2\hat{n}_1\hat{n}_2\cos(\hat{\delta}_1-\hat{\delta}_2)+\hat{n}_2^2)^{\frac{1}{2}} \tag{3-19}$$

Since the denominator is small, the performance variation measure is small only if the numerator is also small. However, it can be easily shown geometrically that the angle mismatches between a collinear process and a diagonal model must be close to the following:

$$|\hat{\delta}_1-\hat{\delta}_2| \doteq \frac{\pi}{2} \tag{3-20}$$

and therefore (3-19) becomes

$$\|\hat{G}G^{-1}\|_E \doteq \frac{1}{\sin\beta}(\hat{n}_1^2+\hat{n}_2^2)^{\frac{1}{2}} \tag{3-21}$$

Hence, the performance variation measure must be large for SISO control of collinear processes, unless the gain vector lengths are deliberately underestimated in controller design (ie. $\hat{n}_1 \doteq \hat{n}_2 \doteq 0$). However, the latter design may create stability problems and shall not be considered. In summary, another property of performance variations using SISO control can be concluded below:

<u>Property 2</u>

For 2×2 collinear processes, multiloop SISO control usually has large performance variations.

3.3.3.2 Stabilizability

Substituting $\beta = \frac{\pi}{2}$ into (3-17), the determinant and trace of $G\hat{G}^{-1}$ reduce to

$$det(G\hat{G}^{-1}) = n_1 n_2 \cos(\delta_1 - \delta_2) > 0 \ \text{ iff } \ |\delta_1 - \delta_2| < \frac{\pi}{2} \qquad (3-22.a)$$

$$tr(G\hat{G}^{-1}) = n_1 \cos\delta_1 + n_2 \cos\delta_2 > 0 \ \text{ if } \ |\delta_1| < \frac{\pi}{2}, |\delta_2| < \frac{\pi}{2} \qquad (3-22.b)$$

It is apparent from Figure-3.6 that whenever the angle mismatch in either gain vector exceeds the magnitude of $\frac{\pi}{2}$, the diagonal model has at least one diagonal element with incorrect sign. Hence a sufficient condition for the trace to be positive in (3-22.b) is simply that the diagonal model gain matrix has all the signs correct. When this sufficient condition is met and multiloop SISO control is applied to processes with *orthogonal* gain vectors (Figure-3.7(a)), the necessary and sufficient condition for the determinant to be positive in (3-22.a) is satisfied simultaneously. Therefore we have the following property:

Property 3

For 2×2 orthogonal processes, multiloop SISO control is always stabilizable if the signs of steady-state model gains in both input/output pairs are correct. Model mismatches due to neglecting the off-diagonal elements (ie. interactions) of the true process are not relevant to the stabilizability problem.

On the other hand, for collinear processes, the same sufficient condition for the trace to be positive is not sufficient to yield a positive determinant in (3-22.a). Consider the example in Figure-3.8(a) below. The diagonal model D1 in Figure-3.6(a) has correct signs with respect to both process P1 and P2. However, a simple application of Theorem 2 indicates that D1 cannot be used to control P2. Therefore we have the following property in terms of MIMO model mismatch.

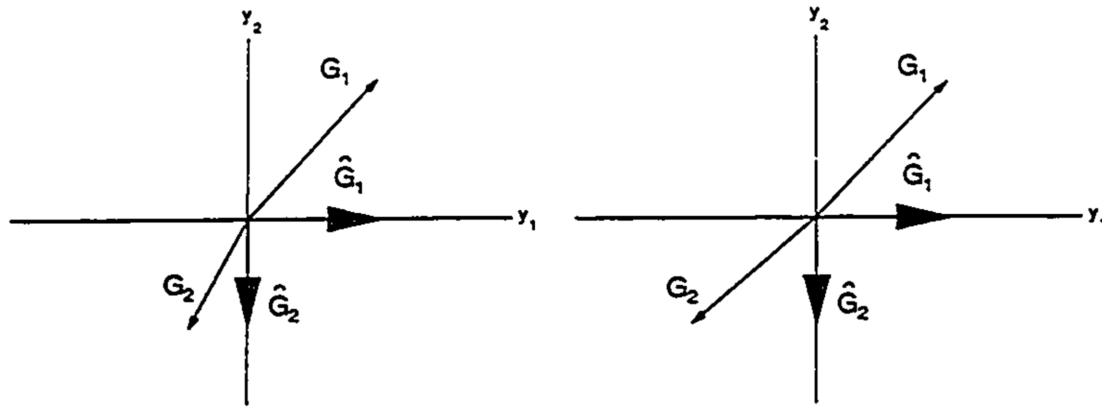

(a) P1 process (b) P2 process

Figure-3.8 Two different collinear processes

Property 4

For 2×2 collinear processes, multiloop SISO control can be unstabilizable even when the signs of steady-state model gains in both input/output pairs are correct. Model mismatches due to neglecting the off-diagonal elements (ie. interactions) of the true process may well cause the stabilizability problem.

Using the same geometric theorems, it can be easily shown that the correct diagonal model for P2 should be similar to D2 as shown in Figure-3.6(b). Note that the major difference between D1 and D2 is that the pairing is changed. Therefore the geometric conditions in Theorem 2 and 3 for the stabilizability of MIMO systems can also be applied as a pairing criterion for SISO control. Relative Gain Array (RGA, Bristol(1966)) is a much better known and more general pairing criterion derived from the viewpoint of "interactions" among SISO loops. According to RGA theories, y_1 must not be paired with m_2 if and only if the corresponding RGA element is negative. Therefore, pairing of input/output variables with negative RGA elements is equivalent to designing multivariable controllers based on a severely mismatched model which does not satisfy the stabilizability condition. More on the relationship between the signs of RGA elements and the stabilizability of general multivariable control will be discussed in the following.

3.3.4 The Signs of RGA Elements and the Stabilizability

RGA is the most widely used interaction measure. For any input/output pair $(y_k - m_j)$, the relative gain γ_{kj} is defined as the ratio of the open-loop steady-state gain between y_k and m_j to its "effective" steady-state gain, in which all other loops with integral action are closed, ie.

$$\gamma_{kj} \stackrel{\Delta}{=} \frac{(\partial y_k/\partial m_j)_{\text{open loop}}}{(\partial y_k/\partial m_j)_{\text{all other loops closed}}} \tag{3-23}$$

Therefore if the γ_{kj} is larger than 1, the steady-state gain between y_k and m_j is reduced by closing all the other loops and therefore multiloop control is more sluggish than single loop control. If γ_{kj} is small than 1 and positive, multiloop control will be more oscillatory than single loop control because the effective gain is increased. Finally, if γ_{kj} is negative, the process gain changes sign when all the other loops are closed and this has been discussed earlier as an unstabilizable situation. Past research work that uses the RGA to infer closed-loop robustness properties includes Skogestad and Morari (1987), Yu and Luyben (1987).

Using the polar coordinate representation in (3-13), it can be easily shown that for 2×2 systems the 1-1 element of the RGA is as follows (Koung and Harris (1989)):

$$\gamma_{11} \stackrel{\Delta}{=} 1 + (1 - \frac{g_{12}g_{21}}{g_{11}g_{22}}) = 1 + \left(1 - \frac{\tan\alpha_1}{\tan\alpha_2}\right) \tag{3-24.a}$$

$$= \frac{\cos\alpha_1 \sin\alpha_2}{\sin\beta} \tag{3-24.b}$$

Note that the collinearity measure $\sin\beta$ again appears in the denominator of (3-24.b) which implies that the identification of RGA can be very sensitive to the mismatches in the gain vector angles for collinear processes. On the other hand, for orthogonal processes this sensitivity does not exist (ie. $\sin(\beta) = \sin(\alpha_2 - \alpha_1) = 1$). The geometric properties of RGA for 2×2 processes can be summarized below:

Property 5

For 2×2 systems, RGA is a function of gain vector angles only. Orthogonal processes always have their γ_{11}'s within a range from 0 to 1, while collinear processes have large magnitudes in the RGA elements and γ_{11} can easily change signs for slight angle mismatches.

The fact that collinear processes can easily have the $\hat{\gamma}_{11}$ of the identified model with the opposite sign to γ_{11} of the true process should be considered carefully in robust model identification. The following theorem whose proof is given in Appendix-3 shows one impact of the sign mismatches in the RGA elements, and also provides a useful criterion for robust linear model synthesis.

Theorem 4

Suppose all elements of a 2×2 model gain matrix have the correct signs. Then the stabilizability condition is satisfied only if

$$\gamma_{11} \cdot \hat{\gamma}_{11} > 0 \qquad (3-25.a)$$

For the same condition to be also sufficient, the following assumption on the gain vector mismatches is required:

$$\frac{|n_1 \sin\delta_1 - n_2 \sin\delta_2|}{n_1 \cos\delta_1 + n_2 \cos\delta_2} < \tan\beta \qquad (3-25.b)$$

Combining Property 5 and Theorem 4, we can reach a conclusion that if we have no prior knowledge of the RGA for a collinear process, it is easy to identify a model with wrong RGA sign and this result is sufficient to have an unstabilizable multivariable controller. On the other hand, if we can choose a model where the gain vectors are not nearly collinear (ie. RGA elements of the model do not have very large magnitudes) and also the mismatches are not very large, then the assumption in (3-25.b) is usually valid. Consequently, if we have the prior knowledge about the sign of the RGA, we can fit the data with correct RGA sign imposed as an additional constraint to yield a model that is guaranteed stabilizable (Marlin, 1991).

3.4 Singular Value Decomposition Approach

A new description of structured uncertainties based on the SVD of the steady-state gain matrix is proposed in this section. The stabilizability and performance variation conditions in (2-4) and (2-11) are then analyzed using this description for several special structures of model uncertainties, which can be directly applied to robust model identification.

A steady-state gain matrix can be decomposed via SVD in the following:

$$\mathbf{G} = \mathbf{U\Sigma V}^T \qquad (3-26.a)$$

$$= [U_1, ..., U_r] \cdot diag(\sigma_1, ..., \sigma_r) \cdot [V_1, ..., V_r]^T \qquad (3-26.b)$$

The **U** and **V** are referred as the output and input rotation matrix respectively, while the diagonal Σ matrix is called the singular value matrix (Stewart, 1973). (3-26.b) describes SVD in terms of the individual singular values and the column vectors of both rotation matrices. Note that both rotation matrices are unitary, ie. for **U** matrix

$$\mathbf{U}^T\mathbf{U} = \mathbf{I} \text{ or } \mathbf{U}^T = \mathbf{U}^{-1} \qquad (3-27.a)$$

or, in terms of column vectors

$$U_j^T U_k = \begin{cases} 0, \text{ for } j \neq k \\ 1, \text{ for } j = k \end{cases} \qquad (3-27.b)$$

(3-27.b) shows that all the column vectors of a rotation matrix are of unit length and orthogonal to each other. In addition, the result of multiplying two unitary matrices is still an unitary matrix, and the determinant of any unitary matrix is 1.

Instead of analyzing the additive or multiplicative mismatch in a gain matrix as a whole (Figure-3.9(a)), we can decompose the model mismatch into those in the decomposition matrices of its SVD (Figure-3.9(b)). The structure of mismatch can be described as some constraints on the individual mismatch matrix of SVD. Although this approach has the advantage over the geometric approach in its applicability to high-dimensional systems, in this study only a few of special structures can be analyzed for their robustness properties. Nevertheless, these special structures are very useful in robust model synthesis.

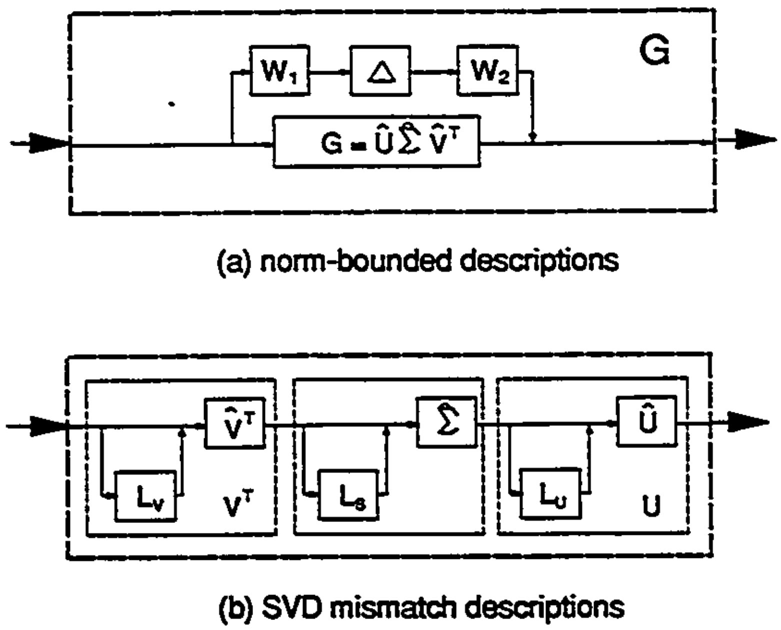

Figure-3.9 Descriptions for structured model uncertainties

3.4.1 The Performance Variation Condition

To analyze the sensitivity of the 2-norm of $\hat{G}G^{-1}$ using the SVD structured uncertainty description, $\hat{G}G^{-1}$ should be first expressed in terms of the SVD matrices of G and $\hat{G}$ as the following:

$$\hat{G}G^{-1} = \hat{U}(\hat{\Sigma}\hat{V}^T V\Sigma^{-1})U^T \qquad (3-28.a)$$

$$\stackrel{\Delta}{=} \hat{U}T_V U^T \stackrel{\Delta}{=} \hat{U}(U_T\Sigma_T V_T^T)U^T \qquad (3-28.b)$$

$$= (\hat{U}U_T)\Sigma_T(UV_T)^T \qquad (3-28.c)$$

where

$$T_V = \begin{bmatrix} \frac{\hat{\sigma}_1}{\sigma_1}\hat{V}_1^T V_1 & \cdot & \frac{\hat{\sigma}_1}{\sigma_r}\hat{V}_1^T V_r \\ \cdot & \cdot & \cdot \\ \cdot & \cdot & \frac{\hat{\sigma}_r}{\sigma_r}\hat{V}_r^T V_r \end{bmatrix} \qquad (3-28.d)$$

Owing to the fact that the product of two unitary matrices is still unitary, we learn from (3-28.c) that the singular value matrix of T_V (Σ_T) is the same as that of $\hat{G}G^{-1}$ and therefore the 2-norms of $\hat{G}G^{-1}$ and T_V are equal. Then we only need to evaluate the 2-norm of the simpler matrix T_V.

When there is no mismatch in the V matrix, T_V is simply a diagonal matrix and the following theorem is thus proven:

Theorem 5

If there is no mismatch in the V matrix, then $\|\hat{G}G^{-1}\|_2 = \underset{j}{\mathrm{Max}} \frac{\hat{\sigma}_j}{\sigma_j}$

On the other hand, if there is significant mismatch in the V matrix and the process is ill-conditioned, then the $(\hat{\sigma}_1/\sigma_r)\hat{V}_1^T V_r$ element on the top right corner of the T_V matrix is usually much larger than 1. Since any matrix norm is always larger than or equal to the largest magnitude of all matrix elements, we have the following property for ill-conditioned systems of arbitrary dimensions.

Property 6

The performance variation measure, $\|\hat{G}G^{-1}\|_2$, in ill-conditioned systems is very sensitive to the mismatch in the V matrix.

3.4.2 The Stabilizability Condition

The stabilizability condition involves the sensitivity of eigenvalue. As an alternative to the norm-bounded perturbation analysis, the sensitivities of the eigenvalues of A can be examined from the sensitivities of the coefficients of Characteristic Polynomial (CP) whose roots are the original definition of eigenvalues: ie.

$$det(\mathrm{A}-\lambda\mathrm{I}) = 0 = (\lambda_1-\lambda)\cdot(\lambda_2-\lambda)\ldots\cdot(\lambda_r-\lambda) \qquad (3-29.a)$$

$$= (-1)^r\lambda^r + (-1)^{r-1}\left[\sum_{i=1}^{r}\lambda_i\right]\lambda^{r-1} + (-1)^{r-2}\left[\sum_{i=1}^{r-1}\sum_{\substack{j=2\\ j>i}}^{r}\lambda_i\cdot\lambda_j\right]\lambda^{r-2} + \ldots + [\lambda_1\lambda_2\ldots\lambda_r] \qquad (3-29.b)$$

As shown in (3-29.b), there are r coefficients influencing the r eigenvalues. Generally speaking, these coefficients are related to the summations of eigenvalue products of various orders. For examples, the second coefficient is plus or minus the summation of the eigenvalues themselves (first order product) and the last one is the product of all the eigenvalues (nth order product). Given some additional specifications other than the magnitude for the perturbation in A, we may be able to see how the CP coefficients of A are perturbed and draw some conclusions on the perturbed eigenvalues. In the following, we will adopt this approach to analyze sensitivity of the eigenvalues of $\mathbf{G}\hat{\mathbf{G}}^{-1}$ when the model mismatch has special structures.

3.4.2.1 Both U and V Matrices Unchanged

Consider first the structured model mismatch which keeps both the U and V matrices unchanged. The $\hat{\mathbf{G}}^{-1}\mathbf{G}$ then becomes

$$\hat{\mathbf{G}}^{-1}\mathbf{G} = \hat{\mathbf{V}}\hat{\Sigma}^{-1}\hat{\mathbf{U}}^T\hat{\mathbf{U}}\Sigma\hat{\mathbf{V}}^T \qquad (3-30.a)$$

$$= \hat{\mathbf{V}}diag\left\{\frac{\sigma_1}{\hat{\sigma}_1},\ldots,\frac{\sigma_r}{\hat{\sigma}_r}\right\}\hat{\mathbf{V}}^{-1} \qquad (3-30.b)$$

Therefore $\hat{\mathbf{G}}^{-1}\mathbf{G}$ is simply a similarity transformation of $\hat{\Sigma}^{-1}\Sigma$, which is diagonal and hence has its eigenvalues equal to the diagonal elements ($\sigma_i/\hat{\sigma}_i$'s). The diagonal elements $\sigma_i/\hat{\sigma}_i$, $i = 1, .., r$ are non-negative by definition. Thus, the condition in (2-4) is always satisfied, and we have proven the following theorem.

Theorem 6

If $\mathbf{G}$ and $\hat{\mathbf{G}}$ are both non-singular and the mismatch between them has the structure that $\hat{\mathbf{U}}^T\mathbf{U} = \mathbf{I}$ and $\hat{\mathbf{V}}^T\mathbf{V} = \mathbf{I}$, then the i-th eigenvalue of $\mathbf{G}\hat{\mathbf{G}}^{-1}$ is the ratio of the i-th singular value of $\mathbf{G}$ to that of $\hat{\mathbf{G}}$, for all the eigenvalues.

3.4.2.2 V Matrix Unchanged

If the structured model mismatch only keeps the $\mathbf{V}$ matrix unchanged, the $\hat{\mathbf{G}}^{-1}\mathbf{G}$ becomes

$$\hat{\mathbf{G}}^{-1}\mathbf{G} = \hat{\mathbf{V}}\hat{\Sigma}^{-1}\hat{\mathbf{U}}^T\mathbf{U}\Sigma\mathbf{V}^T \qquad (3-31.a)$$

$$= \hat{\mathbf{V}}\mathbf{T}\hat{\mathbf{V}}^{-1} \qquad (3-31.b)$$

where $\mathbf{T} = \hat{\Sigma}^{-1}\hat{\mathbf{U}}^T\mathbf{U}\Sigma$ (3-31.c)

The eigenvalues of $\hat{\mathbf{G}}^{-1}\mathbf{G}$ are equal to the eigenvalues of $\mathbf{T}$ due to the similarity transformation in (3-31.b). Therefore we only need to examine the characteristic polynomial of the following matrix

$$\mathbf{T} = \begin{bmatrix} \cdot & \cdot & \cdot & \cdot & \cdot \\ \cdot & \frac{\sigma_i}{\hat{\sigma}_i}\hat{U}_i^T U_i & \cdot & \frac{\sigma_j}{\hat{\sigma}_i}\hat{U}_i^T U_j & \cdot \\ \cdot & \cdot & \cdot & \cdot & \cdot \\ \cdot & \frac{\sigma_i}{\hat{\sigma}_j}\hat{U}_j^T U_i & \cdot & \frac{\sigma_j}{\hat{\sigma}_j}\hat{U}_j^T U_j & \cdot \\ \cdot & \cdot & \cdot & \cdot & \cdot \end{bmatrix} \qquad (3-32.a)$$

$$= \left[\frac{\sigma_j}{\hat{\sigma}_i}\right]_{ij} * \hat{\mathbf{U}}^T\mathbf{U} \qquad (3-32.b)$$

where * denotes the element-by-element product of two matrices

From (3-32.b) we can clearly see that both the singular value mismatches ($[\sigma_j/\hat{\sigma}_i]_{ij}$) and the $\mathbf{U}$ matrix mismatch ($\hat{\mathbf{U}}^T\mathbf{U}$) affect the eigenvalues of $\mathbf{T}$. However, there exist certain structures of $\hat{\mathbf{U}}^T\mathbf{U}$ that will ensure, in spite of the mismatches in the singular values, that the eigenvalues of $\mathbf{G\hat{G}^{-1}}$ satisfy the stabilizability condition in (2-4). In the following, we will present one particular structure of $\mathbf{\hat{U}^T U}$ which is encountered in many situations as discussed in later chapters.

When there is no mismatch in the U matrix, the $\mathbf{\hat{U}^T U}$ is simply an identity matrix, in which all the diagonal elements are 1 and therefore positive, while all the off-diagonal elements are 0 and hence have the minimum magnitude. From this limiting case of $\mathbf{\hat{U}^T U}$ being identity, we therefore propose a mismatch structure of the $\mathbf{\hat{U}^T U}$ matrix as the following:

$$\hat{U}_i^T U_i > 0 \qquad \forall i \qquad (3-33.a)$$

$$\Big|\sum_{\substack{k=1\\k\neq i,j}}^{n} \hat{U}_k^T U_i \cdot \hat{U}_k^T U_j\Big| < |\hat{U}_i^T U_i \cdot \hat{U}_j^T U_j| \quad \forall i,j \qquad (3-33.b)$$

The interpretation for (3-33.a) is that the mismatch in the U matrix is allowed to reduce the diagonal elements from the limiting value of 1 to any value as long as they remain positive. On the other hand, (3-33.b) which involves a pair of column vectors of the $\mathbf{\hat{U}^T U}$ matrix sets the limit on how much the diagonal elements can be reduced. That is, the two diagonal elements of the $\mathbf{\hat{U}^T U}$ matrix in every pair of column vectors should be large enough that their product is larger than the absolute value of the summation of all element-by-element products in these two columns (excluding the two rows containing the diagonal elements). (3-33.b) can also be interpreted as the off-diagonal elements of the $\mathbf{\hat{U}^T U}$ matrix being relaxed from the limiting value of 0 to have significant magnitudes.

It is trivial to find a sufficient condition for (3-33.a) in terms of the differences between U and $\mathbf{\hat{U}}$. That is, there is no *sign mismatch* at all in the U matrix. On the other hand, we cannot find a corresponding general sufficient condition in (3-33.b). However, it should be emphasized that the structure defined in (3-33.b) does cover a wide range of mismatches in the U matrix in many applications. More details are discussed in later chapters. The effects of the mismatch structure in (3-33) on the eigenvalues of $\mathbf{G\hat{G}^{-1}}$ are summarized in Theorem 7 and Theorem 8 below.

Theorem 7

If $\mathbf{G}$ and $\hat{\mathbf{G}}$ are both non-singular and the mismatch between them has the following structure:

1) $\hat{\mathbf{V}}^T\mathbf{V} = \mathbf{I}$

2) If the mismatch between $\mathbf{U}$ and $\hat{\mathbf{U}}$ has the following structure:

i) the signs of all the elements of $\mathbf{U}$ remain the same as those of $\hat{\mathbf{U}}$,

ii) $| \sum_{\substack{k=1 \\ k\neq i,j}}^{n} \hat{U}_k^T U_i \cdot \hat{U}_k^T U_j | < | \hat{U}_i^T U_i \cdot \hat{U}_j^T U_j |$

then the all the *real* eigenvalues of $\mathbf{G}\hat{\mathbf{G}}^{-1}$ must be positive.

The proof is given in the Appendix-4. Remember that the stabilizability condition in (2-4) also requires all the complex roots have positive real parts. It is well known that the Routh test is used to count the number of positive real parts in the roots of arbitrary polynomial with real coefficients. Appendix-5 contains the results of performing the Routh test to $\mathbf{G}\hat{\mathbf{G}}^{-1}$ up to 3×3 systems which are subjected to the structure defined in Theorem 7, and it shows that all the complex roots must have positive real parts. The Routh test can be applied to higher dimension systems and possibly prove that the structure defined in Theorem 7 would ensure the stabilizability for higher dimension systems. However, this analytical approach is very tedious and will not be examined any further. Therefore we simply state the following theorem:

Theorem 8

For at least up to 3×3 systems, if $\mathbf{G}$ and $\hat{\mathbf{G}}$ have the structure in Theorem 7, then all the *complex* eigenvalues of $\mathbf{G}\hat{\mathbf{G}}^{-1}$ have positive real parts. Therefore the control system is stabilizable for the locally linearized process.

For 2×2 systems, the assumption in (3-33.b) is not necessary (ie. always satisfied). Therefore we can conclude from the above theorems that if there is no mismatch in the **V** matrix while the mismatch in the **U** matrix is such that none of its elements changes signs, then the control system is stabilizable for the locally linearized process.

3.4.2.3 U Matrix Unchanged

For the situation where the model mismatch keeps the **U** matrix of its nominal model unchanged, the development is the same as above for the case of a constant **V** matrix. The SVD of $\mathbf{G}\hat{\mathbf{G}}^{-1}$, instead of $\hat{\mathbf{G}}^{-1}\mathbf{G}$ in (3-31), is examined and thus $\mathbf{T} = \Sigma\mathbf{V}^T\hat{\mathbf{V}}\hat{\Sigma}^{-1}$. Then the mismatch structure in (3-33) can be re-defined for the $\mathbf{V}^T\hat{\mathbf{V}}$ matrix. Therefore Theorem 7 and Theorem 8 are all applied to this situation by simply exchanging the **U** with the **V** matrix, and they will not be repeated here.

The most significant and perhaps surprising consequence of Theorems 5, 7 and 8 is that any mismatch in the singular values, or the conditioning of nominal models, does not affect the stabilizability in these situations. Theoretically, in the face of these structured mismatches, the mismatch magnitudes could be very large without making the process unstabilizable. These ideal and somewhat counter-intuitive results arise from the main assumption that either or both of the rotation matrices are exactly unchanged. In the following, we will relax this assumption to examine when and why the mismatch magnitude and the conditioning of a nominal model affect the stabilizability.

3.4.2.4 Both U and V Matrices Changed

(3-31) and (3-32) were developed assuming the **V** matrix of the process remained unchanged. We now investigate the sensitivity of the eigenvalues of $\hat{\mathbf{G}}^{-1}\mathbf{G}$ to additional mismatch in the **V** matrix. The *ij*-th element of $\hat{\mathbf{G}}^{-1}\mathbf{G}$ in (3-31.a) can be derived as

$$[\hat{G}^{-1}G]_{ij} = (\hat{V}TV^{-1})_{ij} \qquad (3-34.a)$$

$$= \sum_{h=1}^{r} \hat{v}_{ih} \sum_{k=1}^{r} t_{hk} v_{jk} \qquad (3-34.b)$$

where $t_{hk} = \frac{\sigma_k}{\hat{\sigma}_h} \hat{U}_h^T U_k$ is the hk-th element of the T matrix.

Given the complexity of (3-34.b), it is virtually impossible to obtain each characteristic polynomial (CP) coefficient of $\hat{G}^{-1}G$ in such a simple expression as that of T in Appendix-4. However, the second CP coefficient which is simply the summation of the diagonal elements of $\hat{G}^{-1}G$ can be derived as

$$\sum_{i=1}^{r} \lambda_i = \sum_{i=1}^{r} \sum_{h=1}^{r} \hat{v}_{ih} \sum_{k=1}^{r} t_{hk} v_{ik} \qquad (3-35.a)$$

$$= \sum_{i=1}^{r} \sum_{\substack{j=1 \\ j \neq i}}^{r} \frac{\sigma_j}{\hat{\sigma}_i} (\hat{U}_i^T U_j)(\hat{V}_i^T V_j) \qquad (3-35.b)$$

$$= \sum_{i=1}^{r} \frac{\sigma_i}{\hat{\sigma}_i} (\hat{U}_i^T U_i)(\hat{V}_i^T V_i) + \sum_{i=1}^{r} \sum_{\substack{j=1 \\ j \neq i}}^{r} \frac{\sigma_j}{\hat{\sigma}_i} (\hat{U}_i^T U_j)(\hat{V}_i^T V_j) \qquad (3-35.c)$$

The first term in (3-35.c) involves only the diagonal elements of T and $\hat{V}^T V$, while the second term involves only the off-diagonal elements. Since a trace is simply the summation of the real parts of eigenvalues in a matrix whose complex eigenvalues are conjugates (ie. the matrix has all its elements being real), a negative trace of $\hat{G}^{-1}G$ is sufficient to conclude that at least one of its eigenvalues is negative or one pair of complex conjugates has a negative real part, and therefore the stabilizability condition is violated.

The second term in (3-35.c) is zero and then the first term is just the summation of the diagonal elements of T in (3-32), if there is no mismatch in the V matrix (ie. $\hat{V}_i^T V_j = 0$ for all $i \neq j$). When an additional V matrix mismatch is introduced, the trace may be very sensitive to this effect because the second term in (3-35.c) contains the ratio of maximum to minimum singular value (ie. $\sigma_1/\hat{\sigma}_r$) which will dominate the magnitude of the trace in ill-conditioned processes. Therefore, unless the mismatches in the U and V matrices are properly correlated such that $(\hat{U}_r^T U_1)(\hat{V}_r^T V_1)$ is positive, the trace can become negative for small mismatches in the two rotation matrices. Therefore we conclude the following qualitative property.

<u>Property 7</u>

> The stabilizability of ill-conditioned systems may be very sensitive to the uncorrelated mismatches in the **U** and **V** matrices.

More quantified treatments for the effect of uncorrelated mismatches in the two rotation matrices on the stabilizability will be postponed to the identification chapter.

3.5 Summary

The geometric analysis results clearly indicate that the critical difference between a 2×2 true process and its model is the angle mismatches. If there is no angle mismatch at all, the stabilizability condition is always satisfied. This has important implications for robust model identification or synthesis. That is, it is necessary to preserve as much as possible the angle between the two true gain vectors in the modelling. For 2×2 processes, there is a direct relationship between this angle and their RGA's. Thus RGA is also an important characteristic for robust model synthesis. It has been shown that for any identified model with the correct signs in all the gain elements, it is a necessary condition that this model has the correct signs in its RGA. The geometric analysis also shows that when the structure of the model which the controller design is based upon is fixed (ie. such as those in multiloop SISO control), different angles between the gain vectors of a true process (ie. collinear or orthogonal process) can have very different effects on the robustness the controller design.

The SVD approach can be regarded as a high-dimensional extension of the geometric approach. In fact, it will be shown in Chapter 4 that the structure of unchanged U and V matrices is equivalent to the structure that the angle between the two gain vectors is unchanged. The major difference between the two approaches is that the SVD approach lacks the flexibility of specifying any mismatch structure that the geometric approach has as an analysis tool. However, the SVD approach is applicable to high-dimensional systems, and the analysis results based on some special mismatch structures (ie. Theorem 5 and 7) are readily applied to robust model identification. The particularly useful result is where the V matrix is unchanged and all the elements in U matrix have unchanged signs. An identified model which is subjected to such an uncertainty structure often satisfies both the stabilizability and performance variation conditions despite the fact that the model is ill-conditioned and the uncertainty magnitude is significant.

4 Structured Uncertainties Arising from Nonlinearities

This chapter applies analysis results in Chapter 3 to the mismatches among the locally linearized gain matrices of nonlinear processes. All the conditions on the gain matrices presented earlier are examined using model gain matrix to be that at the nominal operating point (ie. $\bar{G}$ replaces $\hat{G}$ in the related theorems and properties) and the true gain matrix to be that at various operating points (G) in the uncertainty region. Since such mismatches are completely determined by deterministic physical/chemical phenomena, they can be highly structured. This chapter will first present some theoretical results for some special structures of model uncertainties which may arise from process nonlinearities and lead to good robustness properties of linear multivariable control. Then a few examples are provided to confirm that these structures do exist in physical processes.

4.1 Robustness of Linear Controllers to Special Uncertainty Structures

Four special structures of model mismatches, which can provide useful classifications of process input/output nonlinearities, will be introduced in the following. The first two structures are derived using the geometric sensitivity analysis, while the last two are based on the SVD structured mismatch description. The discussions on both the geometric and SVD structures are organized in the same fashion. More stringent structures are discussed first which deal with both robust stability and performance problems. Then only the stabilizability condition is treated for less stringent structures.

4.1.1 Equal Angle/Length Mismatches of Gain Vectors

Suppose that the angle mismatches of the gain vectors in 2×2 processes have the following constraint:

$$\delta_1 = \delta_2 = \delta \qquad (4-1)$$

This constraint represents the rotation of the two gain vectors with the angle between them unchanged (ie. $\tilde{\beta} = \beta$). Then condition (3-17) for the stabilizability becomes:

$$det(G\tilde{G}^{-1}) = n_1 n_2 \qquad (4-2.a)$$

$$tr(G\tilde{G}^{-1}) = \left[(n_1+n_2)+(n_1-n_2)\frac{\tan\delta}{\tan\beta}\right]\cos\delta \qquad (4-2.b)$$

Since the determinant of $G\tilde{G}^{-1}$ is always positive in this situation, the stabilizability is determined only by the sign of the trace. If $\delta = 0$ (no angle mismatch), the trace is also positive (ie. $tr = n_1 + n_2$) and therefore the 2×2 system is always stabilizable no matter how large the mismatch magnitude that is introduced by the length mismatches in the two gain vectors. Another sufficient condition for the trace to be positive is where both the angle and length mismatches are constrained to be equal (ie. $n_1 = n_2$ in addition to (4-1)).

As to the performance variation problem, it has been shown in the earlier geometric analysis that collinear processes are very sensitive to model mismatches. However, when a collinear process is subject to the mismatch structure of equal angle\length mismatches in the two gain vectors, equation (3-16) is reduced to the following:

$$\|\hat{G}G^{-1}\|_E = \frac{1}{|\sin\beta|}(\hat{n}_1^2 - 2\hat{n}_1\hat{n}_2\cos\beta\cos\beta + \hat{n}_2^2)^{\frac{1}{2}} \qquad (4-3.a)$$

$$= \left[2\hat{n}_1\hat{n}_2 + \frac{(\hat{n}_1-\hat{n}_2)^2}{|\sin\beta|}\right]^{\frac{1}{2}} = \sqrt{2}\hat{n}_1 \qquad (4-3.b)$$

Therefore the high sensitivity of collinear processes due to small $|\sin\beta|$ is completely eliminated. In other words, even though a nominal process is collinear and very ill-conditioned, linear controllers designed for the nominal process can control the locally linearized processes at various operating conditions with minimal impact on the performance variation as long as the above structure holds.

4.1.2 Global Stabilizability of 2×2 Systems

The geometric mismatch conditions for stabilizability as given in Theorem 2 and Theorem 3 are stated in terms of any specific pair of a true process and its model gain matrices. When these conditions are applied to the mismatches among the locally linearized gain matrices of a nonlinear process, we can exploit the continuity of nonlinear steady-state input/output relationship in order to derive a *global* condition for the stabilizability of linear multivariable controllers for controlling nonlinear processes in a *region* of operation.

The nonlinear steady-state relationship between the inputs (m_1, m_2) and outputs (y_1, y_2) of a 2×2 process is best represented by an input contour plot (Figure-4.1). The values of the two outputs under constant values of m_1 are plotted as the solid contours, while the dotted contours are those under constant values of m_2 in this figure. An intersection point of one solid and one dotted contours gives the output values corresponding to a specific pair of input values (ie. an operating point). The gain vector of m_1 at any operating point is along the tangent line, drawn from the intersection point, of the m_2 contour. Similarly, the gain vector of m_2 is along the line tangent to the m_1 contour at the same point (Figure-4.1). These contour plots are usually easily obtained from the nonlinear model. For linear processes, the input contour plot has the following characteristics: 1) parallel straight lines for each input, 2) a pair of contours of different inputs intersect exactly once, 3) equal distances between two parallel contours if the contours are plotted for the same amount of change in that input. Consequently, all operating points have the same gain vectors in a linear process and the stabilizability is never a problem.

Nonlinear processes are always characterized by curved and/or non-uniform contours. In addition, multiple steady states may exist in a nonlinear process. An intersection of two contours of the same input variable indicates that the same pair of output values (y_1, y_2) can result from different values of that input and, in general, from different values of the other input as well (Figure-4.2(a)). This situation has been referred as input multiplicity

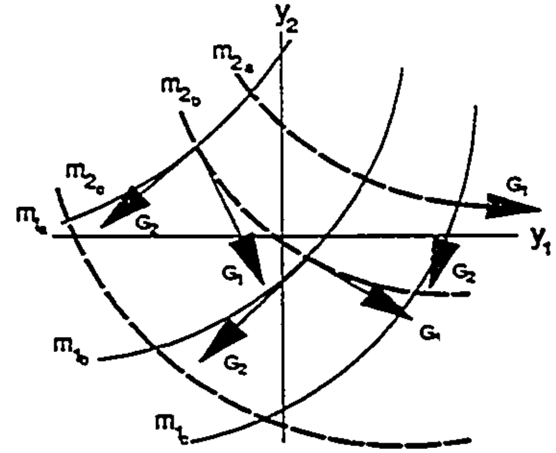

Figure-4.1 Input contour plot and process gain vectors

(Koppel (1982)). Another input multiplicity situation is when the same value of one output is obtained from different values of one input (ie. y_1 and m_2 in Figure-4.2(b)). This type of input multiplicity is characterized by a sign change in one element of a gain vector (ie. the element for y_1 in Figure-4.2(b)). Finally, the output multiplicity appears when different pairs of output values result from the same pair of input values (Figure-4.2(c)). Unless the process output variables are implicit functions of the input variables, it is impossible to have output multiplicity.

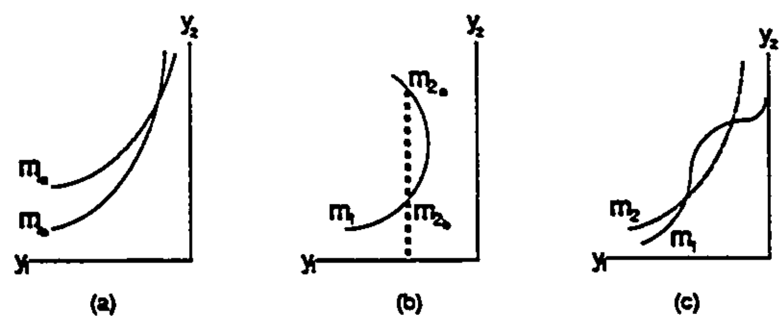

Figure-4.2 Input/output multiplicities

When a nonlinear process has all these multiplicities (ie. almost arbitrarily angle changes) in an operating region, the model mismatch due to process nonlinearities may be considered as unstructured. However, a large class of nonlinear processes only has a simple one to one mapping for the input/output relationship and hence excludes any kind of multiplicity. For these processes, the model mismatch is highly structured because the angle mismatches are severely constrained to avoid the multiplicities. Theorem 9 below is useful to examine the stabilizability problem for some nonlinear processes with this mismatch structure. The proof is given in Appendix-6.

Theorem 9

If the nonlinearities define a one to one mapping for the input/output relationship in an operating region, then the determinant of $G\tilde{G}^{-1}$ is always positive in the region.

Obviously, the structure in (4-1) is just a special case of Theorem 9 with more stringent constraint and (4-2.a) has already shown that the determinant is always positive in this case. The other major difference between the structure in (4-1) and that in Theorem 9 is that the latter is a global condition. To apply this theorem, it is not necessary to actually obtain the contour plot for a nonlinear process as long as we know analytically that the input/output relationship is one-to-one mapping within a given range of inputs (ie. when the nonlinear model is simple enough). For SISO processes, Theorem 9 is equivalent to the well-known condition that if there is no multiplicity then the sign of process gain is always the same as that of the nominal model (Figure-4.3). Unlike with the SISO systems, this theorem alone is not sufficient for 2×2 systems to determine whether the control is stabilizable. Only for those processes which also satisfy the sufficient condition for the positive trace in Theorem 3, can we say that the stabilizability is guaranteed if there are no multiplicities in an operating region. To see if this sufficient condition is met, we will have to obtain the contour plot and examine how the gain vectors change along the contours. For some processes such as binary distillation columns shown later, it is rather obvious to see that this sufficient condition is satisfied.

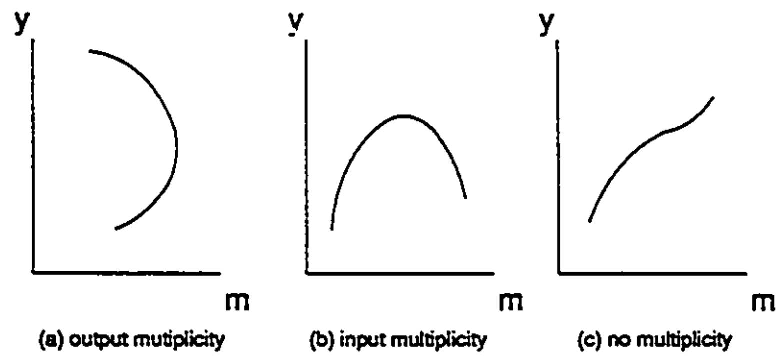

Figure-4.3 Multiplicities in SISO processes

4.1.3 Constant Input Rotation Matrix

Using the structured uncertainty description in Figure-3.9, we may specify a class of nonlinear processes with a mismatch structure of a constant **V** matrix among the locally linearized gain matrices. Then linear multivariable controllers designed for the nominal process may control this class of nonlinear processes over a wide region with robust stability and performance. The robustness properties given in Theorem 5, 6, 7 and 8 are applicable in this situation and therefore will not be repeated here. The emphasis in this section, instead, is on showing the relationship between the structure of constant **V** matrix and the geometric structure of equal angle/length mismatches in 2×2 processes.

For 2×2 systems, an unitary matrix can always be expressed by sine/cosine functions (Noble and Daniel, 1977) and therefore a gain matrix may be expressed as follows:

$$\mathbf{G}=\begin{bmatrix}\cos\theta & -\sin\theta\\ \sin\theta & \cos\theta\end{bmatrix}\begin{bmatrix}\bar{\sigma} & 0\\ 0 & \underline{\sigma}\end{bmatrix}\begin{bmatrix}\cos\phi & -\sin\phi\\ -\sin\phi & -\cos\phi\end{bmatrix}^T \qquad (4-4.a)$$

$$=\begin{bmatrix}\bar{\sigma}\cos\theta\cos\phi+\underline{\sigma}\sin\theta\sin\phi & -\bar{\sigma}\cos\theta\sin\phi+\underline{\sigma}\sin\theta\cos\phi\\ \bar{\sigma}\sin\theta\cos\phi-\underline{\sigma}\cos\theta\sin\phi & -\bar{\sigma}\sin\theta\sin\phi-\underline{\sigma}\cos\theta\cos\phi\end{bmatrix} \qquad (4-4.b)$$

where θ and ϕ are the characteristic angles for the input and output rotation matrices, respectively. For ill-conditioned nonlinear processes with unchanged **V** matrix, it can be easily shown that the two gain vectors in (4-4.b) asymptotically have the following geometric mismatch structure as the minimum singular value approaches to zero:

$$\frac{l_1}{\bar{l}_1} \doteq \frac{l_2}{\bar{l}_2} \doteq \frac{\bar{\sigma}}{\bar{\bar{\sigma}}} \Rightarrow n_1 = n_2 = n \qquad (4-5.a)$$

$$\alpha_1 \doteq \alpha_2 \doteq \theta \Rightarrow \delta_1 = \delta_2 = \delta \qquad (4-5.b)$$

when $\bar{\sigma}$ and θ in terms of SVD description, or n and δ in terms of the geometric description, are functions of operating conditions. Therefore for 2×2 ill-conditioned processes, the special structure of the constant V matrix is equivalent to the geometric structure of equal angle/length mismatches. We may regard a constant V matrix structure as a high-dimensional extension of this geometric structure.

A special case of this structure is where both rotation matrices are unaffected by changing the operating conditions. Then θ is a constant and thus δ is 0 in (4.5.b). In other words, the structure of constant U and V matrices is equivalent to the geometric structure of no angle mismatch in gain vectors. The only mismatches are in the singular values or the magnitudes of the process, and this case is very similar to those SISO systems where nonlinearities only change the magnitude of a nominal process gain.

4.1.4 Correlated Mismatches in the Input and Output Rotation Matrices

Similar to the consecutive developments of the two geometric structures as given in sections 4.1.1 and 4.1.2, this section will relax the stringent assumption of a constant V matrix proposed in the last section. For ill-conditioned processes, Property 6 implies that linear controllers designed for a nominal process must have large performance variations when the locally linearized processes do not have the ideal structure of a constant V matrix. Therefore only the stabilizability problem needs to be examined here.

Suppose that mismatches in both the U and V matrices have the structure of no sign mismatch in all matrix elements. Then the first summation term in (3-35.c) must be positive because all diagonal elements $\sigma_i/\tilde{\sigma}_i$, $\tilde{U}_i^T U_i$ and $\tilde{V}_i^T V_i$ are positive. A simple sufficient condition for the second summation term to be positive as well, and thus for the summation of eigenvalues to be positive, is as follows

$$(\tilde{U}_i^T U_j) \cdot (\tilde{V}_i^T V_j) > 0 \ \forall i, j \tag{4-6}$$

This condition requires that the mismatch in **V** (characterized by $\tilde{\mathbf{V}}^T\mathbf{V}$) is correlated with the mismatch in **U** (characterized by $\tilde{\mathbf{U}}^T\mathbf{U}$) in such a way that each pair of their *ij*-th elements have the same sign. It will be shown later that this correlation between $\tilde{\mathbf{V}}^T\mathbf{V}$ and $\tilde{\mathbf{U}}^T\mathbf{U}$ does exist in physical processes such as catalytic reactors. Unfortunately we are not able to further examine the properties of other CP coefficients of $\tilde{\mathbf{G}}^{-1}\mathbf{G}$ based on this correlation, because of the complexity of these coefficients. Consequently we cannot obtain a sufficient condition for the stabilizability when both rotation matrices have significant mismatches. However, for 2×2 systems, the following theorem has been proven in Appendix-7.

Theorem 10

For 2×2 systems, if both **G** and $\tilde{\mathbf{G}}$ are non-singular and the mismatch between them has the following structure:

i) both rotation matrices have their element signs unaffected by the mismatch,

ii) $\tilde{\mathbf{U}}^T\mathbf{U}$ and $\tilde{\mathbf{V}}^T\mathbf{V}$ are correlated such that they have the same signs in each of their corresponding elements (ie. equation (4-6)),

then the eigenvalues of $\mathbf{G}\tilde{\mathbf{G}}^{-1}$ must be either real and positive, or be complex and with positive real parts, and the control system is stabilizable for the locally linearized process.

Although both Theorem 9 and Theorem 10 deal with the stabilizability problem, the former is a global condition addressing only a necessary condition for the stabilizability (ie. $det(\mathbf{G}\tilde{\mathbf{G}}^{-1})$ is positive) while the latter is a local condition for the stabilizability condition itself.

4.2 Physical Examples

In this section, the numerical results of locally linearized gain matrices at various operating conditions for a few physical processes are obtained to confirm that the theoretically derived structures are realistic for the mismatches arising from process nonlinearities. The examples include a binary distillation column based on a short-cut nonlinear model, a fluidized-bed catalytic reactor based on a rigorous mechanistic model, and a packed-bed catalytic reactor where several linear models have been identified experimentally at various operating conditions.

4.2.1 Dual Composition Control of High-Purity Distillation

The dual-composition control of high-purity distillation columns has been thoroughly studied in recent years because it presents unique challenges from severe process nonlinearities and from ill-conditioned nominal steady-state gain matrices (McAvoy (1983), Skogestad and Morari (1988), Skogestad *et al* (1988)). Two control strategies, LV and DV control, particularly have been the focus of attention. LV control of a column refers to controlling the overhead and bottom compositions with reflux flow (L) and boil-up flow (V), while DV control refers to controlling the dual compositions with overhead product flow (D) and boil-up flow (V).

The steady-state relationship between LV and DV control is just a linear transformation due to material balances

$$\begin{bmatrix} dL \\ dV \end{bmatrix} = \begin{bmatrix} -1 & 1 \\ 0 & 1 \end{bmatrix} \begin{bmatrix} dD \\ dV \end{bmatrix} \overset{\Delta}{=} \mathbf{T}_{BM} \begin{bmatrix} dD \\ dV \end{bmatrix} \qquad (4-8)$$

The more complicated dynamic relationship has been derived by Yang, *et al* (1990), but it is not necessary for this study. Owing to the relationship in (4-8), both the $\mathbf{G}\tilde{\mathbf{G}}^{-1}$ and $\tilde{\mathbf{G}}\mathbf{G}^{-1}$ matrices are the same for LV and DV control because

$$G^{M}(\bar{G}^{M})^{-1}=G^{E}T_{EM}(\bar{G}^{E}T_{EM})^{-1}=G^{E}(\bar{G}^{E})^{-1} \qquad (4-9.a)$$

$$\bar{G}^{M}(G^{M})^{-1}=\bar{G}^{E}T_{EM}(G^{E}T_{EM})^{-1}=\bar{G}^{E}(G^{E})^{-1} \qquad (4-9.b)$$

where the superscript E and M denote LV (energy balance) and DV (material balance) control respectively. Consequently, there is no difference between the robustness of linear LV and DV multivariable controllers designed for the nominal process to control the nonlinear process at any operating point in terms of their stabilizability and performance variation measure ((2-4) and (2-11)).

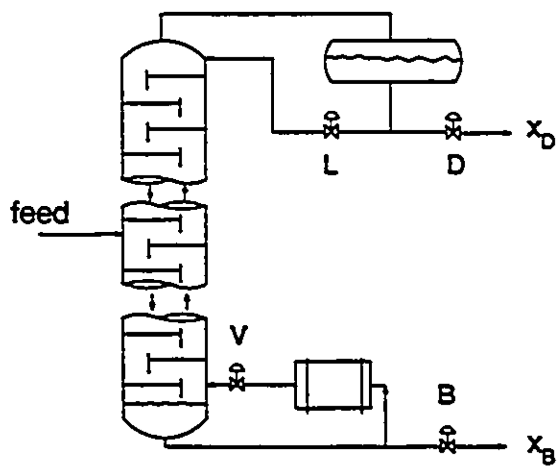

Figure-4.4 Distillation column

The nonlinear steady-state relationship between the inputs (two flows) and the outputs (two compositions) in LV and DV control is approximated in this study using a short-cut model for binary distillation columns which consists the following equations (McAvoy (1983)):

$$\left(\frac{N-N_m}{N+1}\right)=.75\left[1-\left(\frac{R-R_m}{R+1}\right)^{.5668}\right] \qquad (4-10.a)$$

$$R_m=\frac{1}{(\alpha-1)}\left(\frac{X_D}{X_F}-\frac{\alpha(1-X_D)}{(1-X_F)}\right) \qquad (4-10.b)$$

$$N_m=\frac{\ln\left(\frac{X_D}{1-X_D}\cdot\frac{1-X_B}{X_B}\right)}{\ln\alpha} \qquad (4-10.c)$$

where the feed quality is assumed to be 1 (ie. saturated liquid) in this model. Only three parameters need to be specified, ie. the number of trays, the relative volatility and feed composition. Given the product compositions, we can solve (4-10.a) for R and then solve for the other flow-rate from material balance equations

$$F = D + B \tag{4-11.a}$$

$$FX_F = DX_D + BX_B \tag{4-11.b}$$

$$L = D \cdot R \tag{4-11.c}$$

$$V = L + D \tag{4-11.d}$$

Therefore the input contour plots can be obtained. Figure-4.5 and Figure-4.6 are the results of LV and DV processes with specified parameters of twenty seven trays, relative volatility of 1.65 and feed composition of 0.5 in mole fraction.

The gain vectors are along the tangent lines of these contours. These nonlinear contour plots have the following major characteristics: i) the process nonlinearities are prominent in the severely curved, and not equally spaced contours arising from the physical limits on the composition (ie. 0 to 1 for mole fraction), ii) in LV control, the contours of the two inputs are almost overlapped and therefore the gain vectors at any operating point in the region will be nearly collinear (ie. very ill-conditioned), and iii) the contours for constant boil-up flows in DV are the same as those in LV except that, by increasing the other input value on these contours, LV and DV will have the compositions moved in opposite directions along a contour. The last characteristic is because

$$\begin{aligned}[G_D^M, G_V^M] &= [G_L^E, G_V^E]\begin{bmatrix}-1 & 1\\ 0 & 1\end{bmatrix}\\ &= [-G_L^E, G_L^E + G_V^E]\end{aligned} \tag{4-12}$$

and thus the gain vector of distillate flow is simply the negative gain vector of reflux flow.

Consider first the global stabilizability of linear model-based control of the nonlinear process. The nonlinear model in (4-10) is simple and therefore, by inspections of the

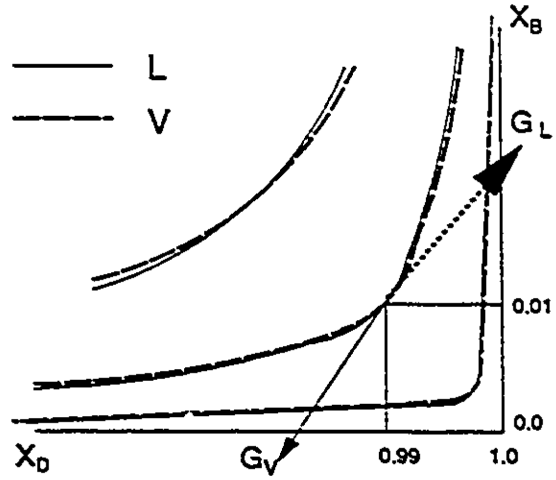

Figure-4.5 Input Contours of LV process

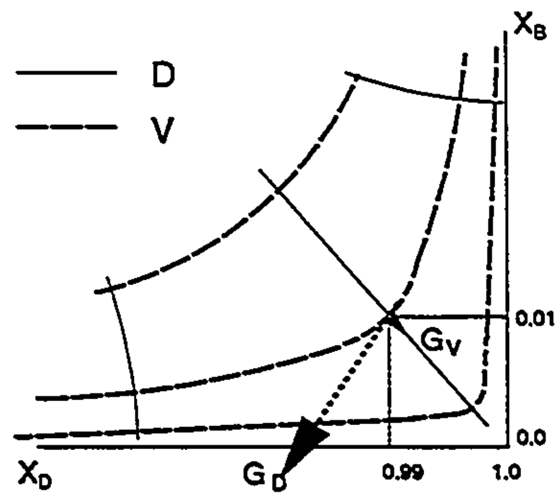

Figure-4.6 Input Contours of DV process

equations, we know that the input/output relationship is a one to one mapping. According to Theorem 9, the determinant of $G\tilde{G}^{-1}$ in the region is always positive. For more complicated models, we should examine the contour plots to see if any multiplicity exists. In DV control, the dotted contours in Figure-4.6 asymptotically approach the two axes. Consequently, the two gain vectors at any point, one tangent to and other normal to a dotted contour, will always remain in their original half planes. This phenomena satisfies the sufficient condition in Theorem 3 for the trace of $G\tilde{G}^{-1}$ to be positive. We conclude that, even though the nominal model in DV (or LV) control is very ill-conditioned, a linear controller is globally stabilizable in a wide region.

The locally linearized process gain matrices are now examined. First, an equal-purity operating condition, in which the light-key mole fraction composition of the top and bottom products are 0.987 and 0.013 respectively, is chosen as the nominal process. The LV control has the steady-state gain matrix as follows (Koung, 1987):

$$\tilde{G}_{LV}=\begin{bmatrix} .4864 & -.4807 \\ .4864 & -.4921 \end{bmatrix}=\begin{bmatrix} .703 & -.711 \\ .711 & .703 \end{bmatrix}\begin{bmatrix} .972 & 0 \\ 0 & .006 \end{bmatrix}\begin{bmatrix} .707 & -.707 \\ -.707 & -.707 \end{bmatrix} \qquad (4-13)$$

Table-1 contains the process gain matrices at four operating points: (1) high purity in the heavy key; (2) high purity in the light key; (3) high purities in both keys; (4) low purity in both keys. These four cases clearly show that the V matrix of this process is not affected by the nonlinearities because $\tilde{\mathbf{V}}^T\mathbf{V}$ matrices are all nearly the identity matrix. Furthermore, the U matrix of the process is also unaffected as long as the relative purity of the keys remains the same as seen in operating points such as (3) and (4) where $\tilde{\mathbf{U}}^T\mathbf{U}$ is also nearly an identity matrix. The $\tilde{\mathbf{U}}^T\mathbf{U}$ matrices in (1) and (2) have the structure as described in Theorem 7.

	X	G	$\tilde{\mathbf{U}}^T\mathbf{U}$	$\tilde{\mathbf{V}}^T\mathbf{V}$	$diag(\tilde{\Sigma}^{-1}\Sigma)$	n_1	n_2	δ_1	δ_2
(1)	$\begin{bmatrix} .9083 \\ .0009 \end{bmatrix}$	$\begin{bmatrix} .813 & -.812 \\ .015 & -.016 \end{bmatrix}$	$\begin{bmatrix} .718 & .698 \\ -.698 & .718 \end{bmatrix}$	$\begin{bmatrix} 1.00 & 0.00 \\ 0.00 & 1.00 \end{bmatrix}$	1.18, 0.13	1.18	1.18	-0.77	-0.78
(2)	$\begin{bmatrix} .9969 \\ .0918 \end{bmatrix}$	$\begin{bmatrix} .018 & -.017 \\ .810 & -.811 \end{bmatrix}$	$\begin{bmatrix} .726 & -.687 \\ .687 & .726 \end{bmatrix}$	$\begin{bmatrix} 1.00 & 0.00 \\ 0.00 & 1.00 \end{bmatrix}$	1.18, 0.13	1.18	1.18	0.76	0.75
(3)	$\begin{bmatrix} .9948 \\ .0052 \end{bmatrix}$	$\begin{bmatrix} .494 & -.493 \\ .494 & -.495 \end{bmatrix}$	$\begin{bmatrix} 1.00 & .005 \\ -.005 & 1.00 \end{bmatrix}$	$\begin{bmatrix} 1.00 & 0.00 \\ 0.00 & 1.00 \end{bmatrix}$	1.02, 0.18	1.02	1.02	0.00	-0.01
(4)	$\begin{bmatrix} .9457 \\ .0543 \end{bmatrix}$	$\begin{bmatrix} .446 & -.394 \\ .446 & -.498 \end{bmatrix}$	$\begin{bmatrix} .999 & -.05 \\ .050 & .999 \end{bmatrix}$	$\begin{bmatrix} 1.0 & -.00 \\ .00 & 1.0 \end{bmatrix}$	9.12, 0.92	0.92	0.92	0.00	0.10

Table-1 LV control

Table 1 also contains the length and angle mismatches of the two gain vectors which confirms that the constant V matrix structure is equivalent to the geometric structure as shown in (4-5). Using the contour plot in Figure-4.5, we can clearly see that when the process is moved to an operating point with high-purity product at one end only, the movement is basically along the sharply curved contours and therefore the two gain vectors are rotated by approximately the same angle. However, there still exist slight differences in the two angle mismatches due to the fact that physical constraints on the compositions must force the angle between the two gain vectors even closer to π when the operating point is closer to either axis than the equal purity situation. This also explains why the process minimum singular values decrease from its nominal value significantly in case (1), (2), and (3) when the product purity at either end increases.

4.2.2 Catalytic Reactor Control

The following two processes to be investigated are pilot plant fluidized-bed and packed-bed reactors carrying out the same butane hydrogenolysis reactions over a nickel on silica gel catalyst. The hydrogenolysis of butane can be represented by the following overall reactions

$$
\begin{aligned}
&C_4H_{10}+H_2 \rightarrow C_3H_8+CH_4\\
&C_4H_{10}+H_2 \rightarrow 2C_2H_6\\
&C_3H_8+H_2 \rightarrow C_2H_6+CH_4\\
&C_2H_6+H_2 \rightarrow 2CH_4 \qquad (4-14)
\end{aligned}
$$

Only three of the above reaction are stochiometically independent, therefore at most three outputs or reaction species can be controlled. The controlled output variables usually are percentage butane conversion, and ethane and propane production rates. The manipulated variables are the total feed flowrate, the feed ratio (ie. hydrogen to butane flowrate), and the reactor temperature. The gain matrices listed later correspond to the process output/input vectors with the elements in the same order as described above. Numerous open-loop and control experiments have been carried out for these pilot plant reactors, including the latest such as Onderwater (1985), Kozub *et al.* (1987) on the packed-bed reactor, and McFarlane *et al.* (1983), Kelly (1991) on the fluidized-bed reactor.

4.2.2.1 The Fluidized-Bed Reactor

Mechanistic steady-state and dynamic models for the fluidized reactor were developed by Shaw (1972) and McFarlane *et al.* (1983) based on a two phase model of Orcutt *et al* (1962). Shaw (1974) has reported that this model, despite its many simplifying assumptions, predicts the conversion and selectivities reasonably well. With this nonlinear model, we can perturb the process at various operating points to obtain different gain matrices. In order to ensure that all regions were adequately considered, in our analysis a three-level factorial design in the three manipulated input variables around the nominal operating point in Table-2 was used to choose the operating points. In total twenty seven operating points were examined.

flowrate (scfm)	ratio	temperature (c)
3.48 ± 2.	10. ± 4.	262. ± 20.

Table-2 Three-level factorial design for the fluidized-bed reactor

The nominal linear process has the following gain matrix

$$\hat{G} = \begin{bmatrix} -1.24 & -.053 & .038 \\ .084 & .152 & -.100 \\ .074 & .127 & -.090 \end{bmatrix}$$

$$= \begin{bmatrix} -.99 & .10 & -.00 \\ .08 & .76 & .65 \\ .07 & .65 & -.76 \end{bmatrix} \begin{bmatrix} 1.28 & 0 & 0 \\ 0 & 0.34 & 0 \\ 0 & 0 & .008 \end{bmatrix} \begin{bmatrix} 1.00 & -.07 & .00 \\ .06 & .83 & .56 \\ -.04 & -.56 & .83 \end{bmatrix} \qquad (4-15)$$

Again, this model is very ill-conditioned with a condition number around 160 and thus a linear controller based on this model will be very sensitive to unstructured model mismatch (ie. according to (3-3.c) for additive mismatch magnitude, less than one percent of the 2-norm of the nominal process can be tolerated). However, by themselves the process nonlinearities in this reactor introduce a very structured model mismatch, in which both **U** and **V** remain roughly unchanged at most of the operating points. More precisely, the gain matrices of all the twenty seven points fall into four categories:

1) Both **U** and **V** are unchanged,

2) Either **U** or **V** is unchanged,

3) Both **U** and **V** are changed but the mismatch has a structure as in (4-6), and

4) The model mismatch leads to unstabilizable linear control.

Table-3 contains one example gain matrix from each category.

	M	$\mathbf{G}$	$\tilde{\mathbf{U}}^T\mathbf{U}$	$\tilde{\mathbf{V}}^T\mathbf{V}$	$(\Sigma^{-1}\Sigma)_{d}$
1	$\begin{bmatrix} 0 \\ 1 \\ 0 \end{bmatrix}$	$\begin{bmatrix} -0.680 & -0.038 & 0.028 \\ 0.005 & 0.152 & -0.103 \\ 0.004 & 0.130 & -0.092 \end{bmatrix}$	$\begin{bmatrix} 0.998 & 0.064 & -0.001 \\ -0.064 & 0.998 & 0.007 \\ 0.001 & -0.007 & 1.000 \end{bmatrix}$	$\begin{bmatrix} 1.000 & -0.011 & 0.001 \\ 0.011 & 1.000 & 0.008 \\ -0.001 & -0.008 & 1.000 \end{bmatrix}$	$\begin{bmatrix} .55 \\ 1.0 \\ .60 \end{bmatrix}$
2	$\begin{bmatrix} -1 \\ -1 \\ 0 \end{bmatrix}$	$\begin{bmatrix} -1.79 & -0.124 & 0.094 \\ 0.807 & 0.206 & -0.132 \\ 0.686 & 0.166 & -0.119 \end{bmatrix}$	$\begin{bmatrix} 0.903 & -0.430 & 0.005 \\ 0.430 & 0.903 & -0.017 \\ 0.003 & 0.017 & 1.000 \end{bmatrix}$	$\begin{bmatrix} 0.998 & -0.071 & 0.004 \\ 0.071 & 0.997 & -0.029 \\ -0.002 & 0.029 & 1.000 \end{bmatrix}$	$\begin{bmatrix} 1.7 \\ 0.83 \\ 2.0 \end{bmatrix}$
3	$\begin{bmatrix} 1 \\ 1 \\ -1 \end{bmatrix}$	$\begin{bmatrix} -0.726 & -0.025 & 0.005 \\ 0.003 & 0.352 & -0.045 \\ 0.002 & 0.169 & -0.029 \end{bmatrix}$	$\begin{bmatrix} 0.998 & 0.066 & -0.027 \\ -0.070 & 0.965 & -0.253 \\ 0.009 & 0.254 & 0.967 \end{bmatrix}$	$\begin{bmatrix} 1.000 & 0.010 & -0.031 \\ -0.023 & 0.896 & -0.444 \\ 0.023 & 0.444 & 0.896 \end{bmatrix}$	$\begin{bmatrix} .58 \\ 1.7 \\ 1.6 \end{bmatrix}$
4	$\begin{bmatrix} -1 \\ 0 \\ 1 \end{bmatrix}$	$\begin{bmatrix} -1.095 & -0.066 & 0.112 \\ 0.108 & 0.084 & -0.167 \\ 0.109 & 0.082 & -0.152 \end{bmatrix}$	$\begin{bmatrix} 0.998 & -0.068 & 0.009 \\ 0.067 & 0.997 & 0.034 \\ -0.011 & -0.034 & 0.999 \end{bmatrix}$	$\begin{bmatrix} 0.996 & -0.090 & -0.026 \\ 0.066 & 0.876 & -0.479 \\ -0.066 & -0.475 & -0.878 \end{bmatrix}$	$\begin{bmatrix} .90 \\ 1.0 \\ .88 \end{bmatrix}$

Table-3 Some 3×3 fluidized-bed reactor linear models

Case 1 have both $\tilde{\mathbf{V}}^T\mathbf{V}$ and $\tilde{\mathbf{U}}^T\mathbf{U}$ being identity matrices and hence the ratios of singular values $(\sigma_i/\tilde{\sigma}_i)$ are the eigenvalues of $\tilde{\mathbf{G}}^{-1}\mathbf{G}$, according to Theorem 6. When a multivariable process has model mismatch in the singular values only, the process nonlinearities in such a process act similarly to those in SISO processes. Case 2 shows that the mismatched gain matrix has virtually the same V matrix as the nominal process, while its U matrix has the structure as described in Theorem 7. The real eigenvalues will be positive and the complex ones will have positive real parts in this situation (Theorem 7 and 8).

In Case 3, there are significant mismatches in both U and V matrices. However, both $\tilde{\mathbf{U}}^T\mathbf{U}$ and $\tilde{\mathbf{V}}^T\mathbf{V}$ have the structure described in Theorem 10, and they are correlated with each other in exactly the same way as (4-6).

The process nonlinearities in some regions do cause the process to have a mismatch that is not stabilizable regardless of how we detune a controller based on the model in (4-15). Case 4 shows one of these gain matrices where the U matrix is essentially unaffected but the V is severely changed by the nonlinearities in that $\tilde{\mathbf{V}}^T\mathbf{V}$ has a negative diagonal element. It can be shown that Case 4 has one negative eigenvalue of $\tilde{\mathbf{G}}^{-1}\mathbf{G}$.

Since the 3×3 process is very ill-conditioned and thus is vulnerable to unstructured uncertainties in the modelling, it is logical to control the reactor as a 2×2 process. The 2×2 nominal process, which has the butane conversion and ethane production rate as the outputs while the feed flowrate and feed ratio as the inputs, has the following gain matrix

$$\tilde{\mathbf{G}}=\begin{bmatrix}-1.267 & -.067\\ .066 & .191\end{bmatrix}=\begin{bmatrix}-.9981 & .0611\\ .0611 & .9981\end{bmatrix}\begin{bmatrix}1.271 & 0\\ 0 & 0.187\end{bmatrix}\begin{bmatrix}.9981 & -.0618\\ .0618 & .9981\end{bmatrix} \qquad (4-16)$$

By reducing the dimension of the process, not only is the tolerable magnitude of additive unstructured uncertainty increased by almost 30 times as seen from the size of the minimum singular value in (4-16), but also it is observed that, under the structured mismatch arising from nonlinearities, all the 27 operating conditions in Table-2 are stabilizable. The U and V matrices at various operating points are generally closer to those of the nominal model than in the 3×3 cases. Three examples are listed in Table-4 which have the same mismatch structures as those in the first three cases in Table-3. Again, we can see that the structured mismatch due to process nonlinearities makes both $\tilde{\mathbf{U}}^T\mathbf{U}$ and $\tilde{\mathbf{V}}^T\mathbf{V}$ meet the sufficient conditions in Theorem 6 (Case (1)), Theorem 7 (Case (2)) and Theorem 10 (Case (3)) for condition (2-4) to be true. Note that the reactor temperature, which is shown as the bottom element of the M vector in Table-4, is not a manipulated input here and is not at its nominal value (ie. 0) in the three cases. This implies that not only the input/output nonlinearities but also the disturbance nonlinearities (ie. reactor temperature) do not affect both rotation matrices or affect them in a favorably correlated fashion.

	M	G	$\tilde{U}^T U$	$\tilde{V}^T V$	$diag(\tilde{\Sigma}^{-1}\Sigma)$
(1)	$\begin{bmatrix} 0 \\ +1 \\ 1 \end{bmatrix}$	$\begin{bmatrix} -.659 & -.024 \\ .004 & .067 \end{bmatrix}$	$\begin{bmatrix} 1.0 & .06 \\ -.06 & 1.0 \end{bmatrix}$	$\begin{bmatrix} 1.0 & .01 \\ -.01 & 1.0 \end{bmatrix}$	.53, .45
(2)	$\begin{bmatrix} -1 \\ -1 \\ 1 \end{bmatrix}$	$\begin{bmatrix} -1.89 & -.0074 \\ .806 & .093 \end{bmatrix}$	$\begin{bmatrix} .95 & -.32 \\ .32 & .95 \end{bmatrix}$	$\begin{bmatrix} 1.0 & 0.0 \\ 0.0 & 1.0 \end{bmatrix}$	1.7, .38
(3)	$\begin{bmatrix} -1 \\ -1 \\ -1 \end{bmatrix}$	$\begin{bmatrix} -1.60 & -.189 \\ .611 & .590 \end{bmatrix}$	$\begin{bmatrix} .94 & -.35 \\ .35 & .94 \end{bmatrix}$	$\begin{bmatrix} .98 & -.19 \\ .19 & .98 \end{bmatrix}$	1.4, 3.2

Table-4 Some 2×2 fluidized-bed reactor linear models

4.2.2.2 The Packed-Bed Reactor

Due to the complexity of a rigorous mechanistic model for the packed-bed reactor, the effects of process nonlinearities on the linear model mismatch will be examined only from the previous experimental works. Onderwater (1985) identified the linear models at three operating conditions which are referred as high, medium, and low stability regions. Kozub *et al.* (1987) also identified a linear model for inverse-based controller designs. In these models, the process output variables are the propane production rate and butane conversion, and the input variables are the hydrogen flowrate and hot spot temperature in the reactor. Suppose that we choose the low stability region as the nominal operating point and the nominal steady-state model is

$$\tilde{G}=\begin{bmatrix}-5.85 & 0.96\\ .95 & .64\end{bmatrix}=\begin{bmatrix}-.990 & -.142\\ .142 & -.99\end{bmatrix}\begin{bmatrix}5.99 & 0\\ 0 & 0.78\end{bmatrix}\begin{bmatrix}.990 & -.144\\ -.144 & -.990\end{bmatrix} \quad (4-17)$$

Three other steady-state models are listed in Table-5.

	G	$\tilde{U}^T U$	$\tilde{V}^T V$	$diag(\tilde{\Sigma}^{-1}\Sigma)$
(1)	$\begin{bmatrix}-6.9 & 0.54\\ 0.0 & 1.42\end{bmatrix}$	$\begin{bmatrix}.99 & -.16\\ .16 & .99\end{bmatrix}$	$\begin{bmatrix}1.000 & .06\\ -.06 & 1.0\end{bmatrix}$	1.18,1.15
(2)	$\begin{bmatrix}-3.9 & 1.21\\ 1.8 & .93\end{bmatrix}$	$\begin{bmatrix}.97 & .23\\ -.23 & .97\end{bmatrix}$	$\begin{bmatrix}1.0 & -.04\\ .04 & 1.0\end{bmatrix}$	1.72,0.72
(3)	$\begin{bmatrix}-3.6 & 1.02\\ 1.4 & 2.33\end{bmatrix}$	$\begin{bmatrix}.98 & .20\\ -.20 & .98\end{bmatrix}$	$\begin{bmatrix}.98 & .20\\ -.20 & .98\end{bmatrix}$	3.34,0.63

Table-5 Some gain matrices of the packed-bed reactor

Despite the fact that the gain matrices in Table-5 were obtained by experiments in which the model mismatch must contain some elements of unstructured uncertainties, the structured mismatch due to nonlinearities still dominates the modelling errors with respect to the nominal model in (4-17). This is evident from the fact that in all cases both $\tilde{U}^T U$ and $\tilde{V}^T V$ meet the sufficient conditions in Theorem 7 and Theorem 10.

4.3 Summary

This chapter first derives some special structures of model uncertainties using the results from Chapter 3, and then shows that such uncertainty structures indeed exist in many physical processes. Structured uncertainties arising from process nonlinearities usually impose certain correlations among the mismatch terms. For example, high-purity distillation columns have the correlation, $\delta_1 = \delta_2$ and $n_1 = n_2$ in a wide operating region, whose physical meaning is also provided using Figure-4.5 and 4.6. This geometric correlation, in ill-conditioned processes, corresponds to the structure that the V matrix is constant. For these nonlinear, ill-conditioned processes, simple linear control systems can have high performance even when the process operating conditions are changed. Another example of mismatch correlations is where the process input/output relationship is a one to one mapping, which is a necessary condition for nonlinear processes to be controlled by linear controllers with the global stabilizability. Binary distillation columns based on the short-cut model definitely satisfy this condition. However, the example of a 3×3 fluidized bed reactor clearly demonstrates that nonlinear processes can have a portion of the entire operating region that is not stabilizable using any linear controller designed for the nominal process. On the other hand, the 2×2 fluidized bed reactor represents a good example in which the robustness of controlling an ill-conditioned process is enhanced by reducing the number of input/output variables. Finally, the packed bed reactor example presents some experimental results on the relative importance of the structured (nonlinearities) vs. unstructured (identification errors) model mismatches.

5 Robust Identification

The identification of robust linear models is considered in this chapter. Since it is well-known that the uncertainties in parameter estimates are controlled by the design of experiments, this chapter focuses on this aspect.

For SISO systems, a traditional two-level input perturbation design such as the Pseudo Random Binary Sequence (PRBS) can provide very efficient estimates of linear model parameters. When applied to multivariable processes, the two-level design is usually applied to every input variable, and employed in such a manner that the inputs are perturbed simultaneously and independently, or one at a time. In the case of Multiple Input Single Output (MISO) model identification, these traditional designs still provide efficient estimates of process models. However, for multiple output systems designs, such as these which were developed for the single output case will not in general provide models that will lead to robust multivariable controllers. There are two reasons for this: 1) in these designs the modelling errors in the MIMO model have not been considered jointly, and therefore the robustness properties of the MIMO model have not been addressed; and 2) an independent design for each output does not consider the directionality of a multivariable processes. These issues are particularly important for ill-conditioned processes where very small mismatch magnitudes can lead to severe problems in closed-loop stability and performance.

This chapter applies the results in Chapter 3 on the analysis and synthesis of robust linear models to develop new criteria for the design of identification experiments. First, robust identification designs for 2×2 systems are rigorously derived from two approaches, namely, a geometric approach for robust stability and an optimal design approach for robust performance. These results lead to a very simple and unified design approach for general 2×2 processes, which can be easily generalized to high-dimensional systems and extended to address the problem of closed-loop identification. Finally, examples on identifying linear MIMO models for distillation control, and on using a sequential design approach for a 3×3 process are provided.

5.1 Criteria for Robust Identification

5.1.1 Geometric Criterion for the Stabilizability of 2×2 Systems

Linear estimation of a MIMO gain matrix considers the parameters row-wise for each output. Therefore the uncertainties of an identified gain matrix are more conveniently addressed in terms of row vectors rather than column (gain) vectors. Since the row vectors are the gain vectors of the transpose of a gain matrix, and the eigenvalues of any matrix and its transpose are the same, ie.

$$\lambda_i[(\mathbf{G}^T)(\hat{\mathbf{G}}^T)^{-1}] = \lambda_i[(\hat{\mathbf{G}}^{-1}\mathbf{G})^T] = \lambda_i(\hat{\mathbf{G}}^{-1}\mathbf{G}) \qquad (5-1)$$

both Theorems 2 and 3 are applicable to the row vectors of gain matrices as well.

Model uncertainties arising from identification errors are likely to be such that the two identified row vectors are independent to each other. In this case, we can apply the mismatch conditions Theorem 2 and Theorem 3 to become one simple condition for the stabilizability in terms of model uncertainties. Define a "singularity line" ($\hbar$) as a straight line passing through the intersection point of the two row vectors. Then a boundary can be drawn around each true row vector to enclose all possible identified row vectors as shown in Figure-5.1, which is referred here as the uncertainty region. Due to the stochastic nature of identification errors, we shall assume that not a single point in either uncertainty region can be excluded from the identification results, and then it can be derived using Theorem 2 and 3 the following property:

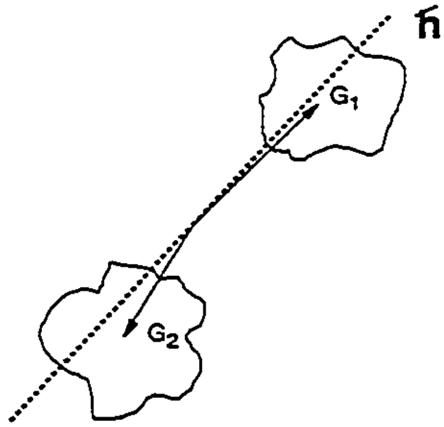

Figure-5.1 Geometric uncertainty condition for the stabilizability

Property 8

Suppose that the uncertainty regions of the two row vectors of a 2×2 gain matrix are independent. Then a multivariable controller design for this process is stabilizable for all possible identified models if and only if there exists no singularity line trespassing both uncertainty regions

This leads to the following geometric criterion. For stabilizability one should design identification experiments to shape the uncertainty regions such that there exists no singularity line trespassing these regions.

5.1.2 Criteria Using SVD Structured Uncertainty Descriptions

5.1.2.1 The Stabilizability Condition

According Theorem 7 and Theorem 8, if we can identify a model with the exact **V** matrix information and the mismatch in the **U** matrix is not too severe, in that the two conditions on the **U** matrix elements are satisfied, then the stabilizability of any controller design based on this identified model can be guaranteed. Furthermore, for the special class of nonlinear processes in which the locally linearized gain matrices at different operating points have the structure given in Theorem 7, the linear multivariable controller can provide stable control of these nonlinear processes over wide operating regions in spite of large mismatch magnitudes due to nonlinearities. Therefore, Theorem 7 also serves as a new criterion for robust identification.

Unfortunately, it is virtually impossible to identify the theoretically *exact* V matrix. Moreover, Property 7 indicates that an ill-conditioned system can be very sensitive to uncorrelated uncertainties in the **U** and **V** matrices which will always be present in identification. Therefore the best we can do is to design the experiments so that the mismatch in the identified **V** matrix is minimized. To establish an upper bound on how much the **V** matrix uncertainties must be reduced, consider the following simplified situation. Assume that the uncertainties in an ill-conditioned gain matrix is so small that all the diagonal elements of $\hat{\Sigma}^{-1}\Sigma$, $\hat{\mathbf{U}}^T\mathbf{U}$ and $\hat{\mathbf{V}}^T\mathbf{V}$ are virtually unity while the magnitudes of off-diagonal elements of the latter two matrices can be estimated by nearly zero constants, $\bar{\varepsilon}_u$ and $\bar{\varepsilon}_v$ respectively, ie.

$$\sigma_i \doteq \hat{\sigma}_i \text{ and } \hat{U}_i^T U_i \doteq \hat{V}_i^T V_i \doteq 1 \ \ \forall i \qquad (5-2.a)$$

$$\hat{U}_i^T U_j \doteq \pm\bar{\varepsilon}_u \text{ and } \hat{V}_i^T V_j \doteq \pm\bar{\varepsilon}_v \ \ \forall i \neq j \qquad (5-2.b)$$

Then (3-35.c) can then be simplified to the following

$$tr(\mathbf{G}\hat{\mathbf{G}}^{-1}) = \sum_{i=1}^{r} \lambda_i = r \ \pm \bar{\varepsilon}_u\bar{\varepsilon}_v \left(\frac{\hat{\sigma}_1}{\hat{\sigma}_r} + \sum_{i=2}^{r} \sum_{\substack{j=1 \\ j \neq i}}^{r-1} \frac{\hat{\sigma}_i}{\hat{\sigma}_j} \right) \qquad (5-3.a)$$

$$= r \pm \bar{\varepsilon}_u\bar{\varepsilon}_v\hat{\kappa}^* \qquad (5-3.b)$$

where $\hat{\kappa}^*$ is a large value greater than the condition number of the nominal process. For 2×2 systems, $\hat{\kappa}^* = \hat{\kappa} + 1/\hat{\kappa}$. Given the fact that we cannot exclude the possibility that the random identification errors in the V matrix make the $\pm\bar{\varepsilon}_u\bar{\varepsilon}_v$ negative, we therefore should establish the upper bound for the $\bar{\varepsilon}_u\bar{\varepsilon}_v$ as:

$$\bar{\varepsilon}_u\bar{\varepsilon}_v < \frac{r}{\hat{\kappa}^*} \qquad (5-4)$$

to guarantee a positive value in the trace. It is clear that as the process gets more ill-conditioned, the tolerable mismatch magnitude in the elements of U and V matrices become smaller. Theorem 11 below summarizes the effect of uncorrelated uncertainties of the U and V matrices on stabilizability.

<u>Theorem 11</u>

Assume that a r dimensional $\hat{\mathbf{G}}$ is ill-conditioned and the uncertainties between $\mathbf{G}$ and $\hat{\mathbf{G}}$ is uncorrelated and characterized by

$$\hat{\Sigma}^{-1}\Sigma = \mathbf{I},\ \hat{U}_i^T U_j = \begin{cases} 1 & i = j \\ \pm\bar{\varepsilon}_u \to 0 & i \neq j \end{cases},\ \hat{V}_i^T V_j = \begin{cases} 1 & i = j \\ \pm\bar{\varepsilon}_v \to 0 & i \neq j \end{cases}$$

then stabilizability of the closed-loop system for the locally linearized process is ensured for

1) high dimensional systems ($n \geq 3$), only if $\bar{\varepsilon}_u \bar{\varepsilon}_v < \frac{r}{\kappa}$

2) for 2×2 systems, if and only if $\bar{\varepsilon}_u \bar{\varepsilon}_v < \frac{1}{\kappa}$

The proof of this theorem for general cases has been derived from (5-2) through (5-4), while for 2×2 processes, the concept that the determinant of $\hat{\mathbf{G}}^{-1}\mathbf{G}$ is positive as shown in Theorem 10 is also needed to claim that the same condition is both necessary and sufficient. Theorem 11 implies that if we cannot reduce the mismatch in the U matrix (for example, due to the process nonlinearities), then we must minimize the uncertainty magnitude in the V matrix to meet the necessary condition for stabilizability. Therefore, this leads to a criterion that for stabilizability one should design the experiments to minimize the uncertainties in the V matrix.

5.1.2.2 The Performance Variation Condition

According to Theorem 5, if we could have the exact V matrix information, then the performance variation condition can be easily derived to be equivalent to:

$$\|\hat{G}G^{-1}\|_2 - 1 = \max_j\left(\frac{\hat{\sigma}_j}{\sigma_j}\right) - 1 \qquad (5-5.a)$$

$$\therefore \quad \min\left(\max_{\substack{\text{all directions}\\ \text{of } \Delta Y_{sp}}} \frac{\|\Psi\|_2}{\|\Delta Y_{sp}\|_2}\right) \Leftrightarrow \min_{\hat{\Sigma}} \left|\max_j \frac{\hat{\sigma}_j - \sigma_j}{\sigma_j}\right| \qquad (5-5.b)$$

Generally speaking, if any of singular values is overestimated and has the largest multiplicative error magnitude which is much larger than 1, then the $\|\hat{G}G^{-1}\|_2$ is large and there will be large performance variations. However, when a process has very different magnitudes in the singular values (ie. ill-conditioned processes), only those relatively small singular values are sensitive to modelling errors and most likely to have large multiplicative error magnitudes.

To illustrate this, consider a simple situation of an ill-conditioned 2×2 processes where the mismatches are present in the singular values only:

$$\|G - \hat{G}\|_2 = \|U(\Sigma - \hat{\Sigma})V^T\|_2 = \|\Sigma - \hat{\Sigma}\|_2 \qquad (5-6.a)$$

$$= \max_j\left(\sigma_j\left|\frac{\hat{\sigma}_j}{\sigma_j} - 1\right|\right) \quad j = 1,2 \qquad (5-6.b)$$

Therefore, given an additive mismatch magnitude of the gain matrix, $l_G = \|G - \hat{G}\|_2$, either the absolute value of the maximum singular value multiplied by its multiplicative error ($\sigma_1|\hat{\sigma}_1/\sigma_1 - 1|$) or that of the minimum singular value ($\sigma_2|\hat{\sigma}_2/\sigma_2 - 1|$) will equal to this value. However, the latter situation corresponds to a much larger multiplicative error, ie.

$$\left|\frac{\hat{\sigma}_2}{\sigma_2} - 1\right| = \frac{l_G}{\sigma_2} \gg \frac{l_G}{\sigma_1} = \left|\frac{\hat{\sigma}_1}{\sigma_1} - 1\right| \qquad (5-7)$$

For example, suppose that the additive mismatch magnitude cannot exceed σ_1, then the multiplicative error magnitude of the maximum singular value on the RHS of (5-7) must be equal to or smaller than 1, while that of the minimum singular value on the LHS can be much larger than 1. Hence, for ill-conditioned 2×2 processes, the RHS of (5-5.b) is equivalent to the following condition:

$$\underset{\Sigma}{\mathrm{Min}} \left| \frac{\hat{\sigma}_2}{\sigma_2} - 1 \right| \qquad (5-8)$$

Extensions of (5-6), (5-7) and (5-8) to high-dimensional processes with more than one small singular values are straightforward and will not be shown here.

Property 9

> Suppose that the V matrix could be exactly identified. Then the performance variation condition in (2-11) is most sensitive to the mismatches in the relatively small singular values.

This provides a performance related criterion that one should identify the smaller singular values as precisely as possible. Anderson and Kummel (1991) drew the same conclusion from a simulation study, in which they found that it is very difficult in ill-conditioned processes to identify the minimum singular value at low frequency with enough accuracy and the control performance will suffer if the accuracy is not improved.

5.2 Design of Experiments

Traditional criteria for the optimal design of identification experiments have always involved minimizing some overall measures of parameter uncertainties associated with one output only (ie. for MISO model). Nevertheless, the above criteria for robust identification imply that we should design the experiments such that the parameter uncertainties associated with all outputs should be treated jointly. In this section, we will discuss two new design approaches which are derived from the above robust identification criteria. The geometric approach for 2×2 processes is to shape the uncertainty regions for the two row vectors in a gain matrix such that Property 8 is satisfied. The other design criteria are to minimize the uncertainties in the input rotation matrix (V) and in the small singular values in order to satisfy Theorem 11 for the stabilizability, and Property 9 for the performance variation. Furthermore, a new concept of designing experiments in the transformed input space is shown to unify all these design approaches and provide a general design criterion.

5.2.1 Geometric Approach for 2×2 Systems

5.2.1.1 Experimental Designs for Stabilizability

Under the assumption that the errors in the k-th output are normally distributed with a mean 0 and variance $\sigma^2_{e_k}$, it is well known that the least square estimates of the parameters in the k-th row of a gain matrix has a joint confidence region defined by the ellipse (Beck and Arnold, 1977):

$$(G_k^* - \hat{G}_k^*)(\mathbf{M}^T\mathbf{M})(G_k^* - \hat{G}_k^*)^T = rs^2_{e_k}F_\alpha(r, n-r) = c^2 \quad k = 1,2 \qquad (5-9.a)$$

or

$$\left(\sum_{i=1}^{n} m_{1i}^2\right)(g_{k1} - \hat{g}_{k1})^2 + 2\left(\sum_{i=1}^{n} m_{1i}m_{2i}\right)(g_{k1} - \hat{g}_{k1})(g_{k2} - \hat{g}_{k2}) + \left(\sum_{i=1}^{n} m_{2i}^2\right)(g_{k2} - \hat{g}_{k2})^2 = c^2 \quad (5-9.b)$$

where $G_k^* = [g_{k1} \quad g_{k2}]$ is the k-th row vector of $\mathbf{G}$, $s^2_{e_k}$ is the estimated variance, $F_\alpha(r, n-r)$ is the critical value of the F-distribution with $r+(n-r)$ degrees of freedom at α level of significance, and $\mathbf{M}$ is the design matrix of manipulated input settings:

$$\mathbf{M} = [m_{1i} \quad m_{2i}]_{n\times 2}\ ,\ \mathbf{M}^T\mathbf{M} = \begin{bmatrix} \sum_{i=1}^{n} m_{1i}^2 & \sum_{i=1}^{n} m_{1i}m_{2i} \\ \sum_{i=1}^{n} m_{1i}m_{2i} & \sum_{i=1}^{n} m_{2i}^2 \end{bmatrix} \qquad (5-9.c)$$

This joint confidence region is the uncertainty region of the k-th row vector defined earlier in discussing Property 8. Note that, aside from their locations, the uncertainty ellipses for the two row vectors are the same because the same $\mathbf{M}^T\mathbf{M}$ matrix appear in (5-9.a) for both vectors. With the additional assumption that the errors in the two outputs are independent, we can apply the geometric necessary and sufficient condition in Property 8 to examine how different designs affect the stabilizability of the closed-loop system using the identified models. The uncertainty regions can be classified as: 1) ellipses with a horizontal or vertical major axis when the cross product term is 0 (ie. the two inputs are designed to be uncorrelated), or 2) ellipses with inclined axes when the two inputs are correlated.

The most common practice in identification is to design the inputs to be uncorrelated. This can be achieved by either perturbing only one input at a time (ie. each $m_{1i}m_{2i}$ is 0), or all inputs simultaneously but independently (ie. $\sum_{i=1}^{n} m_{1i}m_{2i}$ is close to 0). A well-known example for the latter is a two-level design in which each input is perturbed independently at its upper and lower levels. It can be shown that the latter two-level design is also able to minimize the area of the joint confidence region for all the parameters associated with one output ((5-9.b)). This is the so-called "D-optimality" criterion, in which the determinant of M^TM in (5-9.a) is maximized by the design. For dynamic systems, independent PRBS's with well chosen switching intervals are good approximation to the D-optimality design.

Figure-5.2(a) illustrates the joint confidence regions of the two row vectors that would be obtained from applying independent inputs to an ill-conditioned process. We can see from this figure that, because of the collinearity of the true gain vectors coupled with the orientation of the major axis of the uncertainty regions, the necessary and sufficient condition for the stabilizability in Property 8 cannot be satisfied by this uncorrelated design. In order to meet this stabilizability condition, the uncorrelated design would have to be modified to have more experiments or larger magnitudes of input perturbations such that the ellipses would be reduced sufficiently (Figure-5.2(b)) so that there exists no singularity line ($\hbar$) that can intersect both regions. However, for ill-conditioned processes the required number of experiments, or the increased variations in the output responses as a result of increasing the input magnitudes, is often unacceptable.

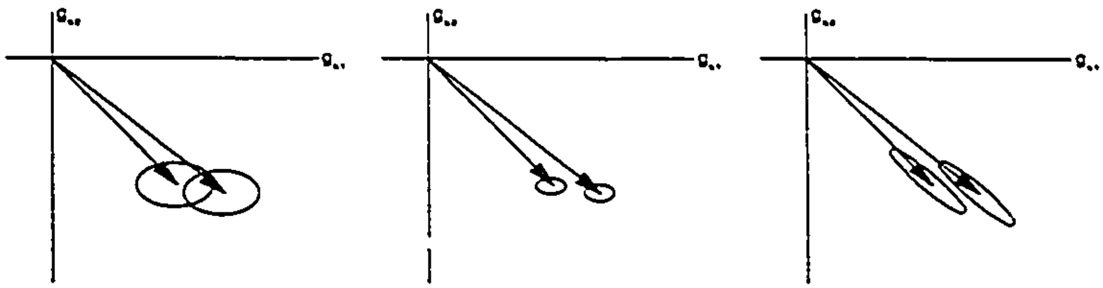

(a) an arbitrarily uncorrelated design

(b) a modified design of (a) with increased magnitudes or number of experiments

(c) the new design of correlated inputs

Figure-5.2 Uncertainties from different input designs

Geometrically, an obvious method to meet the condition in Property 8 is to rotate the ellipse in Figure-5.2(a) such that the major axis is parallel to the row vectors, and to simultaneously decrease the ratio of minor to major axis length such that the major uncertainties are only in the lengths of the two vectors (Figure-5.2(c)). Of course, this design strategy requires some prior knowledge about the direction of the row vectors to be identified. If this is not available, it can be achieved by using a sequential design approach which will be discussed later. The most significant result from Figure-5.2(c) is that proper designs for stabilizability of this type of ill-conditioned process will have correlated input perturbations (ie. the ellipse has an inclined major axis). This is contrary to the general belief that we should use independent perturbations in the two inputs. The latter would provide uncorrelated parameter estimates but less robust models. Another important advantage of taking this approach to design is that the robust identification can be accomplished with many fewer experiments or with input variations that cause much smaller output variations than the case in Figure-5.2(b). More details on the latter will be discussed later.

In summary, we have established a geometric basis for experimental design that mainly considers the orientation of the uncertainty regions for the row vectors in the gain matrix of 2×2 systems. The orientation of the ellipses as well as the required ratio of the minor to major axis lengths depend on the particular MIMO process being considered, Therefore, in the following, we unify the designs for different processes in the transformed input space.

5.2.1.2 Unified Design in Terms of the Rotated Inputs

Consider the following input transformation based on the SVD of a gain matrix:

$$\mathbf{G} \cdot M = (\mathbf{U}\Sigma)(\mathbf{V}^T \cdot M) \stackrel{\Delta}{=} \Omega \cdot \xi \qquad (5-10)$$

where ξ is a result of multiplying the input rotation matrix by the input vector, and therefore will be referred here as a *rotated* or *transformed* input vector. Design of experiments for the settings of ξ will determine the uncertainties in the elements of the *transformed* gain matrix Ω, which can be interpreted as the output rotation matrix being re-scaled column-wise by the singular values. Figure-5.3 provides a geometric interpretation for a transformed gain matrix.

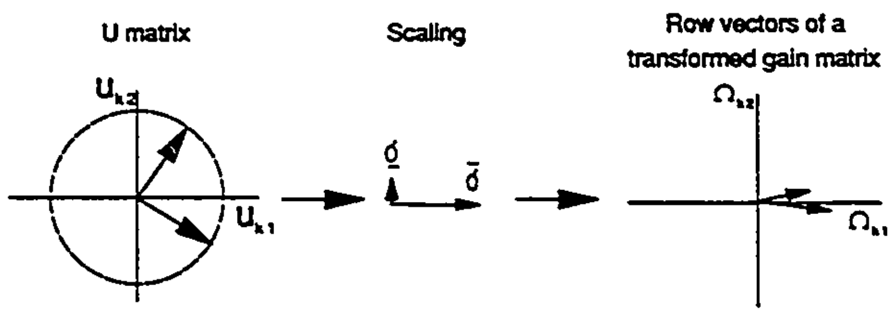

Figure-5.3 The formation of a transformed gain matrix

Figure-5.4(a) shows two circles around the row vectors of the transformed gain matrix. These are the uncertainty regions from an uncorrelated design with the same perturbation magnitude in both rotated inputs. According to Property 8, the design in Figure-5.4(a) does not lead to robust identification. It is clear from this figure that the major problem with ill-conditioned processes is the very small minimum singular value, which scales the vertical components of row vectors to be so small that both uncertainty regions can easily have their vertical components being positive or negative. Then the horizontal axis itself is a singularity line trespassing both uncertainty regions.

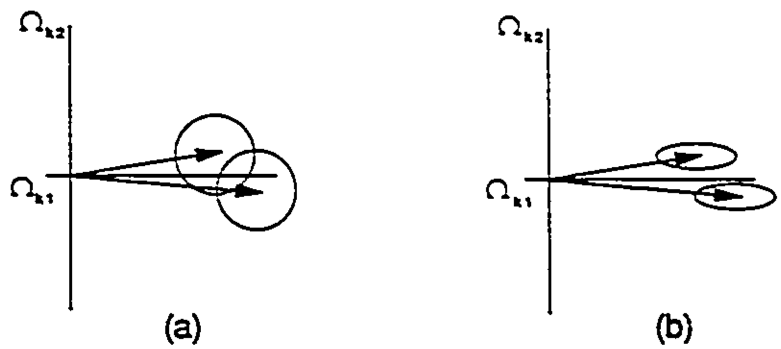

(a) the same perturbation magnitude in two rotated inputs

(b) the second rotated input has a larger magnitude than the first

Figure-5.4 The uncertainties from two uncorrelated designs of experiments

A proper design for the transformed process should yield uncertainty regions similar to Figure-5.4(b). This design would still be an uncorrelated design in the rotated inputs, but would have a larger magnitude in the rotated input corresponding to the smaller singular value. When the input magnitude in this direction is large enough that neither uncertainty region has the possibility of a sign mismatch, then stabilizability is guaranteed because then no singularity line can trespass both regions. This result is totally consistent with Theorem 5, 7 and 8. When there is no sign mismatch in the transformed gain matrix, there is no sign mismatch in the identified **U** matrix because singular values are always positive. Note that the second condition on the **U** matrix elements is always met in 2×2 systems. Therefore, we conclude that an uncorrelated design in the rotated inputs with a sufficiently larger magnitude in the second rotated input perturbation is necessary to identify general transformed processes that satisfy the stabilizability condition.

Given an estimate of the input rotation matrix, the design of rotated inputs discussed above can be easily translated into the design of the physical inputs by a simple inverse calculation, $M = \mathrm{V}\xi$. Consider as an example the ill-conditioned process with nearly collinear column vectors discussed in Figure-5.2 and with the gain matrix given by (2-1.a). This process has its true rotated input vector as following

$$\xi = \begin{bmatrix} 0.71 & -0.71 \\ -0.71 & -0.71 \end{bmatrix} \cdot \begin{bmatrix} m_1 \\ m_2 \end{bmatrix} = \begin{bmatrix} 0.71m_1 - 0.71m_2 \\ -0.71m_1 - 0.71m_2 \end{bmatrix} \qquad (5-11)$$

Suppose we design the rotated inputs using an independent two-level design where the second rotated input has a 10 times larger perturbation than the first. Then the four components of both the rotated and the corresponding physical input perturbations are given below

$$\xi_i \in \left\{ \begin{bmatrix} 1.4 \\ 14 \end{bmatrix}, \begin{bmatrix} -1.4 \\ 14 \end{bmatrix}, \begin{bmatrix} 1.4 \\ -14 \end{bmatrix}, \begin{bmatrix} -1.4 \\ -14 \end{bmatrix} \right\} \Leftrightarrow M_i \in \left\{ \begin{bmatrix} -9 \\ -11 \end{bmatrix}, \begin{bmatrix} -11 \\ -9 \end{bmatrix}, \begin{bmatrix} 11 \\ 9 \end{bmatrix}, \begin{bmatrix} 9 \\ 11 \end{bmatrix} \right\} \qquad (5-12)$$

Note that the two physical inputs always change in the same direction (ie. either increase or decrease simultaneously), and therefore are highly correlated. This result is same as that from the earlier approach shown in Figure-5.2(c) which directly designs the physical inputs based on the geometric analysis of the original gain matrix. It should be emphasized that the new correlated design yields approximately the same output range of $Y_i \doteq [\pm 1 \ \pm 1]^T$ as the traditional uncorrelated design of $M_i = [\pm 1 \ \pm 1]^T$. In other words, the proposed design approach can reduce the parameter uncertainty without the cost of a wider range of output variations. More general treatments on the issue of output variations will be presented later.

If the input rotation matrix could be estimated exactly, then applying the designed physical inputs would yield a physical model with stabilizability because

$$\mathrm{G}\hat{\mathrm{G}}^{-1} = \Omega \mathrm{V}^T (\hat{\Omega} \mathrm{V}^T)^{-1} = \Omega \hat{\Omega}^{-1} \qquad (5-13)$$

However, the true V matrix is never known exactly, and therefore the design of experiments in terms of the rotated inputs will only asymptotically ensure the robustness of physical models. Therefore, it is also crucial to precisely identify the V matrix. This problem is discussed in the following section.

5.2.2 Optimal Design Approach

As discussed earlier in Theorem 11 and Property 9, criteria for robust identification require that mismatches in the identified **V** matrix, and uncertainties in the small singular values be minimized. Therefore, we need to find the optimal designs for the precise estimation of the **V** matrix and the small singular values. Since the parameters in SVD matrices,

$$\mathbf{G} = \mathbf{U}\Sigma\mathbf{V}^T = \begin{bmatrix} u_{11} & . & . \\ . & . & . \\ . & . & u_{rr} \end{bmatrix} \begin{bmatrix} \sigma_1 & . & 0 \\ . & . & . \\ 0 & . & \sigma_r \end{bmatrix} \begin{bmatrix} v_{11} & . & . \\ . & . & . \\ . & . & v_{rr} \end{bmatrix}^T \qquad (5-14)$$

enter the model nonlinearly, we apply some well-established methods on the optimal design of experiments for nonlinear parameter estimation to robust identification in this section. Note that although we consider the nonlinear SVD parameters in the experimental designs, it is not necessary to estimate them using a nonlinear estimation algorithm because, due to the invariance principle of maximum likelihood estimation (Hogg and Craig, 1965), they can always be obtained by performing SVD on the linearly estimated gain matrix.

5.2.2.1 Optimal Designs for a Subset of SVD Parameters

The uncertainties of an estimated nonlinear parameter vector $\hat{\beta}$ can be characterized by the approximate covariance matrix (Beck and Arnold, 1977):

$$\mathbf{cov}(\hat{\beta} - \beta) = \mathrm{E}[(\hat{\beta} - \beta)(\hat{\beta} - \beta)^T]$$

$$\doteq \left\{ \sum_{i=1}^{n} \mathbf{X}_i^T \left[diag\left(\sigma_{e_1}^2, ..., \sigma_{e_r}^2 \right) \right]^{-1} \mathbf{X}_i \right\}^{-1} \qquad (5-15.a)$$

$$= \left(\sum_{i=1}^{n} \mathbf{X}_i^T \mathbf{X}_i \right)^{-1} \sigma_e^2 \text{ if } \sigma_{e_k}^2 = \sigma_e^2 \; \forall k \qquad (5-15.b)$$

$$= (\mathbf{X}^T\mathbf{X})^{-1} \sigma_e^2 \qquad (5-15.c)$$

where $\sigma^2_{e_k}$ is the error variance of the k-th output. To simplify (5-15.a) to become (5-15.b) and (5-15.c), it is assumed that all the output variables are scaled to have the same error variance (σ^2_e). Specifically for estimating the SVD parameters of a gain matrix,

$$\mathbf{X}_i = \mathbf{X}_i(\beta, m_{1i}, \ldots, m_{ri})$$

$$= \begin{bmatrix} \frac{\partial\eta_1}{\partial\beta_{U_1}}|_i & \cdot & \frac{\partial\eta_1}{\partial\beta_{U_p}}|_i & | & \frac{\partial\eta_1}{\partial\sigma_1}|_i & \cdot & \frac{\partial\eta_1}{\partial\sigma_r}|_i & | & \frac{\partial\eta_1}{\partial\beta_{V_1}}|_i & \cdot & \frac{\partial\eta_1}{\partial\beta_{V_p}}|_i \\ \cdot & \cdot & \cdot & | & \cdot & \cdot & \cdot & | & \cdot & \cdot & \cdot \\ \frac{\partial\eta_r}{\partial\beta_{U_1}}|_i & \cdot & \frac{\partial\eta_r}{\partial\beta_{U_p}}|_i & | & \frac{\partial\eta_r}{\partial\sigma_1}|_i & \cdot & \frac{\partial\eta_r}{\partial\sigma_r}|_i & | & \frac{\partial\eta_r}{\partial\beta_{V_1}}|_i & \cdot & \frac{\partial\eta_r}{\partial\beta_{V_p}}|_i \end{bmatrix}_{r\times r^2} \qquad (5-15.d)$$

in which $\eta_k = G_k^* \cdot M$ is the k-th predicted output and $p = (r^2 - r)/2$.

The partition of the X matrix as shown in (5-15.c) is to group the parameters belonging to the U, Σ and V, respectively. Note that although the total number of elements in either the U or V matrix is r^2 the number of independent parameters is $(r^2 - r)/2$ because of the equality constraints arising from orthogonality and the unit length of column vectors in a unitary matrix. In this study, the matrix $\mathbf{X}_i^T\mathbf{X}_i$ in (5-15.b) is referred as the "sample information matrix" at the i-th experiment from which the effects of input variable settings on the uncertainties of the nonlinear parameters can be evaluated. Due to the complexity of $\mathbf{X}_i^T\mathbf{X}_i$ as a function of the input settings, generally we must rely on the numerical results to examine how an experimental design affects the uncertainties of the elements of the SVD matrices. An exception is for 2×2 systems where $\mathbf{X}_i^T\mathbf{X}_i$ is shown later to have a simple analytical form, and this is used to provide a deeper understanding of the uncertainties in the elements of the SVD matrices.

A criterion for experimental design for precise estimation of a subset of nonlinear parameters was proposed by Hunter *et al* (1969). First, the sample information matrix for all the experiments, $\mathbf{X}^T\mathbf{X}$, is partitioned according to the parameters of interest (β_1) and the nuisance parameters (β_2), ie.

$$\mathbf{X}^T\mathbf{X} = \sum_{i=1}^{n} \mathbf{X}_i^T\mathbf{X}_i = \begin{bmatrix} \chi_{11} & | & \chi_{12} \\ -- & + & -- \\ \chi_{21} & | & \chi_{22} \end{bmatrix} \qquad (5-16)$$

where the χ_{11} matrix is the partition for the parameter vector of interest (β_1). Then, the criterion for the experimental design is

$$\underset{M}{\mathrm{Max}}\ det(\chi_{11} - \chi_{12}\chi_{22}^{-1}\chi_{21}) \qquad (5-17)$$

For models linear in the parameters, this criterion minimizes the volume of region of highest posterior probability of the marginal distribution for the parameters of interest. For models nonlinear in the parameters, this yields approximate results. When only the parameters of the V matrix are of interest, the columns of the $\mathbf{X}_i$ in (5-15.c) need to be rearranged to have the sensitivity coefficients for the V matrix parameters in the first columns, and then the resulting $\mathbf{X}^T\mathbf{X}$ partitioned accordingly. The same procedure can be used to obtain the optimal design that minimizes the uncertainties in the small singular values.

The design optimization problem in (5-17) is not complete until some constraints are specified. Traditionally constraints in the optimal design problem are simply the bounds on inputs. However, for a control problem it is more meaningful to constrain the output variables. However, the input bounds are still necessary when they indeed represent the physical limitations. In single-response estimation problems, bounding the inputs is equivalent to bounding the output. On the other hand, when we need to bound all the outputs simultaneously in the multiple-response problem of identifying a gain matrix, the input bounds are not necessarily equivalent to the output bounds. In particular, if the MIMO relationship has strong directionality (ie. is ill-conditioned), the region of output variations resulting from bounding the inputs can be drastically different from the one determined by the actual output bounds. For example, in Figure-5.5 the square region with hard bounds on both outputs defines an area of permissible output variations, while the shaded region is the actual region of output variations when the input hard bounds are specified.

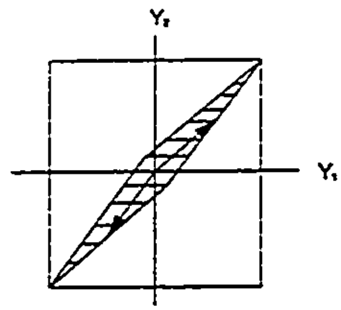

Figure-5.5 Output variation regions from input bounds (shaded area) and from output bounds

It becomes clear that the traditional practice of specifying the input bounds does not provide efficient identification, because a vast portion of the permissible region of output variations (ie. white area within the square) is not exploited. By moving the outputs toward the right bottom corner, input changes with large magnitudes in a certain combination may be required, but this may yield more information on the parameters. Therefore we should impose the output constraint directly in addition to the hard bound input constraints to the optimization problem in (5-17) as follows

$$Y_{low} < \mathbf{G} \cdot M_i < Y_{high} \ \forall i \qquad (5-18)$$

In summary, a new approach for the design of experiments for robust MIMO model identification has been formulated in terms of minimizing the area or volume of the joint confidence region of a subset of the SVD parameters of a gain matrix (ie. for the V matrix parameters or the small singular values). As with the geometric design approach, this optimal design approach will yield results which depend heavily on the specific gain matrix of the MIMO process. Moreover, numerical optimization is usually necessary to maximize (5-17). However, in the following, the analytical solutions to the optimal design problem are derived for 2×2 systems, and it is shown that this design approach can again be unified in terms of the rotated inputs in a very simple fashion.

5.2.2.2 Analytical Solutions for 2×2 Systems

Applying the expression in (4-4) again for 2×2 systems, the linear model in terms of SVD parameters can be simplified as the following:

$$Y_i = \mathrm{G}M_i + E_i = \begin{bmatrix} \cos\theta & -\sin\theta \\ \sin\theta & \cos\theta \end{bmatrix} \begin{bmatrix} \bar{\sigma} & 0 \\ 0 & \underline{\sigma} \end{bmatrix} \begin{bmatrix} \cos\phi & -\sin\phi \\ -\sin\phi & -\cos\phi \end{bmatrix} \cdot M_i + E_i \qquad (5-19.a)$$

$$= \begin{bmatrix} \eta_{1i} \\ \eta_{2i} \end{bmatrix} + E_i \qquad (5-19.b)$$

where
$$\begin{cases} \eta_{1i} = (\bar{\sigma}\cos\theta\cos\phi + \underline{\sigma}\sin\theta\sin\phi)m_{1i} + (-\bar{\sigma}\cos\theta\sin\phi + \underline{\sigma}\sin\theta\cos\phi)m_{2i} \\ \eta_{2i} = (\bar{\sigma}\sin\theta\cos\phi - \underline{\sigma}\cos\theta\sin\phi)m_{1i} + (-\bar{\sigma}\sin\theta\sin\phi - \underline{\sigma}\cos\theta\cos\phi)m_{2i} \end{cases} \qquad (5-19.c)$$

assuming that the element signs in the two rotation matrices are known. An analytical expression for the sample information matrix of these SVD parameters has been derived in Appendix-8 as the following:

$$\mathbf{X}^T\mathbf{X} = \begin{bmatrix} \bar{\sigma}^2 \sum_{i=1}^{n} \xi_{1i}^2 + \underline{\sigma}^2 \sum_{i=1}^{n} \xi_{2i}^2 & -\bar{\sigma}\underline{\sigma}\left(\sum_{i=1}^{n} \xi_{1i}^2 + \sum_{i=1}^{n} \xi_{2i}^2\right) & -\underline{\sigma}\sum_{i=1}^{n} \xi_{1i}\xi_{2i} & \bar{\sigma}\sum_{i=1}^{n} \xi_{1i}\xi_{2i} \\ \cdot & \bar{\sigma}^2 \sum_{i=1}^{n} \xi_{2i}^2 + \underline{\sigma}^2 \sum_{i=1}^{n} \xi_{1i}^2 & \bar{\sigma}\sum_{i=1}^{n} \xi_{1i}\xi_{2i} & -\underline{\sigma}\sum_{i=1}^{n} \xi_{1i}\xi_{2i} \\ \cdot & \cdot & \sum_{i=1}^{n} \xi_{1i}^2 & 0 \\ sym & \cdot & \cdot & \sum_{i=1}^{n} \xi_{2i}^2 \end{bmatrix} \qquad (5-20)$$

where $\xi_{1i} = V_1^T \cdot M_i$ and $\xi_{2i} = V_2^T \cdot M_i$ are the rotated inputs.

Note that this sample information matrix depends upon the data only through the elements of the sample information matrix of the transformed gain matrix Ω in (5-10), ie.

$$\Xi^T\Xi = \begin{bmatrix} \sum_{i=1}^{n} \xi_{1i}^2 & \sum_{i=1}^{n} \xi_{1i}\xi_{2i} \\ \sum_{i=1}^{n} \xi_{2i}\xi_{1i} & \sum_{i=1}^{n} \xi_{2i}^2 \end{bmatrix} \triangleq \begin{bmatrix} \zeta_1 & \zeta_3 \\ \zeta_3 & \zeta_2 \end{bmatrix} \qquad (5-21.a)$$

where $\Xi = [\xi_{1i} \;\; \xi_{2i}]_{n \times 2}$ $\qquad (5-21.b)$

Since it has been shown earlier that an uncorrelated design in the rotated inputs is good for robust identification of the transformed gain matrix, let us examine how the uncertainties of SVD parameters are affected by such designs. Under this situation, the sample information matrix $X^T X$ becomes block diagonal. The sample information matrix for the marginal distribution of each parameter (ie. $\Delta(\beta_1) = det(\chi_{11} - \chi_{12}\chi_{22}^{-1}\chi_{21})$ as given in (5-17)) can be obtained for each of the SVD parameters as the following:

$$\Delta(\theta) = \frac{\left(\overline{\sigma}^2 - \underline{\sigma}^2\right)^2 \zeta_1 \zeta_2}{\overline{\sigma}^2 \zeta_2 + \underline{\sigma}^2 \zeta_1} \qquad (5-22.a)$$

$$\Delta(\phi) = \frac{\left(\overline{\sigma}^2 - \underline{\sigma}^2\right)^2 \zeta_1 \zeta_2}{\overline{\sigma}^2 \zeta_1 + \underline{\sigma}^2 \zeta_2} \qquad (5-22.b)$$

$$\Delta(\overline{\sigma}) = \zeta_1 \qquad (5-22.c)$$

$$\Delta(\underline{\sigma}) = \zeta_2 \qquad (5-22.d)$$

Several important properties of uncorrelated designs in the rotated inputs can be concluded from the above equation.

1) The sample infonnation content on the minimum singular value ($\Delta(\underline{\sigma})$) is equal to the sum of squares of the second rotated input changes. Therefore, the optimal design for estimation of the minimum singular value, under the constraint of uncorrelated rotated inputs, is simply to perturb the second rotated input between its upper and lower bounds.

2) Since the sample information content on the V matrix ($\Delta(\phi)$) is a monotonic function of the rotated inputs, a design that increases $\Delta(\phi)$ will always decrease the inverse of the sample information content ($1/\Delta(\phi)$), which is proportional to the variance of ϕ. The $1/\Delta(\phi)$ can be expressed as

$$\frac{1}{\Delta(\phi)} = \left(\frac{\overline{\sigma}}{\overline{\sigma}^2 - \underline{\sigma}^2}\right)^2 \cdot \frac{1}{\zeta_2} + \left(\frac{\underline{\sigma}}{\overline{\sigma}^2 - \underline{\sigma}^2}\right)^2 \cdot \frac{1}{\zeta_1} \qquad (5-23)$$

Thus increasing the perturbation magnitude of either rotated input always decreases the variance of the V matrix parameter ϕ. However, for ill-conditioned processes, the first term on the RHS of (5-23) dominates. Consequently, the most efficient way to increase the information content of the V matrix is again to increase the perturbation magnitude of the *second rotated input.*

3) Since the minimum of (5-23) is reached when both ζ_1 and ζ_2 are at their maximum values, the two rotated inputs should be designed to have the maximum magnitude in each experiment, ie. a two-level design,

$$|\xi_{1i}| = \bar{\xi}_1 \text{ and } |\xi_{2i}| = \bar{\xi}_2 \quad \forall i \tag{5-24}$$

It can be easily derived that the unconstrained minimum of (5-23) is equal to

$$\left(\frac{1}{\Delta(\phi)}\right)_{\min} = \frac{\bar{\sigma}\underline{\sigma}}{\bar{\sigma}^2 - \underline{\sigma}^2}\sqrt{\frac{1}{\zeta_1\zeta_2}} \tag{5-25.a}$$

and this occurs when

$$\frac{\bar{\sigma}^2}{\zeta_2} = \frac{\underline{\sigma}^2}{\zeta_1} \tag{5-25.b}$$

Translating (5-25.b) into the magnitudes of the rotated inputs for a two-level design, we have

$$\frac{\zeta_2}{\zeta_1} = \frac{n\bar{\xi}_2^2}{n\bar{\xi}_1^2} = \left(\frac{\bar{\sigma}}{\underline{\sigma}}\right)^2 \triangleq \kappa^2 \tag{5-26.a}$$

$$\therefore \quad \left(\frac{\bar{\xi}_2}{\bar{\xi}_1}\right)_{opt} = \kappa \tag{5-26.b}$$

where κ is the condition number. Therefore in the identification of ill-conditioned processes, the magnitude of the second rotated input perturbation should be much larger than the first one. If there is no constraint on the magnitude of input perturbation, the optimum ratio can always be achieved. However, in practice, hard bounds on the physical inputs always exist and they usually limit the magnitude of the second rotated input. In this case, one should not reduce the magnitude of the first rotated input perturbation in order to reach the optimal ratio. Remember that the maximum information content of the V matrix, according to (5-25.a), is proportional to $\sqrt{\zeta_1}$. Therefore one should use the maximum allowable magnitude for the first rotated input, which is determined from its effects on the output variations.

So far we have only examined the optimal designs under the assumption that the rotated inputs are uncorrelated. Without this assumption, analytical expression can still be derived for the information content on the ϕ and $\underline{\sigma}$ for ill-conditioned processes in which the sampled information matrix in (5-20) can be approximated as

$$\mathbf{X}^T\mathbf{X} = \begin{bmatrix} \overline{\sigma}^2\zeta_1 & -\overline{\sigma}\underline{\sigma}(\zeta_1+\zeta_2) & 0 & \overline{\sigma}\zeta_3 \\ \cdot & \overline{\sigma}^2\zeta_2 & \overline{\sigma}\zeta_3 & 0 \\ \cdot & \cdot & \zeta_1 & 0 \\ sym & \cdot & \cdot & \zeta_2 \end{bmatrix} \qquad (5-27)$$

Here all the elements multiplied by only the minimum singular value in (5-20) have been set to zero. Analytical expressions for the information content on ϕ and $\underline{\sigma}$ can then be derived as the following (Appendix-9):

$$\Delta(\phi) = \overline{\sigma}^2\left(\frac{\zeta_1\zeta_2 - \zeta_3^2}{\zeta_1}\right) \qquad (5-28.a)$$

$$\Delta(\underline{\sigma}) = \zeta_2 - \left\{\frac{\overline{\sigma}\underline{\sigma}\zeta_1(\zeta_1+\zeta_2) + \overline{\sigma}^2[\underline{\sigma}(\zeta_1+\zeta_2) + (\zeta_1\zeta_2 - \zeta_3^2)]}{\overline{\sigma}^2\zeta_1(\zeta_1\zeta_2 - \zeta_3^2)}\right\}\zeta_3^2 \qquad (5-28.b)$$

As expected, when the rotated inputs are uncorrelated (ie. $\zeta_3 = 0$), (5-28.b) reduces to (5-22.d) and furthermore when the minimum singular value is negligible, (5-28.a) and (5-22.b) both reduce to $\overline{\sigma}^2\zeta_2$. When the two rotated input perturbations are designed to be correlated, the non-zero ζ_3^2 term always decreases the information content of the V matrix parameter (note that $\zeta_1\zeta_2 - \zeta_3^2$ is always positive because it is the determinant of positive definite $\Xi^T\Xi$ matrix). Similarly, the non-zero ζ_3^2 also always reduce the information content of the minimum singular value since every term in the big bracket is positive. Therefore, we conclude that any correlation between the two rotated inputs must reduce the information contents of the data on both the V matrix and the minimum singular value, thereby implying that orthogonal designs in the rotated inputs are optimal for robust model identification of 2×2 systems.

5.2.3 Generalization to High-Dimensional Systems

For 2×2 systems, the geometric design criterion has shown that the two rotated inputs should be uncorrelated and the second rotated input should have a larger magnitude than the first to better ensure stabilizability. On the other hand, the optimal design criteria require the same orthogonal designs of rotated inputs, and moreover provide an optimum ratio for the two perturbation magnitudes which is equal to the inverse ratio of the two singular values corresponding to the two rotated inputs as given in (5-26). This orthogonal designs of rotated inputs can easily extended to high-dimensional systems, and particularly the ratio of singular values can be generalized as the following:

$$\frac{\sigma_1}{\sigma_k}=\frac{\xi_k}{\xi_1} \qquad \forall k\,,\,k\neq1 \tag{5-29}$$

Therefore, a design strategy for robust identification experiments for multivariable processes of arbitrary dimension is proposed in the following:

1) Scale the outputs to have the same error variance.

2) Given an initial estimate of a gain matrix, we can perform a SVD to obtain the transformed gain matrix and the rotated inputs.

3) When the process to be identified is ill-conditioned, its transformed gain matrix always have some column vectors with very small lengths compared with others. An uncorrelated design of experiments in the transformed space that perturbs the rotated inputs corresponding to these short column vectors as much as possible can better ensure that the transformed gain matrices of the true process and the model satisfy the stabilizability

and performance variation conditions. The same design improves the estimation of the input rotation matrix, and therefore the robustness of the physical closed-loop system is asymptotically ensured.

4) Obtain the physical input settings from the designed settings of rotated inputs to conduct a few more experiments for a better estimate of the gain matrix, and then repeat the above procedures.

These ideas along with some numerical confirmations will be illustrated later in the example of a 3×3 process.

5.3 Closed-Loop Robust Identification

Robust identification designs have so far been discussed in the context of open-loop experiments (ie. input designs), and the proper variations of the process outputs that lead to robust identification have not been considered. In the following, the effects of the proposed designs on the outputs are analyzed. The analysis results explain why closed-loop identification can yield more robust models.

The output directionality distinguishes MIMO from SISO linear processes. In terms of the transformed gain matrix, the output vector is a linear combination of all the column vectors of the U matrix weighted by different singular values

$$Y = U_1 \cdot \sigma_1 \xi_1 + .. + U_j \cdot \sigma_j \xi_j + .. + U_r \cdot \sigma_r \xi_r \qquad (5-30)$$

where U_j is the j-th column vector of the U matrix. When we perturb all the rotated inputs *one at a time* with the same magnitude of 1, the responding output vector will have different magnitudes in different directions. The maximum magnitude of output vector measured in the 2-norm is the maximum singular value in the direction of U_1, while the minimum magnitude is the minimum singular value in the direction of U_r.

Ill-conditioned processes with very different magnitudes in the singular values must have strong directionality. Figure-5.6(a) provides an example of a 2×2 ill-conditioned process in which the strong directionality also makes the two outputs highly correlated (ie. $y_1 \doteq y_2$).

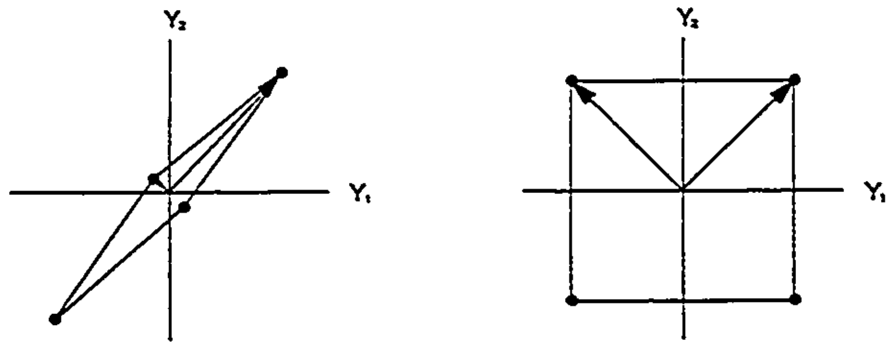

(a) the same magnitude of the two rotated inputs

(b) the optimal relative magnitudes according to Eq.(5-29)

Figure-5.6 Output space interpretations for two different designs

The proposed design strategy of robust identification is to have larger perturbation magnitudes in the rotated inputs corresponding to the smaller singular values. In the extreme, if we do not consider the constraints on the physical inputs, then, when all the rotated inputs reach the ratios defined in (5-29) the process output correlation or directionality will be eliminated as below:

$$Y = \iota\sigma_1\bar{\xi}_1 U_1 + .. + \sigma_j\left(\iota\frac{\sigma_1}{\sigma_j}\bar{\xi}_1\right)U_j + .. + \sigma_r\left(\iota\frac{\sigma_1}{\sigma_r}\bar{\xi}_1\right)U_r \qquad (5-31.a)$$

$$= \sigma_1\bar{\xi}_1 \cdot (\iota U_1 + .. + \iota U_j + .. + \iota U_r) \qquad (5-31.b)$$

where $\iota = \pm 1$

Figure-5.6(b) show the geometric interpretation of (5-31) for 2×2 processes. Therefore, the simple description for the proposed design strategy in terms of output variations is to perturb the outputs in such a fashion that the output correlation is minimized. The design of the output perturbations may be accomplished by using controllers, ie. conducting the identification experiments under closed-loop.

To identify a process model using closed-loop data, independent input perturbations or "dither signals" can be added to the closed-loop system (Box and MacGregor, 1974). The dithers can be added into the set-points or equivalently into the manipulated inputs (Figure-5.7). Since the closed-loop robust identification ideas discussed above set requirements on the outputs, we will consider only the set-point dithers here.

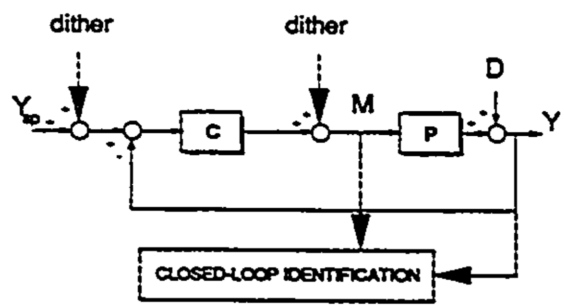

Figure-5.7 Closed-loop identification scheme

A simple design for the set-point dithers is to introduce independent PRBS perturbations in each set-point. If the control were perfect, the optimal design of Figure-5.6(b) would be achieved immediately. However, even when the control is not tight, the controllers will adjust the physical inputs such that the rotated inputs corresponding to the small singular values are increased more whenever a set-point change is made in the direction which is orthogonal to that of the process output correlation. In other words, the required characteristics of the physical inputs from the open-loop identification are met automatically without any knowledge of the input rotation matrix and the process singular values. This is the unique advantage of MIMO closed-loop identification; it inherently produces input variations with the correct correlations and relative magnitudes which will lead to the identification of more robust models. Since tight control of ill-condition processes is not possible before we identify a robust model, the set-point changes should be held for a long enough duration so that the process outputs can approach the steady-state points as shown in Figure-5.6(b).

Anderson and Kummel (1991) have reported that a closed-loop identification scheme using two proportional controllers to perturb the compositions of a binary distillation column can yield a good estimate of the minimum singular value at low frequency. This result is perfectly consistent with the output space interpretations for the design of robust identification proposed here.

5.4 Examples

Two examples are presented to illustrate the theoretical developments through simulations. The first example is a high-purity distillation column which has been discussed in Chapter 4 for its structured model uncertainties. In this example, it is assumed that a good prior knowledge of the process is available, and emphasis is on the physical interpretations of the new design strategy using the rotated inputs. The second example uses a hypothetical 3×3 process to illustrate how the design approach can be applied sequentially.

5.4.1 A Physical 2×2 Process: High-Purity Distillation

5.4.1.1 Rotated Inputs

As shown in Figure-4.4, three flowrates can be used as manipulated inputs in LV and DV control of a distillation column, ie. reflux flow, boilup flow and distillate flow. Both the reflux flow and boil-up flow circulate within the distillation column, and therefore if they are increased/decreased simultaneously the changes are in the *internal flows*. The distillate flow is the product flowing out of the column and therefore called the *external flow* (Skogestad *et al.*, 1988).

It has been shown in Chapter 4 that for the LV and DV control of this process the input rotation matrices are given by:

$$\begin{bmatrix} \xi_1^E \\ \xi_2^E \end{bmatrix} = \begin{bmatrix} 0.707 & -0.707 \\ -0.707 & -0.707 \end{bmatrix} \begin{bmatrix} L \\ V \end{bmatrix} = 0.707 \cdot \begin{bmatrix} L-V \\ L+V \end{bmatrix} \qquad (5-32.a)$$

$$\begin{bmatrix} \xi_1^M \\ \xi_2^M \end{bmatrix} = \begin{bmatrix} 1 & 0 \\ 0 & 1 \end{bmatrix} \begin{bmatrix} D \\ V \end{bmatrix} = \begin{bmatrix} D \\ V \end{bmatrix} \qquad (5-32.b)$$

for LV and DV control respectively. It was also shown that for this nonlinear process these input rotation matrices remain virtually unchanged throughout the operating range of the column. Since the steady-state relationship between LV and DV control is just a linear transformation as given in (4-8), the directions of the rotated inputs for the LV and DV configurations will be essentially the same. The first rotated input is the overhead product flow (ie. $D = -(L-V)$, an external flow) in both configurations. For high-purity distillation where the reflux ratio (L/D) is large (usually over 10), then the second rotated input of LV control approximately equals to 1.4 times of that of the DV control:

$$\xi_2^E = 0.707(L+V) \doteq 0.707(2V) \quad \text{when } L \gg D \qquad (5-33.a)$$

$$= \sqrt{2}\,\xi_2^M \qquad (5-33.b)$$

In other words, both control strategies have the internal flow as their second rotated input.

The proposed design strategy for robust identification experiments is to perturb the second rotated input with a much larger magnitude than the first rotated input when the process to be identified is very ill-conditioned. When applied to distillation processes, this experimental design strategy requires much larger changes in the internal flows than the external flows. Such a requirement can almost always be fulfilled in practice because the reflux flow and boil-up flow are indeed able to have much larger variations than the two product flows. However, there are still some physical constraints such as flooding of the columns that will limit the perturbation magnitudes of the internal flows.

In terms of the changes in the external flow (first rotated input) and internal flow (second rotated input), there is virtually no difference in the design of experiments for LV and DV control. Therefore in the following, we will only examine the LV process. The simple, well-scaled nominal gain matrix used in the illustration example in Chapter 2 will be used here. This gain matrix whose SVD matrices are given by

$$\mathbf{G}=\begin{bmatrix}0.505 & -.495\\ 0.495 & -.505\end{bmatrix}=\begin{bmatrix}0.707 & -.707\\ 0.707 & 0.707\end{bmatrix}\begin{bmatrix}1.0 & 0\\ 0 & 0.01\end{bmatrix}\begin{bmatrix}0.707 & -.707\\ -.707 & -.707\end{bmatrix} \quad (5-34)$$

is very similar to those of many columns with equal purities in both top and bottom products.

5.4.1.2 Experimental Designs

Three experimental designs to identify the distillation column gain matrix will be compared here. Two of them are open-loop designs and the other is a closed-loop design. For a fair comparison, all designs are restricted to yield approximately the same range of variation in each output. From (5-34), the output vector is dominated by the first rotated input as the following:

$$\begin{bmatrix}X_D\\ X_B\end{bmatrix}=\frac{1}{\sqrt{2}}\begin{bmatrix}1\\ 1\end{bmatrix}\cdot\xi_1+\frac{0.01}{\sqrt{2}}\begin{bmatrix}-1\\ 1\end{bmatrix}\cdot\xi_2 \quad (5-35)$$

where X_D and X_B are scaled deviation variables for composition. Therefore, if we choose the first rotated input magnitude to be $\sqrt{2}$, the two outputs will be limited approximately between -1 and 1 when there is no noise.

The first design considered here (Design A) is a traditional design with uncorrelated physical inputs, in which the physical input perturbations have the components of $[\pm 1 \;\; \pm 1]$. Note that the component $[1 \;\; -1]$ or $[-1 \;\; 1]$ corresponds to the first rotated input change with the magnitude of $\sqrt{2}$, and zero second rotated input change, while the component $[1 \;\; 1]$ or $[-1 \;\; -1]$ corresponds to zero first rotated input change and the second rotated input change with the magnitude of $\sqrt{2}$. Therefore, the traditional identification is conducted by perturbing the external and internal flow with the same magnitude in an uncorrelated fashion. Since the two rotated inputs have the same magnitude, the second term on the RHS of (5-35) has negligible effects on the output vector. As a result, the output space is virtually along the $[1\ 1]^T$ vector (ie. $X_D = X_B$), which indicates a strong directionality of the output space. The proposed design for robust identification is to reduce this directionality of the output space. In open-loop experiments, this can be achieved by having a larger change magnitude in the internal flow. Therefore in the second design (Design B) we choose to increase the magnitude of the internal flow change to be ten times larger than the external flow change (note that the theoretical value for the optimal ratio in (5-26.b) is 100). The corresponding physical input settings of Design B have been shown in (5-12) and they are highly correlated. The third design (Design C) is for closed-loop identification where dithers in the set-points are used. Given the range of output variations (ie. between -1 and 1 for both outputs), we can simply design the set-point dithers to be -1 and 1 in both outputs. As discussed earlier, such a design of uncorrelated output perturbations can eliminate the output directionality completely if the controllers have high-performance. However, it is impossible to have high-performance control prior to a good identification of the process. Thus we need to make each set-point dither last long enough to allow the loosely tuned controllers to move the outputs in all directions. Moreover, in the following simulation, the set-point dither are deliberately chosen smaller than the tolerable range of output variations (ie. 1 and -1) to allow some output overshoots due to the control actions.

Table-6 provides a summary of the three designs of experiments used later in simulations. It contains the perturbation components, duration of every perturbation (more details discussed later), characteristic matrices for the physical inputs (ie. information matrix for the gain elements in a row) and for the rotated inputs (ie. Defined in (5-21)) respectively, and finally the estimated variance of the deterministic outputs (ie. noise free).

	Design A	Design B	Design C
Perturbation Components	$\begin{bmatrix}L\\V\end{bmatrix} \in \{\begin{bmatrix}1\\1\end{bmatrix},\begin{bmatrix}1\\-1\end{bmatrix},\begin{bmatrix}-1\\-1\end{bmatrix},\begin{bmatrix}-1\\1\end{bmatrix}\}$	$\begin{bmatrix}L\\V\end{bmatrix} \in \{\begin{bmatrix}11\\9\end{bmatrix},\begin{bmatrix}9\\11\end{bmatrix},\begin{bmatrix}-11\\-9\end{bmatrix},\begin{bmatrix}-9\\-11\end{bmatrix}\}$	$\begin{bmatrix}X_D\\X_B\end{bmatrix}_{sp} \in \{\begin{bmatrix}0.7\\0.7\end{bmatrix},\begin{bmatrix}0.7\\-0.7\end{bmatrix},\begin{bmatrix}-0.7\\-0.7\end{bmatrix},\begin{bmatrix}-0.7\\0.7\end{bmatrix}\}$
duration	one time constant	one time constant	five time constants
M^TM	$\begin{bmatrix}200 & 0\\0 & 200\end{bmatrix}$	$\begin{bmatrix}20200 & 19800\\19800 & 20200\end{bmatrix}$	$\begin{bmatrix}403 & 490\\490 & 992\end{bmatrix}$
$\Xi^T\Xi$	$\begin{bmatrix}200 & 0\\0 & 200\end{bmatrix}$	$\begin{bmatrix}400 & 0\\0 & 40000\end{bmatrix}$	$\begin{bmatrix}207 & 294\\294 & 1188\end{bmatrix}$

Table-6 Summary of the three designs

5.4.1.3 Simulations

In order to make the simulations more realistic, a common first-order dynamic term, $1-0.6z^{-1}$, is brought into the transfer function matrix (ie. $0.4/(1-0.6z^{-1})$ multiplied by the gain matrix in (5-34)) for dynamic simulations. The three designs discussed earlier will be applied to identify this simple dynamic process. Dynamic identifications have another design parameter in addition to the input perturbation magnitude, namely, the switching period. The switching period of open-loop experiments (ie. Design A and B) is chosen as one time constant as a rule of thumb, while that of the set-point dither in closed-loop experiments is chosen to have a longer duration of five time to allow the controllers to track the designed steady-state values of the outputs. The other simulation specifications includes: 1) the sampling interval is taken as one half of the time constant, 2) 200 data points are collected in each design of experiments, and 3) two PI controllers are used to control the column in Design C (the pairing of LV control is X_D - L and X_B - V) and the proportional gain is 0.5 while the reset time is 10 in each loop. Note that although we recognize that different controller designs affect the identification quality, in practice we do not have enough information to fine tune the controllers in the identification stage. Figure-5.8 and Figure-5.9 contain the input sequences of two open-loop designs (Design A and B) and the corresponding noise-free output responses. Figure-5.10 shows the noise-free, closed-loop input/output responses to the designed set-point dithers (Design C).

The ill-conditioned nature of LV control of the distillation process is evident from the output plot of Figure-5.8 where the two output responses are virtually overlapped in Design A where the two physical inputs are uncorrelated. This is owing to the strong output directionality as discussed earlier. On the other hand, Design B achieves some separations in the output curves (Figure-5.9) and therefore reduces the output directionality. Obviously the directionality has been transferred from the outputs to the inputs in Design B where the two inputs are almost overlapped (ie. the changes in the two always have the same sign).

The input/output responses of closed-loop identification using Design C are similar to those of the open-loop Design B in one aspect: the curves of two output responses exhibit small separations. The reason that these separations are much smaller than the designed ones (ie. $[0.7\ -0.7]^T$ and $[-0.7\ 0.7]^T$) is due to the well-known fact that severe interaction exists between the individual loops of LV control, and multiloop controllers always have sluggish performances to set-point changes in these directions (Skogestad and Morari, 1988). This is the major incentive for employing a high-performance controller based on a MIMO model, which in turn requires the robust identification. Despite the sluggish performance of the PI controllers as shown in Figure-5.10, the two manipulated inputs are still adjusted in a somewhat correlated fashion that they both increase or decrease together most of the times, and the corresponding internal flow changes have larger magnitudes than those of external flow changes (see Table-6). However, the closed-loop design there is no direct control over the input perturbations and hence we may not have sufficiently large ratio of $\bar{\xi}_2/\bar{\xi}_1$, and furthermore we may have correlation between the two rotated inputs (ie. the appearance of non-zero off-diagonal elements in $\Xi^T\Xi$, see Table-6). Both situations will make the closed-loop identification quality worse than that of a well-designed open-loop identification.

In order to make fair comparisons among the designs in simulations, the same sets of measurement error signals were added into the two outputs in every case. Ten simulations of 200 points for each design were made using a random number generator with independent, normally distributed signals with mean 0 and a variance of $(0.25)^2$ (ie. the signal to noise ratio is 4 for the largest output variations). MATLAB identification tool box (Ljung, 1988) was used to estimate the parameters of discrete transfer functions based on a prediction error method (Ljung, 1987). The gain matrix is then calculated from the identified transfer functions. Table 7 summarizes the identification results using the three designs. It contains the average values for the ten simulations of the 2-norm of the additive mismatch of the identified gain matrix, the 2-norm of $\hat{G}G^{-1}$ which should be minimized for the robust performance, and the squared errors of the four estimated nonlinear parameters. In addition, the proportion of identified models leading to unstabilizable control is listed for each design.

As shown in Table 7, the independent PRBS design has six out of ten cases where the identified models do not satisfy the stabilizability condition in (2-4), and moreover the identified models have the average value of $\|\hat{G}G^{-1}\|_2$ four times higher than that in Design B which implies a lack of robust performance. On the other hand, the models identified from all the simulation runs for both Designs B and C lead to stabilizable control. The major difference between the latter two designs is that the estimated variances of the minimum singular value and the V matrix parameter in Design C are both more than three times larger than those of Design B, and therefore the average value of $\|\hat{G}G^{-1}\|_2$ in Design C is larger than that in Design B. This is the result of insufficient ratio of $\bar{\xi}_2/\bar{\xi}_1$ being achieved in the input perturbations of the feedback Design C (see Table-6).

Noise-Free Output Responses

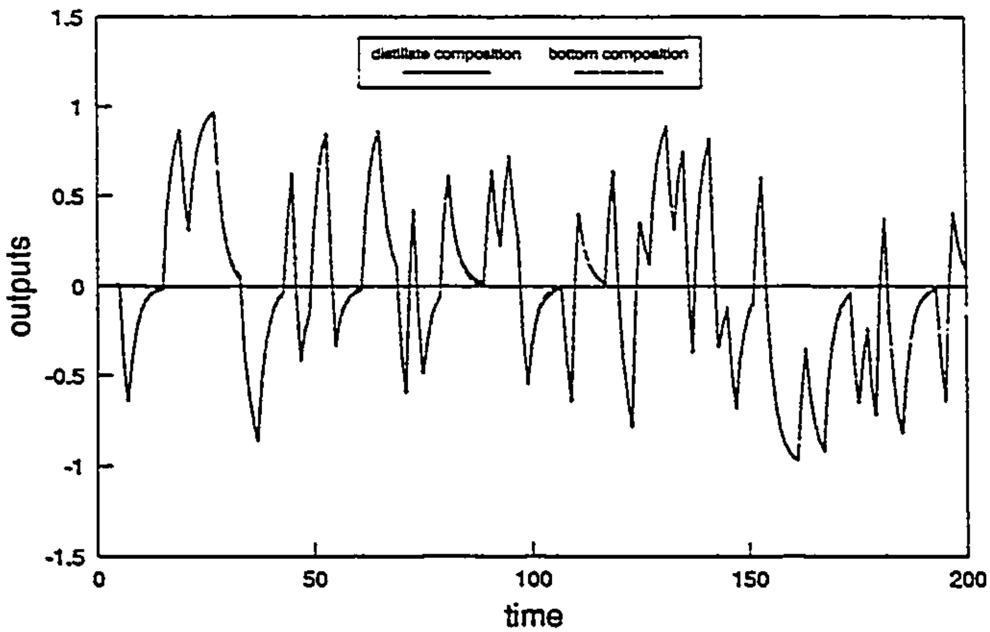

Designed Input Sequences

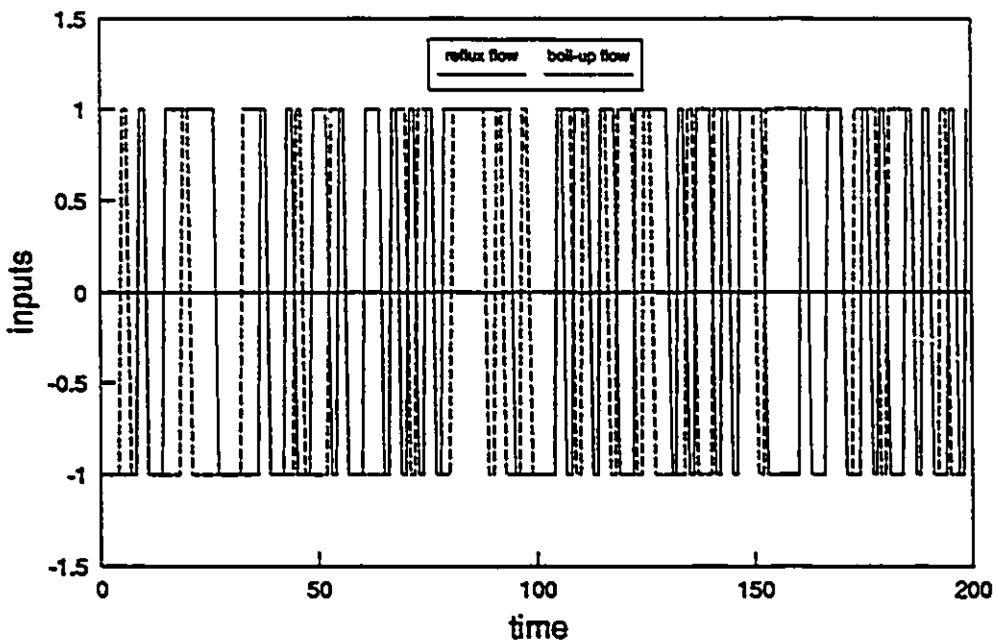

Figure-5.8 Open-loop PRBS design (Design A)

Noise-Free Output Responses

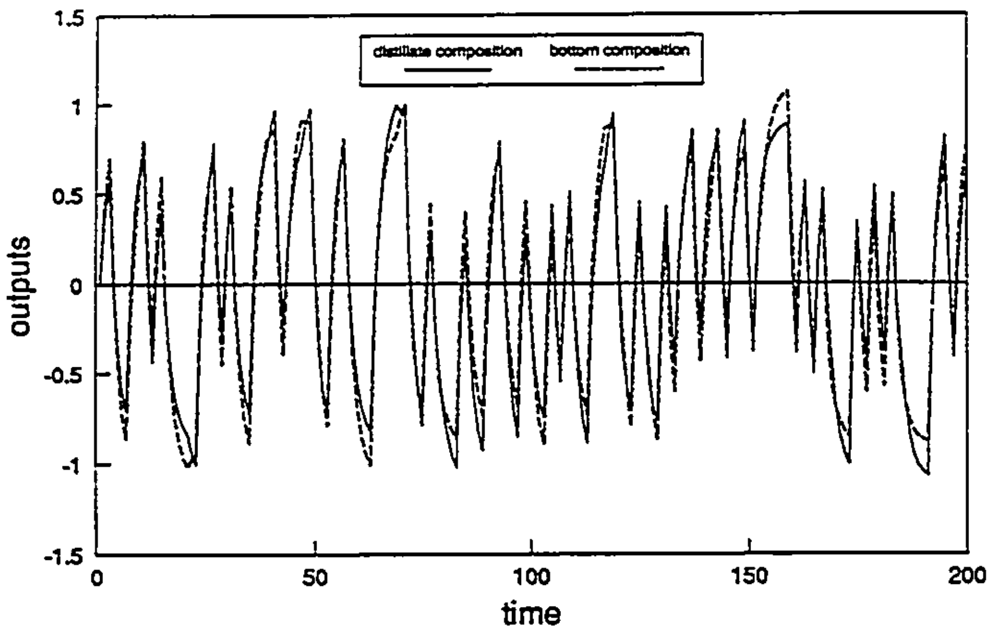

Designed Input Sequences

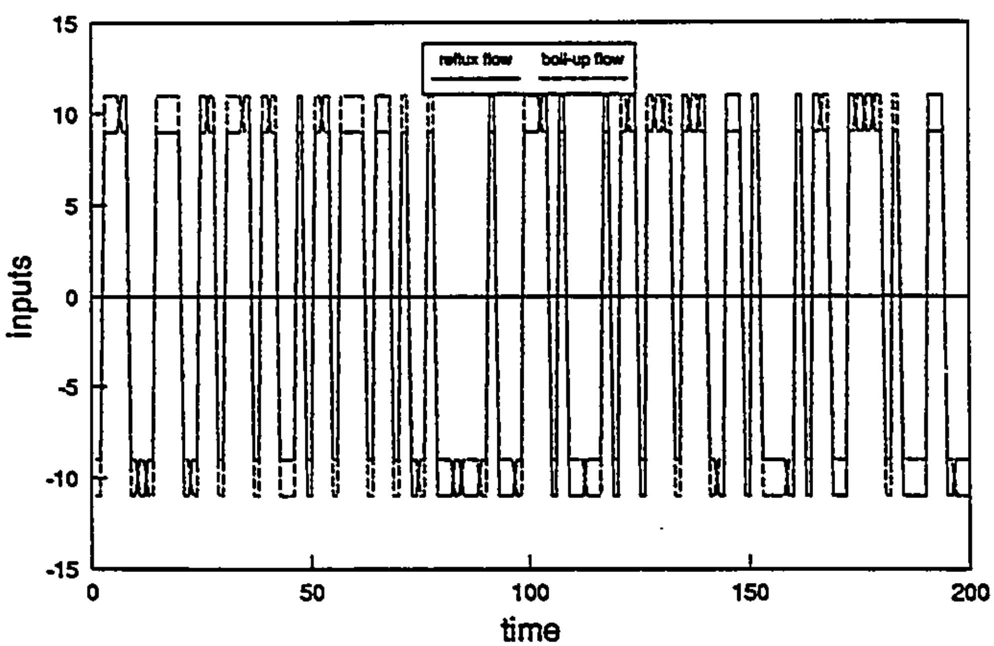

Figure-5.9 Open-loop correlated design (Design B)

Set-point Dither and Controlled Output Responses

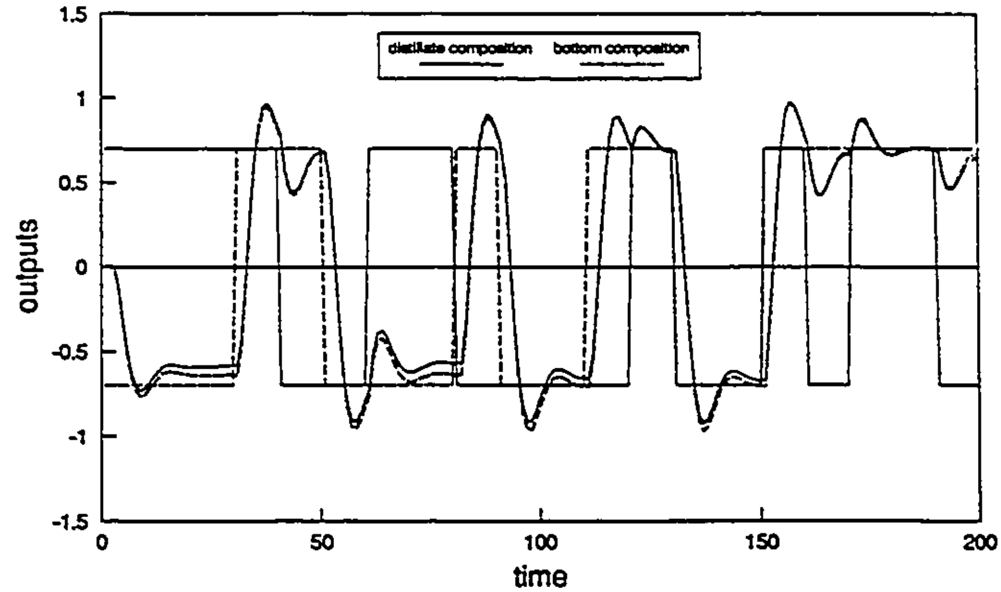

Manipulated Inputs

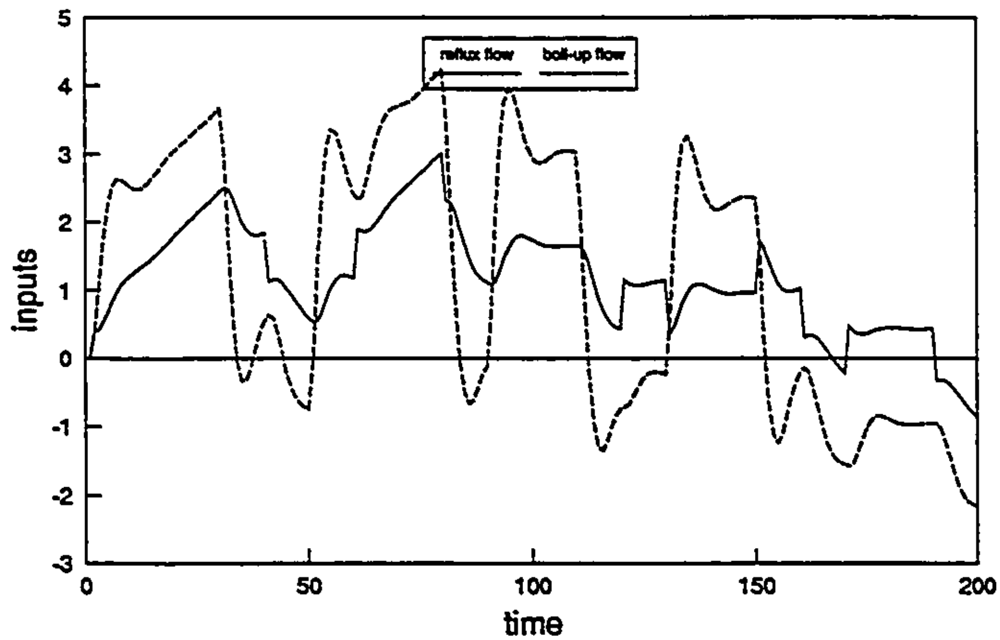

Figure-5.10 Closed-loop identification (Design C)

Design	$\lVert \hat{G}-G \rVert_2$	proportion	$\lVert \hat{G}G^{-1} \rVert_2$	$(\hat{\theta}-\theta)^2$	$(\hat{\phi}-\phi)^2$	$(\hat{\sigma}_1-\sigma_1)^2$	$(\hat{\sigma}_2-\sigma_2)^2$
A	0.076	6/10	4.77	0.00118	0.003530	0.00233	0.000180
B	0.033	0/10	1.16	0.00091	0.000008	0.00093	0.000018
C	0.039	0/10	1.80	0.00061	0.000058	0.00097	0.000071

Table-7 Identification results

5.4.2 Sequential Designs for a Hypothetical 3×3 Process

In this example, a hypothetical 3×3 process will be used to demonstrate the effectiveness of a sequential design of experiments to identify a robust model, and to illustrate the effects of more than one small singular values. The true process is specified as the following:

$$P(z)=\frac{0.4\cdot G}{1-0.6z^{-1}}=\frac{0.4}{1-0.6z^{-1}}\begin{bmatrix}0.0245 & 0.1007 & -0.0957\\ 0.1007 & 0.5204 & -0.4871\\ 0.0957 & 0.4871 & -0.4641\end{bmatrix} \tag{5-36.a}$$

$$G=\begin{bmatrix}0.141 & -0.822 & 0.552\\ 0.720 & 0.468 & 0.513\\ 0.680 & -0.325 & -0.658\end{bmatrix}\begin{bmatrix}1 & 0 & 0\\ 0 & 0.005 & 0\\ 0 & 0 & 0.004\end{bmatrix}\begin{bmatrix}0.141 & -0.822 & 0.552\\ 0.720 & 0.468 & 0.513\\ -0.680 & 0.325 & 0.658\end{bmatrix}^T \tag{5-36.b}$$

This process is ill-conditioned with two small singular values. The condition number is 250. If we knew the true singular values as given in (5-36.b) and supposed that there were no physical input constraints in the hypothetical process, the three rotated inputs could be designed as independent PRBS's with the following relative magnitudes:

$$\frac{\bar{\xi}_2}{\bar{\xi}_1}=200\,,\ \frac{\bar{\xi}_3}{\bar{\xi}_1}=250 \tag{5-37}$$

The corresponding physical input settings could then be converted from the designed rotated input sequence using the true input rotation matrix.

In practice, when we do not have any prior information on the process to be identified, the traditional designs must be used for a first subset of experiments to start a sequential design strategy. In each of the subsequent experiments, the relative magnitudes of the rotated inputs are obtained from (5-37) using the updated estimates of the singular values and the physical inputs are obtained from the corresponding estimate of the V matrix. However, remember that large magnitudes of physical input perturbation in ill-conditioned processes introduce relatively small output variations only when the physical input changes are aligned in the proper direction defined by the true input rotation matrix. When the V matrix estimate is not accurate enough, large magnitudes of the rotated inputs for the small singular values can yield unacceptable output variations. Therefore, if the estimates of singular values from the first few subsets of data indicate that some rotated inputs should have very large magnitudes according to (5-37), we should discount these magnitudes in designing the next subset of experiments because the V matrix estimates in the first few subsets may be far from the true one. Instead of trying to provide some guidelines for the discounting factor, we suggest a simple approach that we adjust the magnitudes of rotated inputs *on-line* for any given V matrix estimation to make sure the output variations are within the tolerable range.

In the simulations, 200 data were collected and the experiment was divided into five subsections with 40 observations each. During the first subsection independent PRBS's were used in all physical inputs with a magnitude of 1. In this particular simulation example, the parameter estimates are obtained using only the data from the immediately preceding subsection and these estimates were used to design the inputs for the next subsection. A better practice would be to use all past data points, however, it does not make much difference here due to the fact that the early designs contribute much less than the subsequent ones. A summary of this sequential identification is provided in Table-8, which contains: 1) the adjustments of the relative magnitudes of the rotated input perturbation (note that the first rotated input has a fixed magnitude of 1), 2) ratios of the identified singular values to the true ones, 3) information on the accuracy of the V matrix estimation, 4) the eigenvalues of $G\hat{G}^{-1}$, and 5) the 2-norm of $\hat{G}G^{-1}$. For comparisons, the identification results using a straightforward independent PRBS for the physical inputs throughout 200 experiments are shown in the following:

$$\frac{\hat{\sigma}_i}{\sigma_i} = 1\,,24.64\,,5.26 \tag{5-38.a}$$

$$\hat{V}^{-1}V = \begin{bmatrix} 0.998 & 0.050 & -0.050 \\ -0.070 & 0.696 & -0.714 \\ 0.003 & -0.716 & -0.698 \end{bmatrix} \tag{5-38.b}$$

$$\lambda_i(G\hat{G}^{-1}) = -0.04\,.\,1.02\,,0.22 \tag{5-38.c}$$

$$\|\hat{G}G^{-1}\|_2 = 32 \tag{5-38.d}$$

Note that the noise signals are the same for all the two identification schemes in the simulations. The noise is simulated to have a mean 0 and variance of $(0.25)^2$.

Exp. No.	1-40	41-80	81-120	121-160	161-200
$\xi_2/\xi_1, \xi_3/\xi_1$	1, 1	2, 3	2, 3	3, 100	6, 50
$\hat{\sigma}_i/\sigma_i$	1.7 , 59 , 35	1.0 , 54 , 33	0.9 , 6.4 , 0.2	0.99 , 3.11 , 0.8	1.37 , 8.88 , 0.98
$\hat{V}^{-1}V$	$\begin{bmatrix} 0.71 & -0.69 & 0.16 \\ 0.45 & 0.27 & -0.85 \\ -0.54 & -0.67 & -0.50 \end{bmatrix}$	$\begin{bmatrix} 1.00 & -0.02 & -0.06 \\ -0.01 & 0.71 & -0.70 \\ -0.04 & -0.70 & -0.72 \end{bmatrix}$	$\begin{bmatrix} 1.00 & 0.01 & 0.02 \\ -0.00 & 0.98 & -0.19 \\ -0.02 & 0.19 & 0.98 \end{bmatrix}$	$\begin{bmatrix} 0.99 & 0.04 & -0.01 \\ -0.04 & 0.96 & -0.28 \\ -0.00 & 0.28 & 0.96 \end{bmatrix}$	$\begin{bmatrix} 1.00 & -0.00 & -0.00 \\ -0.00 & 0.95 & -0.31 \\ 0.00 & 0.31 & 0.95 \end{bmatrix}$
$\lambda_i(G\hat{G}^{-1})$	0.23 , −0.1 , 0.01	0.02 , 1.0 , −0.03	$8.4, 0.26 \pm 0.2i$	$0.31, 1.13 \pm 0.2i$	$0.12, 0.62 \pm 0.6i$
$\|\hat{G}G^{-1}\|_2$	250	61	6.5	8.6	9.1

Table-8 A summary of the five subsets of a sequential design

Judging from the final identification results after 200 experiments, it is obvious that in this sequential SVD-based design the estimates of the small singular values and the V matrix are progressively improved, and the performance variation measure $\|\hat{G}G^{-1}\|_2$ is improved over that of the traditional design. Furthermore, the PRBS design does not yield a model that satisfies the stabilizability condition even if used for all 200 points, while the sequential rotated input design consistently provides a robust model with only 40 data points in the last three subsections of experiments.

The input and output time series of the sequential design are plotted in Figure-5.11. We can clearly see that the designed inputs start from small, uncorrelated perturbations and gradually become highly correlated with very large perturbations in the directions of small singular values at the end. Most importantly, the output variations do not increase at all in responding to the increase of input perturbation magnitudes. In fact, the largest output variations in the new design appear in the second subset of experiments (ie. interval 41 to 80) where the input perturbation magnitudes are still small. This is due to the fact that the initial estimate of the V matrix from the first subset of experiments is very rough, and therefore the physical input perturbations are not aligned in the correct direction. Under this situation, even a slight increase of perturbation magnitudes can cause large output variations.

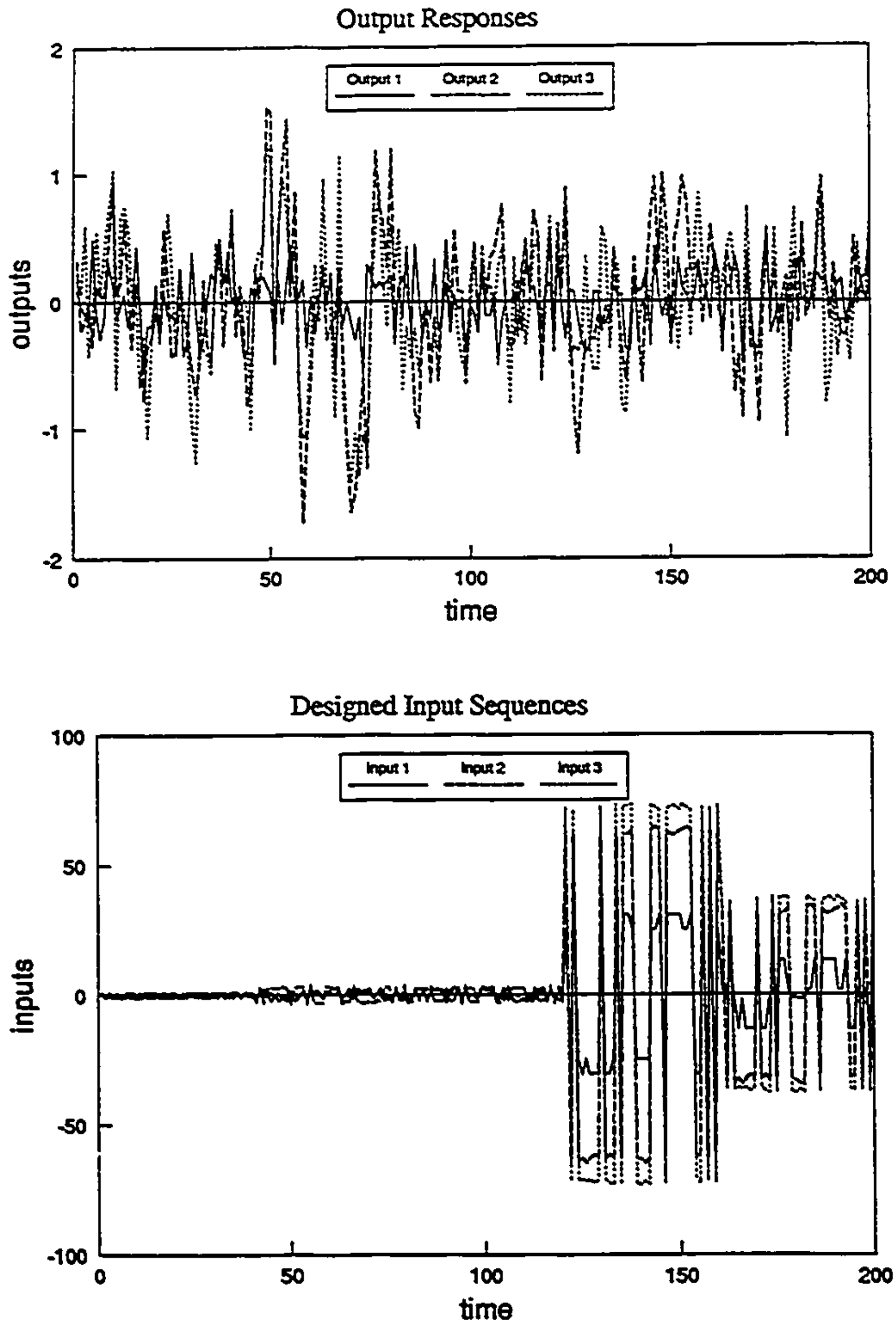

Figure-5.11 A sequential design

5.5 Summary

An unified approach to the design of experiments for general MIMO processes has been developed in terms of the SVD of the process gain matrix. A rigorous derivation for 2×2 processes showed that an uncorrelated design in the rotated inputs with sufficiently larger magnitude in the second rotated input can: 1) prevent the existence of a singularity line that trespasses both uncertainty region of the two row vectors in transformed space and thus ensures the stabilizability of transformed model, 2) minimize the multiplicative mismatch in the small singular value and hence ensures minimal performance variation of the transformed model, and 3) maximize the information content on the input rotation matrix and therefore asymptotically ensure.a robust model.

In addition, the relationship between open-loop and closed-loop robust identification experiments is established in this chapter. The latter is a more convenient method for identifying robust MIMO models because it does not require prior knowledge of the V matrix. However, the closed-loop identification results rely on the controller tuning, and hence may be less effective than using a well-designed, sequential open-loop approach.

In the examples, the physical interpretations of the SVD-based design were illustrated for distillation processes, and the effectiveness of a sequential design strategy was demonstrated through simulations. These case studies reveal that the robust identification designs for ill-conditioned MIMO processes can greatly improve the robustness of multivariable control systems which use these identified model.

6 Conclusions and Recommendations

6.1 Conclusions

This study proposes methodologies for the analysis and identification of linear models that lead to robust controller designs. Both stabilizability and performance variation conditions are investigated. Stabilizability is determined exclusively by the steady-state mismatches between the process and the model for general systems, while the performance condition is an exclusive function of steady-state mismatches only for those systems in which steady-state model uncertainties are dominant, and only for limited controller design methods (however, these designs as given in (2-8.b) and (2-10) cover a wide range of applications). The unique advantage of examining control problems in the above manner is that the robustness of closed-loop systems is completely determined by the model being used and has nothing to do with the controller designs or tuning. In other words, this is a study of robust models rather than robust controllers.

There are two ways to analyze the robustness of linear MIMO models, and they yield the so-called "mismatch conditions" and "uncertainty conditions", respectively. The mismatch conditions can reveal the critical differences as well as crucial similarities between a given process and a model that determine the robustness of the closed-loop system, and therefore they provide not only analysis but also synthesis insight into robust MIMO models. On the other hand, the uncertainty conditions based on the unstructured or structured norm-bound descriptions of model uncertainties only contribute to the analysis of robust models (and the synthesis of robust controllers). Any uncertainty condition with an uncertainty structure specified *a priori* cannot be applied to the robust model identification problems, in which the uncertainty structures are synthesized to ensure the robustness of the identified model.

Two new analysis approaches are developed for the stabilizability and performance variation problems. Contrary to the norm-bounded uncertainty conditions which always relate the uncertainty magnitude to the robustness properties, the mismatch conditions derived in the new approaches clearly emphasize the importance of the mismatch structure over the mismatch magnitude. For instance, the critical difference between the process and model gain matrices for the stabilizability condition is whether or not the model gain vectors need to across the half planes to become the process gain vectors in 2×2 systems, or in high-dimensional systems, whether or not there are sign mismatches in the elements of the **U** matrix. The crucial MIMO characteristic that should be preserved in the modelling for the performance variation condition is the angle between the two process gain vectors for 2×2 systems, or the **V** matrix as its high-dimensional counterpart. All the mismatch conditions from the geometric and SVD analysis approaches have useful model synthesis insights and are readily applied to robust identification.

It is shown that there are some nonlinear, time-variant MIMO processes that can be controlled by linear and time-invariant multivariable controllers to yield robust stability and/or robust performance. Examples of such processes are those which have locally linearized gain matrices with an unchanged angle between the gain vectors or a constant **V** matrix. For these processes, simple linear control systems can have high performance even when the processes are ill-conditioned. Some nonlinear processes have the uncertainty structure that there is no multiplicity in the input contours, or the **U** and **V** matrices of the locally linearized gain matrices are correlated in a favorable fashion. As a result, linear control systems for these processes are always stabilizable regardless of changing operating conditions. For these particular classes of nonlinear processes, the impacts of model mismatches on the stability and performance of linear control systems are minimized, and therefore the benefits of having sophisticated nonlinear or adaptive control schemes may be only marginal.

Finally, this study introduces new ideas on linear model identification that integrates multivariable robust control conditions with the statistical design of experiments. The robust model synthesis conditions developed in this study are used to provide new criteria for experimental designs where the structure of model uncertainties arising from identification errors are manipulated or synthesized such that the crucial MIMO characteristics for the stabilizability and performance variation conditions are precisely identified. These robust identification designs for various processes have been unified to yield a very simple design approach in terms of the rotated inputs for open-loop experiments, or the output variations for closed-loop experiments. For ill-conditioned processes, these robust identification designs typically distinguish themselves from traditional designs in the following characteristics: (1) the inputs are highly correlated; (2) the inputs are not binary sequences; and (3) the perturbation magnitudes in low-gain directions are much larger than those in high-gain directions. It has been rigorously derived and confirmed in simulations that such new designs are far better than the traditional designs in providing robust models.

6.2 Recommendations for Future Research

As a preliminary research work on the analysis and synthesis of robust linear models, this Ph.D. study has only solved the simplest (but important) problems in the area of robust process control. Future research studies may extend this work in the following directions:

1) The robust stability problem considered here is limited to a stabilizability condition in which controller performance is not considered. Therefore the mismatch condition only involves the steady-state gains. Suppose that we want to set a bound on some robust performance measures (ie. the stabilizability condition is the special case where such a bound is infinity). Then it is expected that the generalized mismatch condition in terms of $\mathbf{P}(s)$ and $\hat{\mathbf{P}}(s)$ is much more complicated, because it is coupled with robust

performance measures and thus will no longer involve only the steady-state model mismatch. Under this situation, what are the critical process characteristics that need to be preserved in the model to ensure the robustness properties ?

2) The simplifying assumption behind the performance variation condition in (2-11) is too stringent. The more useful condition for the performance variation problem (ie. minimizing the time integral in (2-6)) will be a function of dynamic model mismatches and more general controller designs. Similar to the generalized robust stability condition, it is expected that the generalized performance variation condition will set limits on the mismatches in the dynamic parameters. Therefore these new conditions may provide some insights into the design of experiments to synthesize the model uncertainties in a wider range of frequency (ie. only zero frequency is considered in this study). In other words, the design of experiments that meets the new robust model synthesis conditions may require some special frequency contents in addition to the correct structural information as derived in this study.

7 Appendices

Appendix-1 : Geometric Expressions for $G\hat{G}^{-1}$ *and* $\hat{G}G^{-1}$

$$G\hat{G}^{-1}=\begin{bmatrix} n_1\hat{l}_1\cos(\hat{\alpha}_1+\delta_1) & n_2\hat{l}_2\cos(\hat{\alpha}_2+\delta_2) \\ n_1\hat{l}_1\sin(\hat{\alpha}_1+\delta_1) & n_2\hat{l}_2\sin(\hat{\alpha}_2+\delta_2) \end{bmatrix}\begin{bmatrix} \hat{l}_1\cos\hat{\alpha}_1 & \hat{l}_2\cos\hat{\alpha}_2 \\ \hat{l}_1\sin\hat{\alpha}_1 & \hat{l}_2\sin\hat{\alpha}_2 \end{bmatrix}^{-1}=\frac{1}{\sin\hat{\beta}}\times \qquad (A-1.1)$$

$$\begin{bmatrix} n_1\sin(\hat{\alpha}_1+\delta_1)\cos\hat{\alpha}_2-n_2\sin(\hat{\alpha}_2+\delta_2)\cos\hat{\alpha}_1 & -n_1\sin(\hat{\alpha}_1+\delta_1)\sin\hat{\alpha}_2+n_2\sin(\hat{\alpha}_2+\delta_2)\sin\hat{\alpha}_1 \\ n_1\cos(\hat{\alpha}_1+\delta_1)\cos\hat{\alpha}_2-n_2\cos(\hat{\alpha}_2+\delta_2)\cos\hat{\alpha}_1 & -n_1\cos(\hat{\alpha}_1+\delta_1)\sin\hat{\alpha}_2+n_2\cos(\hat{\alpha}_2+\delta_2)\sin\hat{\alpha}_1 \end{bmatrix}$$

$$\hat{G}G^{-1}=\begin{bmatrix} \hat{n}_1l_1\cos(\alpha_1+\hat{\delta}_1) & \hat{n}_2l_2\cos(\alpha_2+\hat{\delta}_2) \\ \hat{n}_1l_1\sin(\alpha_1+\hat{\delta}_1) & \hat{n}_2l_2\sin(\alpha_2+\hat{\delta}_2) \end{bmatrix}\begin{bmatrix} l_1\cos\alpha_1 & l_2\cos\alpha_2 \\ l_1\sin\alpha_1 & l_2\sin\alpha_2 \end{bmatrix}^{-1}=\frac{1}{\sin\beta}\times \qquad (A-1.2)$$

$$\begin{bmatrix} \hat{n}_1\sin(\alpha_1+\hat{\delta}_1)\cos\alpha_2-\hat{n}_2\sin(\alpha_2+\hat{\delta}_2)\cos\alpha_1 & -\hat{n}_1\sin(\alpha_1+\hat{\delta}_1)\sin\alpha_2+\hat{n}_2\sin(\alpha_2+\hat{\delta}_2)\sin\alpha_1 \\ \hat{n}_1\cos(\alpha_1+\hat{\delta}_1)\cos\alpha_2-\hat{n}_2\cos(\alpha_2+\hat{\delta}_2)\cos\alpha_1 & -\hat{n}_1\cos(\alpha_1+\hat{\delta}_1)\sin\alpha_2+\hat{n}_2\cos(\alpha_2+\hat{\delta}_2)\sin\alpha_1 \end{bmatrix}$$

where

$$l_j=n_j\hat{l}_j\,,\ \hat{l}_j=\hat{n}_jl_j \qquad (A-1.3)$$

$$\alpha_j=\hat{\alpha}_j+\delta_j\,,\ \hat{\alpha}=\alpha_j+\hat{\delta}_j \qquad (A-1.4)$$

$$\therefore\quad n_j=\frac{1}{\hat{n}_j}\,,\ \delta_j=-\hat{\delta}_j \qquad (A-1.5)$$

Appendix-2: Proof for Theorem 2 and Theorem 3

For an arbitrary 2×2 process, the model is represented by two model gain vectors in which we can always find a ε which has a range between 0 and $\frac{\pi}{2}$ to replace $\hat{\beta}$ to characterize the angle between the nominal gain vectors (Figure-A.1). The determinant can then be rewritten as

$$det(G\hat{G}^{-1})=n_1n_2\frac{\sin(\varepsilon+\delta_1-\delta_2)}{\sin\varepsilon} \qquad (A-2.1a)$$

or

$$det(G\hat{G}^{-1})=n_1n_2\frac{\sin(\varepsilon-\delta_1+\delta_2)}{\sin\varepsilon} \qquad (A-2.1b)$$

depending on the relative positions of the vectors in Figure-A.1 (ie. $\hat{G}_2$ may be in one of the four quadrants, (1) to (4), defined by the dotted lines).

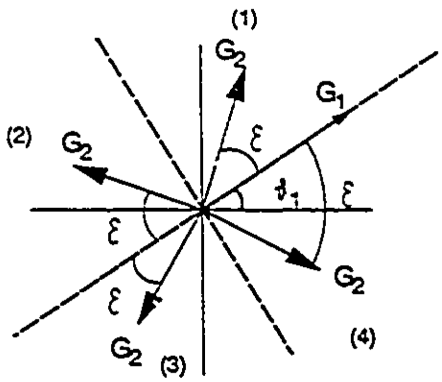

(1) $\beta=\varepsilon$, (2) $\beta=\pi-\varepsilon$, (3) $\beta=\pi+\varepsilon$, (4) $\beta=2\pi-\varepsilon$

Figure-A.1 Possible relative positions of the process gain vectors

Therefore the determinant is positive if and only if (note that n's and $\sin\varepsilon$ are positive)

$$-\varepsilon < \alpha_1-\alpha_2 < \pi-\varepsilon \qquad (A-2.2a)$$

or

$$-\varepsilon < \alpha_2-\alpha_1 < \pi-\varepsilon \qquad (A-2.2b)$$

By setting either α_1 or α_2 to be zero (ie. specifying an unchanged vector) in Eq.(A-2), we can see that the changing vector should remain in its nominal half plane to have a positive determinant.

Let $\mathbf{G}^*$ be the intermediate gain matrix in which only the first model gain vector is changed. Algebraically, the combined effect of changing both model vectors to be the true gain vectors is given by:

$$\mathbf{G}\hat{\mathbf{G}}^{-1} = (\mathbf{G}\mathbf{G}^{*-1})(\mathbf{G}^*\hat{\mathbf{G}}^{-1}) \qquad (A-2.3)$$

Since

$$det(\mathbf{G}\hat{\mathbf{G}}^{-1}) = det(\mathbf{G}(\mathbf{G}^*)^{-1})det(\mathbf{G}^*\hat{\mathbf{G}}^{-1}) \qquad (A-2.4)$$

we can apply (A-2.2) twice (ie. for $det(\mathbf{G}(\mathbf{G}^*)^{-1})$ and $det(\mathbf{G}^*\hat{\mathbf{G}}^{-1})$) and Theorem 2 is proven.

As to the trace of $G\hat{G}^{-1}$ can also be rewritten in term of ε:

$$tr(G\hat{G}^{-1}) = \frac{[n_1 \sin(\varepsilon - \delta_1) + n_2 \sin(\varepsilon + \delta_2)]}{\sin\varepsilon} \qquad (A-2.5a)$$

or

$$tr(G\hat{G}^{-1}) = \frac{[n_1 \sin(\varepsilon + \delta_1) + n_2 \sin(\varepsilon - \delta_2)]}{\sin\varepsilon} \qquad (A-2.5b)$$

depending on the relative positions of the vectors in Figure-A.1. The trace is positive if both terms in the numerator on the RHS of Eq.(A-2.5a) or Eq.(A-2.5b) are positive, and is negative if both terms are negative. Since

$$\sin(\varepsilon \pm \delta_j) > 0 \;\; \text{iff} \;\; 0 < \varepsilon \pm \delta_j < \pi \qquad (A-2.6)$$

geometrically, Eq.(A-2.6) corresponds to Theorem 3.

Appendix-3: Proof for Theorem 4

When there is no sign mismatch in the gain matrix, we have

$$\cos\hat{\alpha}_1 \cdot \cos\alpha_1 > 0 \;\; \text{and} \;\; \sin\hat{\alpha}_2 \cdot \sin\alpha_2 > 0 \qquad (A-3.1)$$

Then $\hat{\gamma}_{11} \cdot \gamma_{11} > 0$ if and only if $\sin\hat{\beta} \cdot \sin\beta > 0$. Since (3-17.a) can be rewritten as:

$$det(G\hat{G}^{-1}) = \frac{det(G)}{det(\hat{G})} = \frac{l_1 l_2 \sin\beta}{\hat{l}_1 \hat{l}_2 \sin\hat{\beta}} \qquad (A-3.2a)$$

$$= n_1 n_2 \frac{\sin\beta}{\sin\hat{\beta}} \qquad (A-3.2b)$$

we have proved that the condition $det(G\hat{G}^{-1}) > 0$, which is necessary for the stabilizability condition, is satisfied if and only if $\hat{\gamma}_{11} \cdot \gamma_{11} > 0$ when there is no sign mismatch in the gain matrix.

The trace in (3-17.b) can be expanded as the following:

$$tr(G\hat{G}^{-1}) = \frac{1}{\sin\hat{\beta}}(n_1 \sin\beta\cos\delta_1 + n_1\cos\beta\sin\delta_1 + n_2\sin\beta\cos\delta_2 - n_2\cos\beta\sin\delta_2) \qquad (A-3.3a)$$

$$= (n_1\cos\delta_1 + n_2\cos\delta_2) + \frac{1}{\tan\beta}(n_1\sin\delta_1 - n_2\sin\delta_2) \qquad (A-3.3b)$$

The first bracket term is always positive when there is no sign mismatch (ie. $|\delta_j| < \frac{\pi}{2}$), and therefore the trace is negative only if the second bracket term is negative. However, if the second bracket term has the magnitude bound given in Theorem 4, the trace is positive even when the second bracket term is negative.

Appendix-4: Proof for Theorem 7

To simplify the notations, the i-th row, j-th column element of T in (3-32) is denoted as

$$\frac{\sigma_j}{\sigma_i}\hat{U}_i^T U_j \overset{\Delta}{=} q_{ii} d_i \quad i = j \qquad (A-4.1a)$$

$$\overset{\Delta}{=} q_{ij} e_{ij} \quad i \neq j \qquad (A-4.1b)$$

Consider that **T** is obtained by perturbing a diagonal matrix **D** in the following way

$$\mathbf{T} \overset{\Delta}{=} \mathbf{D} + \mathbf{E} \qquad (A-4.2a)$$

$$\begin{bmatrix} q_{11}d_1 & . & . & q_{1r}e_{1r} \\ . & . & . & . \\ . & . & . & . \\ q_{r1}e_{r1} & . & . & q_{rr}d_r \end{bmatrix} = \begin{bmatrix} q_{11}d_1 & . & 0 & 0 \\ . & . & 0 & 0 \\ 0 & 0 & . & . \\ 0 & 0 & . & q_{rr}d_r \end{bmatrix} + \begin{bmatrix} 0 & . & . & q_{1r}e_{1r} \\ . & 0 & . & . \\ . & . & . & . \\ q_{r1}e_{r1} & . & . & 0 \end{bmatrix} \qquad (A-4.2b)$$

where **E** is a full matrix except that all the diagonal elements are 0. The eigenvalues of the **D** matrix are simply the diagonal elements. According to the first condition of mismatch structure in the **U** matrix stated in Theorem 7, we have

$$d_i = \hat{U}_i^T U_i = \sum_{k=1}^{n} \hat{u}_{ki} u_{ki} > 0 \ \forall i \quad \text{since } \hat{u}_{ki} u_{ki} > 0 \ \forall i, k \qquad (A-4.3)$$

and therefore all the eigenvalues of the **D** matrix are positive. The next step is to prove that none of the eigenvalues of the **D** matrix will be perturbed by the **E** matrix in Eq.(A-4.2a) to become a negative eigenvalue of the **T** matrix. We will prove this by considering the Characteristic Polynomials (CP) of the **D** and **T** matrices.

According to the well-known Descartes rule of signs for the real roots of a polynomial (Perry and Chilton, 1973), if the CP's of **T** and **D** have the same sign in each of the corresponding coefficients then the CP of **T** must have the same number of positive/negative real roots as the CP of **D** (or that number less a multiple of two). That is, all the real eigenvalues of the **T** matrix are positive because the **D** matrix only has positive eigenvalues (ie. $q_{ii}d_i$'s). Therefore we shall prove the CP's of **T** and **D** matrices satisfy the above stated sufficient condition next.

A principle sub-matrix of order i of **T** is defined as an i-dimensional square matrix where the diagonal elements are a subset of those of **T**, and the h-th row, k-th column off-diagonal element has its row/column index equal to the index of **T** for the h-th and k-th diagonal elements, (Stewart, 1973)

$$\mathbf{T}_{S_i}^{[id]} = \begin{bmatrix} t_{hh} & \cdot & t_{hk} & \cdot \\ \cdot & \cdot & \cdot & \cdot \\ t_{kh} & \cdot & t_{kk} & \cdot \\ \cdot & \cdot & \cdot & \cdot \end{bmatrix}_{i\times i} \quad h < k \qquad (A-4.4)$$

The index $[id]$ identifies different sub-matrices of the same order. For example, a 3×3 matrix has three order 2 principle sub-matrices

$$\mathbf{T}_{S_2}^{[1]} = \begin{bmatrix} t_{11} & t_{12} \\ t_{21} & t_{22} \end{bmatrix} \; \mathbf{T}_{S_2}^{[2]} = \begin{bmatrix} t_{11} & t_{13} \\ t_{31} & t_{33} \end{bmatrix} \; \mathbf{T}_{S_2}^{[3]} = \begin{bmatrix} t_{22} & t_{23} \\ t_{32} & t_{33} \end{bmatrix} \qquad (A-4.5)$$

In general, the principle sub-matrices of order 1 are the diagonal elements of **T** and the principle sub-matrix of order r is just **T** itself.

The i-th coefficient, p_i, in the characteristic polynomial of **T**

$$\begin{aligned} 0 &= det(\mathbf{T}-\lambda\mathbf{I}) \\ &= (-1)^r\lambda^r + (-1)^{r-1}p_1\lambda^{r-1} + \cdots + (-1)^0 p_r \end{aligned} \qquad (A-4.6)$$

is the summation of the determinants of all principle sub-matrices of order i of **T**, ie.

$$p_i = \sum_{id=1}^{C_i^r} det\left(\mathbf{T}_{S_i}^{[id]}\right) \qquad (A-4.7)$$

The above developments from (A-4.4) to (A-4.7) are valid for any square matrix. There is a special property of T matrix involving the q_{ij} terms in (A-4.1), which is critical to the simplification of (A-4.7),

$$q_{ij}\cdot q_{ji}=\frac{\sigma_i}{\hat{\sigma}_j}\cdot\frac{\sigma_j}{\hat{\sigma}_i}=\frac{\sigma_i\sigma_j}{\hat{\sigma}_i\hat{\sigma}_j}=q_{ii}\cdot q_{jj}$$

$$q_{ij}\cdot q_{jk}\cdot q_{ki}=\frac{\sigma_i\sigma_j\sigma_k}{\hat{\sigma}_j\hat{\sigma}_k\hat{\sigma}_i}=\frac{\sigma_i\sigma_j\sigma_k}{\hat{\sigma}_i\hat{\sigma}_j\hat{\sigma}_k}=q_{ii}\cdot q_{jj}\cdot q_{kk} \qquad (A-4.8)$$

$$\vdots$$

etc.

Then, we can derive the CP coefficients of T to have the following simple format:

$$p_1=q_{11}d_1+\dots\dots+q_{rr}d_r \qquad (A-4.9a)$$

$$p_2=\begin{vmatrix} q_{11}d_1 & q_{12}e_{12} \\ q_{21}e_{21} & q_{22}d_2 \end{vmatrix}+\dots.+\begin{vmatrix} q_{r-1,r-1}d_{r-1} & q_{r-1,r}e_{r-1,r} \\ q_{r,r-1}e_{r,r-1} & q_{rr}d_r \end{vmatrix}$$

$$=q_{11}q_{22}(d_1d_2-e_{12}e_{21})+\dots+q_{r-1r}q_{rr-1}(d_{r-1}d_r-e_{rr-1}e_{r-1r}) \qquad (A-4.9b)$$

$$p_3=\begin{vmatrix} q_{11}d_1 & q_{12}e_{12} & q_{13}e_{13} \\ q_{21}e_{21} & q_{22}d_2 & q_{23}e_{23} \\ q_{31}e_{31} & q_{32}e_{32} & q_{33}d_3 \end{vmatrix}+\dots$$

$$=\{q_{11}q_{22}q_{33}[d_1d_2d_3-(d_1e_{23}e_{32}+d_2e_{13}e_{31}+d_3e_{12}e_{21})+(e_{12}e_{23}e_{31}+e_{21}e_{32}e_{12})]\}+\dots \qquad (A-4.9c)$$

$$p_4=\begin{vmatrix} q_{11}d_1 & q_{12}e_{12} & q_{13}e_{13} & q_{14}e_{14} \\ q_{21}e_{21} & q_{22}d_2 & q_{23}e_{23} & q_{24}e_{24} \\ q_{31}e_{31} & q_{32}e_{32} & q_{33}d_3 & q_{34}e_{34} \\ q_{41}e_{41} & q_{42}e_{42} & q_{43}e_{43} & q_{44}d_4 \end{vmatrix}+\dots$$

$$=\{q_{11}q_{22}q_{33}q_{44}[d_1d_2d_3d_4-(d_1d_2e_{34}e_{43}+d_1d_3e_{24}e_{42}+d_1d_4e_{23}e_{32}+d_2d_3e_{14}e_{41}$$

$$+d_2d_4e_{13}e_{31}+d_3d_4e_{12}e_{21})+[d_1(e_{23}e_{34}e_{42}+e_{32}e_{43}e_{24})+d_2(e_{13}e_{14}e_{34}+e_{31}e_{41}e_{43})$$

$$+d_3(e_{12}e_{14}e_{24}+e_{21}e_{41}e_{42})+d_4(e_{12}e_{13}e_{23}+e_{21}e_{31}e_{32})]+(e_{ij}^4 \text{ terms })\}+\dots \qquad (A-4.9d)$$

$$\vdots$$

$$p_r=det(\mathbf{T}) \qquad (A-4.9e)$$

Since e_{ij} is closer to 0 than to 1, we can drop the summation terms involving third order (and above) product terms of e_{ij}'s in (A-4.9). Then the following approximate CP coefficients of the **T** matrix are obtained:

$$\sum_{i=1}^{r} \lambda_i = q_{11}d_1 + \ldots + q_{rr}d_r \qquad (A-4.10a)$$

$$\sum_{\substack{i=1 \\ j>i}}^{r} \lambda_i\lambda_j = q_{11}q_{22}(d_1d_2 - e_{12}e_{21}) + \ldots$$

$$+ q_{r-1,r-1}q_{rr}(d_{r-1,r-1}d_{rr} - e_{r-1,r}e_{r,r-1}) \qquad (A-4.10b)$$

$$\sum_{\substack{i=1 \\ k>j>i}}^{r} \lambda_i\lambda_j\lambda_k = q_{11}q_{22}q_{33}[d_1d_2d_3 - (d_1e_{23}e_{32} + d_2e_{13}e_{31} + d_3e_{12}e_{21})] + \ldots \qquad (A-4.10c)$$

$$+ q_{r-2,r-2}q_{r-1,r-1}q_{rr}[d_{r-2}d_{r-1}d_r - (d_{r-2}e_{r-1,r}e_{r,r-1} + d_{r-1}e_{r-2,r}e_{r,r-2} + d_re_{r-2,r-1}e_{r-1,r-2})]$$

$$\vdots$$

$$\lambda_1 \cdot \lambda_2 \cdots \lambda_r = q_{11} \cdot q_{22} \cdots q_{rr}[d_1 \cdot d_2 \cdots d_r \qquad (A-4.10d)$$

$$-(d_1 \cdot d_2 \cdots d_{r-2}e_{r-1,r}e_{r,r-1} + \ldots + d_3 \cdot d_4 \cdots d_re_{12}e_{21})]$$

As shown in the above equations, every approximate CP coefficient of the **T** matrix, except (A-4.10a), can be decomposed into the corresponding CP coefficient of the **D** matrix (A-4.2b) (those terms without e_{ij}) and a perturbation (those terms with the product of $e_{ij} \cdot e_{ji}$) due to **E** in Eq.(A-4.2b). Note that the first coefficient has no perturbation terms, and therefore it definitely has the same sign as that of the **D** matrix. As to all the other coefficients, if we can prove the following:

$$e_{ij}e_{ji} \ll d_id_j \quad \text{if } e_{ij}e_{ji} > 0 \qquad (A-4.11)$$

then any of the perturbation effects in Eq.(A-4.10) (ie. the products of $e_{ij} \cdot e_{ji}$'s) can only either increase the CP coefficients of the **D** matrix when $e_{ij} \cdot e_{ji}$ is negative, or decrease them without changing the signs when $e_{ij} \cdot e_{ji}$ is positive. Therefore all the summation terms are positive and each corresponding CP coefficients of the **T** and **D** matrices have the same signs.

Since the product of two unitary matrices is still a unitary matrix, any two column vectors of $\hat{\mathbf{U}}^T\mathbf{U}$ will have their scalar product to be 0, ie.

$$0=[\hat{U}_1^TU_i,...,\hat{U}_r^TU_i]\cdot[\hat{U}_1^TU_j,..\hat{U}_r^TU_j]^T \qquad (A-4.12a)$$

$$=d_ie_{ij}+d_je_{ji}+\sum_{\substack{k=1\\k\neq i,j}}^{n} e_{ri}e_k \qquad (A-4.12b)$$

$$\Rightarrow |d_ie_{ij}+d_je_{ji}| = |\sum_{\substack{k=1\\k\neq i,j}}^{r} e_{ki}e_{kj}| \qquad (A-4.12c)$$

If e_{ij} and e_{ji} have the same sign then Eq.(A.6.c) can be rewritten as

$$|d_ie_{ij}|+|d_je_{ji}| = |\sum_{\substack{k=1\\k\neq i,j}}^{r} e_{ki}e_{kj}| \qquad (A-4.13)$$

According to the second condition on the mismatch structure of the **U** matrix stated in Theorem 7, we can prove the condition in Eq.(A-4.11) as the following

$$|\sum_{\substack{k=1\\k\neq i,j}}^{r} e_{ki}e_{kj}| < d_id_j \qquad (A-4.14a)$$

$$\Rightarrow (|d_ie_{ij}|+|d_je_{ji}|)^2 < (d_id_j)^2 \qquad (A-4.14b)$$

$$\Rightarrow e_{ij}e_{ji} < \frac{1}{2}\left[d_id_j-\left(e_{ij}^2\frac{d_i}{d_j}+e_{ji}^2\frac{d_j}{d_i}\right)\right]$$

$$\ll d_id_j \qquad (A-4.14c)$$

Theorem 7 is thus proven.

Appendix-5: Proof for Theorem 8

For 2×2 systems, the CP of the **T** matrix is as follows

$$\lambda^2-(q_{11}d_1+q_{22}d_2)\lambda+q_{11}q_{22}(d_1d_2-e_{12}e_{21})=0 \qquad (A-5.1)$$

The corresponding Routh test array is

$$\begin{matrix} 1 & q_{11}q_{22}(d_1d_2-e_{12}e_{21}) \\ -(q_{11}d_1+q_{22}d_2) & 0 \end{matrix} \qquad (A-5.2)$$

The left column has one sign change in its two elements and therefore the complex roots of (A-5.1) will have one positive real part. Since the two complex roots must be conjugates, this positive real part appears in both complex roots.

The CP of the T matrix in 3×3 systems is as the following

$$(-1)\lambda^3+(q_{11}d_1+q_{22}d_2+q_{33}d_3)\lambda^2-\tau_1\lambda+\tau_2=0 \qquad (A-5.3a)$$

where $\tau_1=q_{11}q_{22}(d_1d_2-e_{12}e_{21})+q_{11}q_{33}(d_1d_3-e_{13}e_{31})+q_{22}q_{33}(d_2d_3-e_{23}e_{32})$ $\qquad (A-5.3b)$

$$\tau_2=q_{11}q_{22}q_{33}[d_1d_2d_3-(d_1e_{23}e_{32}+d_2e_{13}e_{31}+d_3e_{12}e_{21})+(e_{12}e_{23}e_{31}+e_{21}e_{32}e_{13})] \qquad (A-5.3.c)$$

and its corresponding Routh test array is

$$\begin{array}{cc} -1 & -\tau_1 \\ (q_{11}d_1+q_{22}d_2+q_{33}d_3) & \tau_2 \\ \tau_3 & 0 \end{array} \qquad (A-5.4)$$

The second element in the left column of Routh array is always positive because q_{ii}'s are the ratios of singular values, and from (A-4.3) d_i's are positive. The last element in the left column can be derived as the following

$$\begin{aligned}\tau_3=-\{\, & q_1^2d_1[q_2(d_1d_2-e_{21}e_{12})+q_3(d_1d_3-e_{13}e_{31})]+q_2^2d_2[q_1(d_1d_2-e_{21}e_{12})+q_3(d_1d_3-e_{13}e_{31})]\\ & q_3^2d_3[q_1(d_1d_3-e_{31}e_{13})+q_2(d_2d_3-e_{23}e_{32})]+2q_{11}q_{22}q_{33}[d_1d_2d_3\\ & -(d_1e_{23}e_{32}+d_2e_{13}e_{31}+d_3e_{12}e_{21})-\frac{1}{2}(e_{12}e_{23}e_{31}+e_{21}e_{32}e_{13}]\,\}<0 \qquad (A-5.5)\end{aligned}$$

Only the last two summation terms with negative signs in Eq.(A-5.5) may have the opposite sign to the other summation terms which are all positive. However, if this is true, the magnitudes of these two summation terms will be smaller than others as implied by (A-4.11). Therefore τ_3 is negative and there are two sign changes in the left column. Thus the complex roots of (A-5.3) will have two positive real parts. Third order polynomials with real coefficients can only have one pair of complex roots and thus we have proved that the complex eigenvalues of the **T** matrix must have positive real parts.

Appendix-6: Proof for Theorem 9

It is equivalent to prove that if the determinant is negative then there must exist multiplicities. From Theorem 2, we know that the determinant is negative if and only if one gain vector is on the other side of its nominal half plane while the other gain vector is not. However, it is shown that it is impossible to connect the process gain vectors at two operating points by the contours without including some type of multiplicities.

Given an arbitrary $\bar{G}$, we can draw the gain vectors of G at certain point we choose and have negative $det(G\bar{G}^{-1})$ in a systematic way in Figure-A.2: 1) passing the chosen point, draw a parallel line to the nominal gain vector which will remain in its nominal half plane (ie. $\bar{G}_1$ in this figure), 2) at the chosen point, first reproduce the other nominal gain vector (ie. $\bar{G}_2$ in this figure) and then rotate it anywhere to the other side of this line to obtain G_2, 3) at the same point, reproduce $\bar{G}_1$ and rotate it anywhere, without crossing the new line extended from G_2, to obtain G_1.

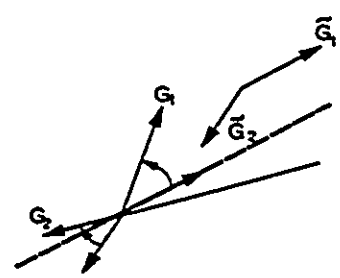

Figure-A.2 A systematic way to have $det(G\bar{G}^{-1}) < 0$

To connect such a pair of $\bar{G}$ and G (ie. four gain vectors) in Figure-A.2, there three possibilities:

a) the two gain vectors of the both inputs are connected by one contour (Figure-A.3(a)),

b) the two gain vectors of one input are connected by one contour, while the two gain vectors of the other input belong to two separate contours (Figure-A.3(b)),

c) the four gain vectors belong to four contours (ie. two for each input) (Figure-A.3(c)).

Possibility a) is the situation of output multiplicity in Figure-4.2(a). In possibility b), the contour passing G_2 in Figure-A.3(b) has to meet one of the following condition: i) intersect with the contour passing $\tilde{G}_2$ (ie. an input multiplicity), ii) intersect once again with the contour of G_1 (ie. an output multiplicity), iii) curve in a way that there must exist a horizontal or vertical gain vector on this contour (ie. an input multiplicity). Possibility c) has the same situations as in possibility b) and will not be repeated here.

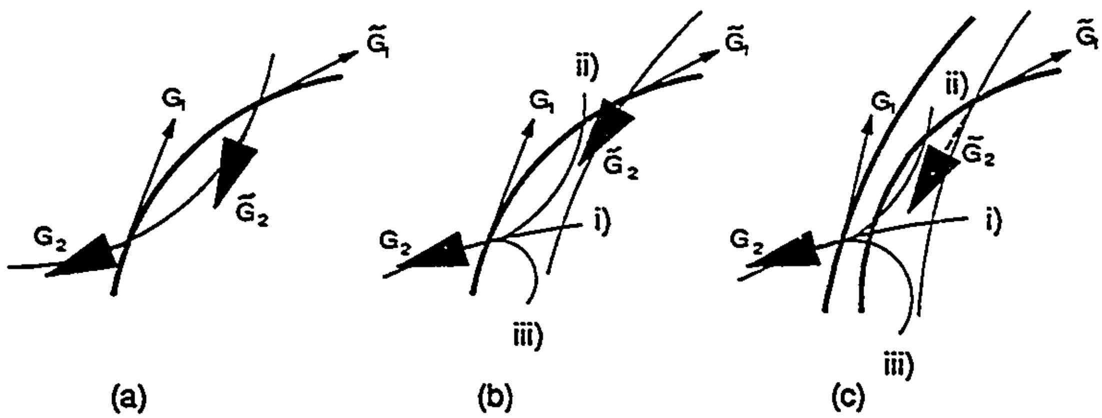

Figure-A.3 Possible relationship between gain vectors at two operating points

Appendix-7: Proof for Theorem 10

Since the determinants of **V** and $\tilde{\mathbf{V}}$ are of the same sign when their elements have the same signs in at least 2×2 systems, the determinant of $\tilde{\mathbf{G}}^{-1}\mathbf{G}$ will simply equal that of **T**, ie.

$$det(\tilde{\mathbf{G}}^{-1}\mathbf{G}) = det(\tilde{\mathbf{V}})det(\mathbf{T})det(\mathbf{V}^{-1}) = det(\mathbf{T}) \qquad (A-7.1)$$

According to Theorem 7, the fact that elements in the **U** matrix do not have their signs changed is a sufficent condition for the product of eigenvalues (ie. determinant) of **T** being positive. Therefore, both the trace and determinant of $\tilde{\mathbf{G}}^{-1}\mathbf{G}$ have been proved to be positive in this situation.

Appendix-8: Derivation of (5-20)

The sensitivity matrix for SVD parameters, $\mathbf{X}$, is obtained by first taking the partial derivatives of the η_{1i} and η_{2i} in (5-19.c) with respect to parameters $\theta, \phi, \bar{\sigma}$ and $\underline{\sigma}$ as the following:

$$\begin{cases} x_{11i} \triangleq \dfrac{\partial \eta_{1i}}{\partial \theta} = (-\bar{\sigma}\sin\theta\cos\phi + \underline{\sigma}\cos\theta\sin\phi)m_{1i} + (\bar{\sigma}\sin\theta\sin\phi + \underline{\sigma}\cos\theta\cos\phi)m_{2i} \\ x_{21i} \triangleq \dfrac{\partial \eta_{2i}}{\partial \theta} = (\bar{\sigma}\cos\theta\cos\phi + \underline{\sigma}\sin\theta\sin\phi)m_{1i} + (-\bar{\sigma}\cos\theta\sin\phi + \underline{\sigma}\sin\theta\cos\phi)m_{2i} \end{cases} \qquad (A-8.1a)$$

$$\begin{cases} x_{12i} \triangleq \dfrac{\partial \eta_{1i}}{\partial \phi} = (-\bar{\sigma}\cos\theta\sin\phi + \underline{\sigma}\sin\theta\cos\phi)m_{1i} + (-\bar{\sigma}\cos\theta\cos\phi - \underline{\sigma}\sin\theta\sin\phi)m_{2i} \\ x_{22i} \triangleq \dfrac{\partial \eta_{2i}}{\partial \phi} = (-\bar{\sigma}\sin\theta\sin\phi - \underline{\sigma}\cos\theta\cos\phi)m_{1i} + (-\bar{\sigma}\sin\theta\cos\phi + \underline{\sigma}\cos\theta\sin\phi)m_{2i} \end{cases} \qquad (A-8.1b)$$

$$\begin{cases} x_{13i} \triangleq \dfrac{\partial \eta_{1i}}{\partial \bar{\sigma}} = (\cos\theta\cos\phi)m_{1i} + (-\cos\theta\sin\phi)m_{2i} \\ x_{23i} \triangleq \dfrac{\partial \eta_{2i}}{\partial \bar{\sigma}} = (\sin\theta\cos\phi)m_{1i} + (-\sin\theta\sin\phi)m_{2i} \end{cases} \qquad (A-8.1c)$$

$$\begin{cases} x_{14i} \triangleq \dfrac{\partial \eta_{1i}}{\partial \underline{\sigma}} = (\sin\theta\sin\phi)m_{1i} + (\sin\theta\cos\phi)m_{2i} \\ x_{24i} \triangleq \dfrac{\partial \eta_{2i}}{\partial \underline{\sigma}} = (-\cos\theta\sin\phi)m_{1i} + (-\cos\theta\cos\phi)m_{2i} \end{cases} \qquad (A-8.1d)$$

and then substituting the settings of m_{1i} and m_{2i} for each experiment (from 1 to n) as below:

$$X_i \triangleq \begin{bmatrix} x_{11i} & x_{12i} & x_{13i} & x_{14i} \\ x_{21i} & x_{22i} & x_{23i} & x_{24i} \end{bmatrix} \qquad (A-8.2a)$$

$$\mathbf{X} = \begin{bmatrix} X_1 \\ \cdot \\ \cdot \\ X_n \end{bmatrix}_{2n \times 4} \qquad (A-8.2b)$$

The information matrix $\mathbf{X}^T\mathbf{X}$ can be easily derived in terms of the sensitivity coefficients as the following:

$\mathbf{X}^T\mathbf{X} =$

$$\begin{bmatrix} \sum_{i=1}^{n} x_{11i}^2 & \sum_{i=1}^{n} x_{11i}x_{12i} & \sum_{i=1}^{n} x_{11i}x_{13i} & \sum_{i=1}^{n} x_{11i}x_{14i} \\ . & \sum_{i=1}^{n} x_{12i}^2 & \sum_{i=1}^{n} x_{12i}x_{13i} & \sum_{i=1}^{n} x_{12i}x_{14i} \\ . & . & \sum_{i=1}^{n} x_{13i}^2 & \sum_{i=1}^{n} x_{13i}x_{14i} \\ sym & . & . & \sum_{i=1}^{n} x_{14i}^2 \end{bmatrix} + \begin{bmatrix} \sum_{i=1}^{n} x_{21i}^2 & \sum_{i=1}^{n} x_{21i}x_{22i} & \sum_{i=1}^{n} x_{21i}x_{23i} & \sum_{i=1}^{n} x_{21i}x_{24i} \\ . & \sum_{i=1}^{n} x_{22i}^2 & \sum_{i=1}^{n} x_{22i}x_{23i} & \sum_{i=1}^{n} x_{22i}x_{24i} \\ . & . & \sum_{i=1}^{n} x_{23i}^2 & \sum_{i=1}^{n} x_{23i}x_{24i} \\ sym & . & . & \sum_{i=1}^{n} x_{24i}^2 \end{bmatrix} \quad (A-8.3)$$

Substituting Eq.(A-8.1) into Eq.(A-8.3), the diagonal elements of $\mathbf{X}^T\mathbf{X}$ can be derived as:

$$\sum_{i=1}^{n} x_{11i}^2 + x_{21i}^2 = \sum_{i=1}^{n}\left[\bar{\sigma}^2(\cos\phi m_{1i} - \sin\phi m_{2i})^2 + \underline{\sigma}^2(\sin\phi m_{1i} + \cos\phi m_{2i})^2\right] \quad (A-8.4a)$$

$$\sum_{i=1}^{n} x_{12i}^2 + x_{22i}^2 = \sum_{i=1}^{n}\left[\bar{\sigma}^2(\sin\phi m_{1i} + \cos\phi m_{2i})^2 + \underline{\sigma}^2(\cos\phi m_{1i} - \sin\phi m_{2i})^2\right] \quad (A-8.4b)$$

$$\sum_{i=1}^{n} x_{13i}^2 + x_{23i}^2 = \sum_{i=1}^{n}(\cos\phi m_{1i} - \sin\phi m_{2i})^2 \quad (A-8.4c)$$

$$\sum_{i=1}^{n} x_{11i}^2 + x_{21i}^2 = \sum_{i=1}^{n}(\sin\phi m_{1i} + \cos\phi m_{2i})^2 \quad (A-8.4d)$$

and the off-diagonal elements in the upper triangle are:

$$\begin{aligned} \sum_{i=1}^{n} x_{11i}x_{12i} + x_{21i}x_{22i} &= -\bar{\sigma}\underline{\sigma}\sum_{i=1}^{n}(m_{1i}^2 + m_{2i}^2) \\ &= -\bar{\sigma}\underline{\sigma}\sum_{i=1}^{n}[(\cos\phi m_{1i} - \sin\phi m_{2i})^2 + (\sin\phi m_{1i} + \cos\phi m_{2i})^2] \end{aligned} \quad (A-8.5a)$$

$$\begin{aligned} \sum_{i=1}^{n} x_{11i}x_{13i} + x_{21i}x_{23i} &= -\underline{\sigma}\sum_{i=1}^{n}[\sin\phi\cos\phi(m_{1i}^2 - m_{2i}^2) + (\cos^2\phi - \sin^2\phi)m_{1i}m_{2i}] \\ &= -\underline{\sigma}\sum_{i=1}^{n}(\cos\phi m_{1i} - \sin\phi m_{2i})(\sin\phi m_{1i} + \cos\phi m_{2i}) \end{aligned} \quad (A-8.5b)$$

$$\sum_{i=1}^{n} x_{11i}x_{14i} + x_{21i}x_{24i} = \bar{\sigma}\sum_{i=1}^{n}(\cos\phi m_{1i} - \sin\phi m_{2i})(\sin\phi m_{1i} + \cos\phi m_{2i}) \quad (A-8.5c)$$

$$\sum_{i=1}^{n} x_{12i}x_{13i} + x_{22i}x_{23i} = \bar{\sigma}\sum_{i=1}^{n}(\cos\phi m_{1i} - \sin\phi m_{2i})(\sin\phi m_{1i} + \cos\phi m_{2i}) \quad (A-8.5d)$$

$$\sum_{i=1}^{n} x_{12i}x_{14i} + x_{22i}x_{24i} = -\underline{\sigma}\sum_{i=1}^{n}(\cos\phi m_{1i} - \sin\phi m_{2i})(\sin\phi m_{1i} + \cos\phi m_{2i}) \quad (A-8.5e)$$

$$\sum_{i=1}^{n} x_{13i}x_{14i} + x_{23i}x_{24i} = 0 \quad (A-8.5f)$$

From (5-19.a) we know that the two rotated inputs are:

$$\xi_{1i} = \cos\phi m_{1i} - \sin\phi m_{2i} \qquad (A-8.6a)$$

$$\xi_{2i} = -(\sin\phi m_{1i} + \cos\phi m_{2i}) \qquad (A-8.6b)$$

Substitute (A-8.6) into (A-8.4) and (A-8.5), and then (5-20) can be obtained.

Appendix-9: Derivation of (5-28)

The information matrix in (5-27) to have the parameter of the V matrix in the first column as below:

$$\mathbf{X}^T\mathbf{X} = \begin{bmatrix} \bar{\sigma}^2\zeta_2 & -\bar{\sigma}\underline{\sigma}(\zeta_1+\zeta_2) & \bar{\sigma}\zeta_3 & 0 \\ . & \bar{\sigma}^2\zeta_1 & 0 & \bar{\sigma}\zeta_3 \\ . & . & \zeta_1 & 0 \\ sym & . & . & \zeta_2 \end{bmatrix} \qquad (A-9.1a)$$

$$= \begin{bmatrix} \chi_{11} & \chi_{12} \\ \chi_{21} & \chi_{22} \end{bmatrix} \qquad (A-9.1b)$$

where $\chi_{12} = \chi_{21}^T = [-\bar{\sigma}\underline{\sigma}(\zeta_1+\zeta_2) \quad \bar{\sigma}\zeta_3 \quad 0]$ $\qquad (A-9.1c)$

$$\text{and } \chi_{22} = \begin{bmatrix} \bar{\sigma}^2\zeta_1 & 0 & \bar{\sigma}\zeta_3 \\ . & \zeta_1 & 0 \\ sym & . & \zeta_2 \end{bmatrix} \qquad (A-9.1d)$$

It is trivial to derive the inverse of χ_{22} as:

$$\chi_{22}^{-1} = \frac{1}{\bar{\sigma}^2\zeta_1(\zeta_1\zeta_2-\zeta_3^2)} \begin{bmatrix} \zeta_1\zeta_2 & 0 & -\bar{\sigma}\zeta_1\zeta_3 \\ . & \bar{\sigma}^2(\zeta_1\zeta_2-\zeta_3^2) & 0 \\ sym & . & \bar{\sigma}^2\zeta_1^2 \end{bmatrix} \qquad (A-9.2)$$

Similarly, the information matrix with the minimum singular value in the first column is as the following

$$X^T X = \begin{bmatrix} \zeta_2 & 0 & 0 & \bar{\sigma}\zeta_3 \\ \cdot & \bar{\sigma}^2\zeta_2 & \bar{\sigma}\zeta_3 & -\bar{\sigma}\underline{\sigma}(\zeta_1+\zeta_2) \\ \cdot & \cdot & \zeta_1 & 0 \\ sym & \cdot & \cdot & \bar{\sigma}^2\zeta_1 \end{bmatrix} \qquad (A-9.3a)$$

$$= \begin{bmatrix} \chi_{11} & \chi_{12} \\ \chi_{21} & \chi_{22} \end{bmatrix} \qquad (A-9.3b)$$

where $\chi_{12} = \chi_{21}^T = [0 \quad 0 \quad \bar{\sigma}\zeta_3]$ $\qquad (A-9.3c)$

$$\text{and } \chi_{22} = \begin{bmatrix} \bar{\sigma}^2\zeta_2 & \bar{\sigma}\zeta_3 & -\bar{\sigma}\underline{\sigma}(\zeta_1+\zeta_2) \\ \cdot & \zeta_1 & 0 \\ sym & \cdot & \bar{\sigma}^2\zeta_1 \end{bmatrix} \qquad (A-9.3d)$$

and the corresponding inverse of χ_{22} is:

$$\chi_{22}^{-1} = \frac{\begin{bmatrix} \bar{\sigma}^2\zeta_1^2 & -\bar{\sigma}^3\zeta_1\zeta_3 & \bar{\sigma}\underline{\sigma}\zeta_1(\zeta_1+\zeta_2) \\ \cdot & \bar{\sigma}^4\zeta_1\zeta_2 - [\bar{\sigma}\underline{\sigma}(\zeta_1\zeta_2-\zeta_3^2)]^2 & \bar{\sigma}^2\underline{\sigma}\zeta_3(\zeta_1+\zeta_2) \\ sym & \cdot & \bar{\sigma}^2(\zeta_1\zeta_2-\zeta_3^2) \end{bmatrix}}{\bar{\sigma}^2[\bar{\sigma}^2\zeta_1(\zeta_1\zeta_2-\zeta_3^2) - \underline{\sigma}^2(\zeta_1+\zeta_2)^2]} \qquad (A-9.4)$$

Then the information contents of ϕ and $\underline{\sigma}$ are straightforward calculations of the following:

$$\chi_{11} - \chi_{12}\chi_{22}^{-1}\chi_{21} \qquad (A-9.5)$$

with (A-9.1b) and (A-9.2) substituted for the former, and (A-9.3.b) and (A-9.4) substituted for the latter. The results are as follows

$$\Delta(\phi) = \bar{\sigma}^2\zeta_2 - \left\{ \underline{\sigma}^2 \left[\frac{(\zeta_1+\zeta_2)^2\zeta_2}{\zeta_1\zeta_2 - \zeta_3^2} \right] + \bar{\sigma}^2 \left(\frac{\zeta_3^2}{\zeta_1} \right) \right\} \qquad (A-9.6a)$$

$$\Delta(\underline{\sigma}) = \zeta_2 - \left\{ \frac{\bar{\sigma}\underline{\sigma}\zeta_1(\zeta_1+\zeta_2) + \bar{\sigma}^2[\underline{\sigma}(\zeta_1+\zeta_2) + (\zeta_1\zeta_2-\zeta_3^2)]}{\bar{\sigma}^2\zeta_1(\zeta_1\zeta_2-\zeta_3^2) - \underline{\sigma}^2(\zeta_1+\zeta_2)^2} \right\} \zeta_3^2 \qquad (A-9.6b)$$

By neglecting small terms involving the minimum singular value, (5-28) is obtained.

8 Notation

A = an arbitrary matrix
B = bottom product flowrate change
c^2 = a constant for the parameter uncertainty ellipse
d_i = the i-th diagonal element of $\hat{\mathbf{U}}^T\mathbf{U}$ as defined in (A-4.1a)
D = distillate flowrate change
D = disturbance vector
D = a diagonal matrix defined in (A-4.2)
e_{ij} = the i-th row, j-th column off-diagonal element of $\hat{\mathbf{U}}^T\mathbf{U}$ as defined in (A-4.1b)
E_i = identification error vector at the i-th experiment
E = an additive perturbation matrix
f_k = filter time constant for the k-th output variable
f^* = the common controller design transfer function
F = filter transfer function matrix
$\mathbf{F}^*$ = controller design transfer function matrix defined in Eq.(8.b)
g_{kj} = the kj-th element of the gain matrix
G_D = gain vector of the distillate flow
G_j = the j-th column vector of a gain matrix
G_k^* = the k-th row vector of a gain matrix
G_L = gain vector of the reflux flow
G_V = gain vector of the boil-up flow
G = gain matrix
I = the identity matrix
l_j = length of the j-th gain vector
l_G = the 2-norm of the additive mismatch matrix $\mathbf{G}-\hat{\mathbf{G}}$
L = reflux flowrate change
$\mathbf{L}_A$ = additive mismatch matrix
$\mathbf{L}_I$ = multiplicative input mismatch matrix
$\mathbf{L}_O$ = multiplicative output mismatch matrix
$\mathbf{L}_S$ = $\hat{\Sigma}^{-1}\Sigma-\mathbf{I}$, mismatch in the singular value matrix
$\mathbf{L}_U$ = $\hat{\mathbf{U}}^{-1}\mathbf{U}-\mathbf{I}$, mismatch in the output rotation matrix
$\mathbf{L}_V$ = $\hat{\mathbf{V}}^{-1}\mathbf{V}-\mathbf{I}$, mismatch in the input rotation matrix
m_{ji} = designed value of the j-th input at the i-th experiment
M = manipulated input vector
M = design matrix of physical inputs (Eq.8.(c))
n_j = length mismatch in the j-th gain vector
N = number of trays in distillation column
N_m = minimum number of trays
P = transfer function matrix
q_{ij} = ratio of the j-th true singular value to the i-th model singular value ((A-4.1)).
Q = controller transfer function matrix in IMC structure
R = reflux ratio
R_m = minimum reflux ratio

$s_{e_k}^2$ = estimated variance of the k-th output errors
T = matrix defined in (3-31)
$\mathbf{T_V}$ = matrix defined in (3-28)
$\mathbf{T}_{EM}$ = transformation matrix between LV and DV control
$\mathbf{T}_{S_i}^{[id]}$ = matrix defined in (A-4.4)
u_{kj} = the kj-th element of the output rotation matrix in SVD
U_j = the j-th column vector of the output rotation matrix in SVD
U = output rotation matrix in SVD
v_{kj} = the kj-th element of the input rotation matrix in SVD
V_j = the j-th column vector of the input rotation matrix in SVD
V = boil-up flowrate change
V = input rotation matrix in SVD
$\mathbf{X}_D$ = distillate composition (mole fraction of light component)
$\mathbf{X}_B$ = bottom product composition (mole fraction of light component)
$\mathbf{X}_F$ = feed composition (mole fraction of light component)
$\mathbf{X}_i$ = sensitivity matrix of the i-th experiment (defined in Eq.(10.c)
X = sensitivity matrix of all experiments
Y = measured output vector
Y_{sp} = set-point change vector
ΔY_{sp} = a step change in set-point vector
$\hbar$ = singularity line (Eq.(5))

Greek letters

α = relative volatility
α_j = the angle of the j-th gain vector
β = angle between the two gain vectors
β_p = vector of nonlinear parameter set
β_{U_j} = the j-th independent parameter in the **U** matrix
β_{V_j} = the j-th independent parameter in the **V** matrix
γ_{kj} = kj-th element in the relative gain array
Γ = eigenvector matrix
δ_j = angle mismatch of the j-th gain vector
σ_e^2 = the common variance of all output errors
$\sigma_{e_k}^2$ = the variance of the k-th output errors
Ψ = a vector of integral perfomance variation due to a step set-point change
Δ = norm-bounded uncertainty matrix
Φ = information content = $|\chi_{11} - \chi_{12}\chi_{22}^{-1}\chi_{21}|$
ζ = element in the design matrix of the rotated inputs (Eq.(23))
Z = design matrix of the rotated inputs (Eq.(23))
η_i = model predition of the k-th output
θ = parameter of the **U** matrix in 2×2 gain matrix

ι = ± 1
κ = condition number
κ^* = minimum condition number
K = summation of singular value ratios
λ_i = the i-th eigenvalue of a matrix
ξ_j = the j-th rotated input
$\bar{\xi}_j$ = magnitude of the j-th rotated input change
ξ = vector of the rotated inputs
Ξ = design matrix of the rotated inputs
σ_j = the j-th singular value of a matrix
$\bar{\sigma}$ = the maximum singular value
$\underline{\sigma}$ = the minimum singular value
Σ = diagonal matrix containing the singular values
ϕ = parameter of the V matrix in 2×2 gain matrix
χ_{ij} = the ij-th sub-matrix of a partitioned information matrix
Ω = transformed gain matrix
ε = the angle between the two gain vectors (defined in Figure-A.1)
$\bar{\varepsilon}_u$ = small error in the output rotation matrix
$\bar{\varepsilon}_v$ = small error in the input rotation matrix
Ω_{kj} = the kj-th row vector of the transformed gain matrix

Superscripts

$\hat{}$ = identified value
$\bar{}$ = true value at nominal operating point
E = LV control
M = DV control

Subscripts

i = experiment or sample index
j = matrix column index
k = matrix row index
n = number of experiments or samples
r = dimension of a gain matrix

9 References

Anderson, H.W. and Kummel, M., 1990, "Evaluating Estimation of gain Directionality. Part II: A Case study of Binary distillation", *Chem. Eng. Sci.*, (submitted for publication).

Beck, J.V. and K.J. Arnold, 1977, *Parameter Estimation in Engineering and Science*. John Wiley & Sons Inc., New York.

Box, G.E.P. and MacGregor, J.F., 1974, "The Analysis of Closed-Loop Dynamic-Stochastic Systems", *Technometrics*, **16**, No.3, 391-398.

Bristol, E.H. 1966, "On a New Measure of Interactions for Multivariable Process Control", *IEEE Trans. Auto. Control* **11**, 133-134.

Doyle, J.C. and Stein, G., 1981, "Multivariable Feedback Design: Doncepts for a Classical/Modern Synthesis. *IEEE Trans. Auto. Control*, **AC-26**, 4-16.

Doyle, J.C., 1982, "Performance and Robustness Analysis for Structured Uncertainty", *Proc. IEEE Conf. on Decision and Control*, Orlando, FL.

Frank, P.M., 1974, *Design of Control Circuits with Prescribed Behavior*. G. Braun, Karlsruhe.

Garcia, C.E. and Morari, M., 1982, "Internal Model Control. 1. A Unifying Review and Some New Results", *Ind. Eng. Chem. Process Des. Dev.*, **21**, 308-323.

Garcia, C.E. and Morari, M., 1985, "Internal Model Control. 2. Design Procedure for Multivariable Systems", *Ind. Eng. Chem. Process Des. Dev.*, **24**, 472-484.

Grosdidier, P.; Morari, M.; Holt, B.R., 1985, "Closed-Loop Properties from Steady-State Gain Information", *Ind. Eng. Chem. Fundam.* **24**, 221-235.

Hunter, W.G., Hill, W.J. and Henson, T.L., 1969, "Designing Experiments for Precise Estimation of All or Some of the Constants in a Mechanistic Model", *Can. J. Chem. Eng.*, **47**, 76-80.

Kelly, J.D., 1990, *Design, Construction, Modelling, Simulation and Multivariable Control of a Pilot Plant Fluidized Bed Catalytic Reactor*. M.Eng. thesis, McMaster University, Canada.

Koppel, L.B., 1982 "Input Multiplicities in Nonlinear, Multivariable Control Systems", *AIChE*, **28**, 935-945.

Koung, C.-W., 1987, *Analysis and Control of High-Purity Distillation Columns*. M.Sc. thesis, Queen's University, Canada.

Koung, C.W. and Harris, T.J., 1989, "Sensitivity of the Relative Gain Array". Presented at the 39th Canadian Chemical Engineering Conference, Hamilton, Ontario, Canada; paper A2d.

Kozub, D.J, MacGregor, J.F. and Wright, J.D., 1987, "Application of LQ and IMC Controllers to a Packed-Bed Reactor", *AIChE*, **33**, 1496-1506.

Ljung, L., 1987, *System Identification: Theory for the User*. Prentice-Hall, Englewood Cliffs, NJ.

Ljung, L., 1988, *System Identification Toolbox: For Use with MATLAB*. The MathWork, Inc.

Marlin, T.E., McAvoy, T.J., Marino-Galarraga, M. and Kapoor N., 1986, "A short-Cut Method for Process Control and Operability Analysis", *Chemical Process Control-III*, CACHE, Elsevier Science Publishers Inc., New York.

Marlin, T.E., 1991, Personal communication.

McAvoy, T.J., 1983, *Interaction Analysis*. ISA monograph, NC.

McDonald, K., Palazoglu, A. and Bequette, B.W., 1988, "Impact of Model Uncertainty Descriptions for High-Purity Distillation Control", *AIChE*, 34, 1996-2004.

McFarlane, R.C. Hoffman, T.W., Taylor, P.A. and MacGregor, J.F., 1983, "Control of Fluidized Bed Reactors. 1. Modelling, Simulation, and Single-Loop Control Studies", *Ind. Eng. Chem. Process Des. Dev.*, 22, 22-31.

Morari M. and Zafiriou, E., 1989, *Robust Process Control*. Prentice-Hall, Englewood Cliffs, NJ.

Noble, B. and Daniel, J.W., 1977, *Applied Linear Algebra*. Prentice-Hall, Englewood Cliffs, NJ.

Onderwater, D., 1985, *Control System Configuration and Multivariable Identification of a Packed Bed Tubular Reactor*. M.Eng. thesis, McMaster University, Canada.

Orcutt, J.C., Davidson, J.F. and Pigford, R.L., 1962, "Reaction Time Distributions in Fluidized Catalytic Reactors", *Chem. Eng. Prog. Symp. Series*, 58, 38, 1-15.

Perry, R.H. and Chilton, C.H., 1973, *Chemical Engineer's Handbook*, 4-th ed., pp.2-52. McGraw-Hill, New York.

Shaw, I.S.D., 1972, *Modelling and Discrimination Studies in a Catalytic Fluidized Bed Reactor*. Ph.D. thesis, McMaster University, Canada.

Skogestad, S; Morari, M. "Implications of Large RGA Elements On Control Performance", *Ind. Eng. Chem. Res.* **1987**, 26, 2323-2330.

Skogestad, S and Morari, M., 1988, "LV Control of a High-Purity Distillation Column", *Chem. Eng. Sci.*, 43, 33-46.

Skogestad, S and Morari, M., 1989, "Robust Performance of Decentralized Control Systems by Independent Designs", *Automatica*, 25, 119-126.

Skogestad, S., Morari, M. and Doyle, J.C., 1988, "Robust Control of Ill-Conditioned Plant: High-Purity Distillation", *IEEE Trans. Auto. Control*, 33, 1092-1105.

Stewart, G.W., 1973, *Introduction to Matrix Computations*, Academic Press, New York.

Yang, D.R., Waller, K.V. Seborg, D.E. and Mellichamp, D.A., 1990, "Dynamic Structural transformations for Distillation Control Configurations", *AIChE Journal*, 36, 1391-1402.

Yu, C.-C. and Luyben, W.L., 1987, "Robustness with Respect to Integral Controllability", *Ind. Eng. Chem. Res.* 26, 1043-1045.

Zames, G., 1981, "Feedback and Optimal Sensitivity: Model Reference Transformations, Multiplicative Seminorms and Approximate Inverses", *IEEE Trans. Auto. Control,* 26, 310.